論文 / 著書情報
Article / Book Information

題目(和文)	
Title(English)	Nuclear transglutaminase 2-mediated human hepatic injury by interaction with pathogenic fungi
著者(和文)	SHRESTHARONAK
Author(English)	Ronak Shrestha
出典(和文)	学位:博士(学術), 学位授与機関:東京工業大学, 報告番号:甲第10926号, 授与年月日:2018年6月30日, 学位の種別:課程博士, 審査員:梶原 将,一瀬 宏,長田 俊哉,山本 直之,小畠 英理,小嶋 聡一
Citation(English)	Degree:Doctor (Academic), Conferring organization: Tokyo Institute of Technology, Report number:甲第10926号, Conferred date:2018/6/30, Degree Type:Course doctor, Examiner:,,,,,
学位種別(和文)	博士論文
Type(English)	Doctoral Thesis

Doctoral Thesis (2018)

Nuclear transglutaminase 2-mediated human hepatic injury by interaction with pathogenic fungi

Ronak Shrestha

Department of Life Science

Faculty of Bioscience and Biotechnology

Tokyo Institute of Technology

Table of Contents

List of figures

List of Tables

Chapter 1

1. Introduction

1.1 Fungi

Yeasts and molds containing chitin in their cell wall are classified under the eukaryotic super kingdom, Fungi [1]. Some fungi have provided various benefits to human being. They are the principal decomposers in the ecological systems and acts as bio-fertilizers [2] and extensively used as a food or food processors like leavening agent in bread and for fermentation of beer, wine and soy sauce. They are also used in production of enzyme, vitamin and various medicinal agents like penicillin cephalosporin, immunosuppressant and steroid [3]. On the other hand, other species of fungi sometimes caused various diseases to humans.

1.2 Fungi and diseases

Being ubiquitous in environment, fungal infections, mycoses, are very common. The infections in most of clinical cases are limited as superficial infection of skin and oral cavity of human body, but in immunocompromised individuals, fungi can invade the host and result in systemic infections, often referred as caused by opportunistic fungal pathogens. The major opportunistic fungal pathogens are *Candida*, *Aspergillus*,

Cryptococcus and *Pneumocystis spp.* and cause more than 90% of human deaths related to fungal diseases [4]. The incidence of candidiasis, aspergillosis, cryptococcusis, and pneumocystisis is clinically more prevalent in patients receiving organ transplantation, AIDS patients, patients receiving cancer chemotherapy and haemato-oncological patients [4]. Although current trends showed an increased incidence of invasive fungal diseases with high morbidity and mortality rates, their incidence is usually underestimated [5]. Their diagnosis and timely treatment to mycoses often depend on clinical suspicion and require attention for its better prevention and treatment.

1.3 *Candida species*-host interaction and pathogenicity

Over the last decades, fungal diseases have become a major problem especially in the clinical settings. *Candida* species is a ubiquitous commensal of human, generally found in the oral cavity and gastrointestinal tract. In this species, *C. albicans* and *C. glabrata* are ranked as the first and second opportunistic fungal pathogens [6]. Collectively, they account for 65-75 % of all systemic candidiasis followed by *C. parapsilosis* and *C. tropicalis* [7].

C. albicans is a diploid fungus, can grow as a yeast cells, pseudohyphae and filamentous hyphae forms known as polymorphism [8, 9] **(**Figure 1.1**)**. This

morphological change is thought to aid for the survival, growth and dissemination in human host [4, 7, 8]. In contrast, *C. glabrata* is a haploid that strictly grows as a yeast form, actually resembles to a bakers' yeast *Saccharomyces cerevisiae* [8]. Compared with *C. albicans* morphological flexibility, the behavior of *C. glabrata* to the host is independent of morphology. Yet, both species are successful commensals of human gut flora, that habitually lives in a benign state. Beside human gastro intestine, these fungi are frequent colonizer of skin, respiratory and reproductive tract and becomes pathogenic in response to changes in human immune state and microflora, brought in due to antibiotics, diabetes, cancer, extreme age, immunosuppression, intravenous catheters and long-term hospitalization. This overgrowth of *Candida* species in the host is known as candidiasis [4, 10].

Unlike most other medically important fungi, such as, *C. neoformans* and *A. fumigatus*, *C. albicans* is rarely found in environmental niches such as soil. Hence, it is highly adapted to and specialized to sustain in host environment [9]. *C. albicans* causes almost of mild cases of fungal infections, furthermore, in some severe cases *C. albicans* is the top pathogen of fungal infection. This fungus can penetrate in the deeper tissue and enters the bloodstream leading to invasive into almost all body sites and organs causing severe life-threating systemic infections [7, 11, 12].

C. albicans constitute various virulent traits to become pathogenic to immuno-compromised individuals. These specialized attributes facilitate *C. albicans* for adaptation and survival in various environmental stresses including host immune system, pH, nutrition acquisition, and competition with the other microorganisms in the microflora. *C. albicans* implicates a number of strategies to escape and/or evade host immune system [13, 14] and cause infections such as morphogenesis; yeast to hypha transition, a major virulence trait. Non-filamentous *C. albicans* strains have been shown to be avirulent or less virulent with defective transcriptional factors [15]. Interestingly, hyphae locked- and yeast locked- mutants of *C. albicans* were also found less virulent than wild type strains [16]. This implies that the morphological switch between yeast phase and hyphae phase is a virulent trait of *C. albicans*. Likewise, the epithelium invasion and the escape from phagocytosis are other important interaction mechanisms between *C. albicans* and host immune response. Shielding *C. albicans'* surface substrates associated molecular patterns through pattern recognition receptors of phagocytes aids in the escape of fungi, which further could be achieved by avoiding activation of complement system and reduce production of proinflammatory cytokines [13]. In addition, *C. albicans* can inhibit the formation of phagolysosome in phagocytes, an important step in pathogen killing by fusion of phagosome containing microorganism

and lysosome by phagocytes. Recently, it has been reported that a live *C. albicans*, but not heat-killed *C. albicans* was able to inhibit phagolysosome formation, suggesting the inhibition of phagocytosis is dependent on the viability of fungus. Also, mutants unable to grow as filamentous forms fail to show the inhibition of phagolysosome formation in comparison to wild type strains [17, 18]. Another important antifungal mechanism shown by *C. albicans* is inhibition of reactive oxygen species (ROS) produced by phagocytes. In an experimental model, catalases [19] and superoxide dismutase [20] genes were found to be responsible to counteract ROS production. Further, Wellington and colleagues have demonstrated that a live *C. albicans* and *C. glabrata*, but not *Saccharomyces cerevisiae*, can actively suppress ROS production in a murine macrophage cell line [21]. Hence, the interaction between *Candida* and host defense system is of the most important factor in making it opportunistic fungal pathogen.

1.4 Liver and liver diseases

Liver has a wide array of functions such as detoxification of various metabolites, production of biochemical necessary for digestion, and protein synthesis. Likewise, this organ also aids in hormone production, breakdown of red blood cells, regulation of glycogen storage and important role in metabolism [22]. It is the largest internal organ, receiving the blood supply from both hepatic artery and hepatic portal vein **(Figure 1.2)**. Impressive amount of blood, approximately 80 % blood entering liver originates from portal vein, while remaining 20% from arterial supply. Hence, liver is continuously exposed to blood borne pathogens, most of which are derived from gut [23, 24]. Failure in the detection and/or clearance of pathogens in blood might result in systemic infection (sepsis) often life threatening. Liver is the first lines of defense between host and external environment [25]. To accomplish variety of functions, liver contains different cells such as liver resident macrophages (kupffer cells), liver sinusoidal epithelial cells, hepatic stellate cells and hepatocytes. Hepatocytes are the parenchymal cells, primarily functions in metabolism, protein production, toxin neutralization and detection of pathogens and aids in host immune response [22].

Being a vital organ and supporting other organs in the body with multidimensional functions, liver is vulnerable to different diseases. Liver disease also

referred as hepatic disease, means any disturbance in the liver functions as a consequence of various factors such as infectious hepatitis virus, drugs and alcohol. One of most common and emerging chronic liver conditions is Steatosis. It is accumulation of fat (triglycerides and other lipids) in hepatocytes of liver and commonly known as fatty liver. This accumulation is a result of defective fatty acid metabolism caused by unbalance between energy intake and utilization, mitochondrial damage, insulin resistance, and defect in receptors and enzymes involved [26]. Steatosis is classified into two types, one is associated with alcohol and known as alcohol-related fatty liver disease and the other is not related to alcohol and known as non-alcoholic fatty liver disease. These lipid accumulations can progress to develop inflammation and become steatohepatitis. Alcohol-related fatty liver with inflammation is known as alcoholic steatohepatitis (ASH), Non-alcoholic fatty liver disease with inflammation is known as non-alcoholic steatohepatitis (NASH). Both ASH and NASH can progress to cirrhosis and later to hepatocellular carcinoma [26, 27].

1.5 *Candida species* and liver injury

Among *Candida* species, *C. albicans* and *C. glabrata* are two common species that are commensals of human digestive tract and habitually lives in a benign state [28].

In immuno-compromised individuals such as patients treated with antibiotics, diabetes and cancer patients, elderly people and infants overgrowth of these fungi occurs and this disease is known as candidiasis. In such cases, these fungi invade intestine and reach liver through hepatic portal vein **(Figure 1.2)**. Liver acts as the first barrier against spreading of these pathogens and prevents severe systemic fungal infections [6, 29, 30]. A prospective study from two and half decade ago reported that fungal infection was present in 32 % of patients with acute liver failure and *Candida* species were major fungus present [31]. Hepatic *Candida* infection is still commonly recognized complication in patients with acute leukaemia and other haematological malignancies [30]. This fact is also anevidence that *Candida* species play an important role in gut microbiota such as bacteria-liver interaction in the pathogenesis of ASH and NASH [32-35]. Recently, sequencing of the fecal microbiome showed overgrowth of *C. albicans* in ASH patients [36]. Although prevalence of pathogenic fungi like *C. albicans* and *C. glabrata* has been shown in the liver injury by several studies, the detailed relation between Candida infection and hepatic injury has not been addressed yet.

1.6 Transglutaminase 2 in liver injury

Transglutaminases (TGs) is a group of enzymes that catalyze the formation of an isopeptide bond between a free amine group (e.g., protein- or peptide-bound lysine) and an acyl group at the end of the side chain of protein- or peptide-bound glutamine. A total of eight TGs have been characterized as given in **Table 1.1** [37]. Among these TGs, Transglutaminase 2 (TG2, EC 2.3.2.13) is the most ubiquitously expressed multifunctional protein-crosslinking enzyme of the TG family [38, 39]. Unlike other TGs, the transamidase reaction of TG2 is a Ca^{2+}-dependent formation of a covalent bond between γ-carboxamide groups of peptide-bound glutamine residues and the primary amino groups of a wide range of proteins. This crosslinking activity has been implicated in various physiological activities such as cell growth and differentiation, cell adhesion and apoptosis [40]. In as low intracellular Ca^{2+} concentrations as 10 nM, ATP/GTP/GDP forms complex with TG2 and render TG2 in a "closed" conformation [41, 42]. In this conformation, it mainly acts as a GTPase supporting growth [43-45]. In contrast, when cells are injured and the intracellular Ca^{2+} concentration exceeds 700–800 nM, Ca^{2+} binds with TG2 to make an extended "open" conformation [46] exposing the catalytic site of TG2 [47, 48]. In this conformation, TG2 mainly acts as a crosslinking enzyme and induces apoptosis [45, 49]. TG2 is predominantly a cytosolic

protein but can localize in extracellular matrix, the membrane, mitochondria and nucleus [39]. Only small portions (5-7 %) is expressed in the nuclear region, which is generally stimulated by various stimuli via cellular stress such as ROS and/or an increased Ca^{2+} concentration [38]. Depending upon its cellular location and biological activity TG2 induces cell growth, differentiation and apoptosis [37, 39, 50].

TG2-dependent hepatic cell death has been previously reported in alcohol, free fatty acid, and acyclic retinoid (ACR) treated cell culture systems, animal models and patients with ASH and NASH [51-54]. In hepatic cells, treatment with alcohol and free fatty acid increases crosslinking activity of TG2 in nucleus. The increased nuclear TG2 activity causes excessive crosslinking of transcription factor Sp1 and inactivates it. This inactivation decreases expression of c-Met, one of the major receptor for hepatocyte growth factors, leading to caspase-independent hepatic cell death **(**Figure 1.3**)** [51, 52]. Increased nuclear TG2 activity dependent cell death was also reported in ACR treated hepatic cellular carcinoma cells [53, 54].

Prevalence of pathogenic fungi like *C. albicans* and *C. glabrata* in liver injury has been revealed by number of researches, signifying that an important role of these fungi in hepatic injury, but the relation between these fungi infection and hepatic injury

remains to be elucidated. Hence, in this study I have investigated on involvement of TG2 activity in regulation of *Candida* species induced liver cell death.

1.7 Aim, objectives and research contribution

1.7.1 Aim

The aim of this study is to explore the hypothesis that *C. albicans* and *C. glabrata* might increase nuclear activity of TG2 in hepatic cells and apoptosis of hepatic cells.

1.7.2 Objective

This study has been carried out with an objective to

- investigate the effect of fungus-host interaction to TG2 activity and death of the host cells.
- Screen and identify fungal factor(s) that can affect TG2 activity of the host cells
- establish the role of identified factor in TG2-mediated hepatic cell injury.

1.7.3 Research contributions

This study demonstrated that co-incubation of hepatic cells and opportunistic fungi such as *C. albicans* and *C. glabrata*, but not edible yeasts, such as *S. cerevisiae*, induced hepatic cell death by enhancing TG activity, at least in part through the

production of ROS such as hydroxyl radicals (·OH). Pharmacological and genetic approaches were used to demonstrate these phenomena. Irreversible inhibitor of TG2, 6-diazo-5-oxo-norleucine tetrapeptide (ZDON), was used to study *C. albicans*-induced cell death as measured by caspase-3 activation. An inhibitor of ROS, N-acetyl cysteine (NAC), and *NADPH* oxidase gene (*NOX1*) mutant in *C. glabrata* were used to confirm whether these phenomena were mediated by fungus-derived ROS.

Table 1.1 TG family

Name	Gene
Factor XIII A	F13A1
Keratinocyte transglutaminase	TGM1
Tissue transglutaminase	TGM2
Epidermal transglutaminase	TGM3
Prostate transglutaminase	TGM4
TGM X	TGM5
TGM Y	TGM6
TGM Z	TGM7

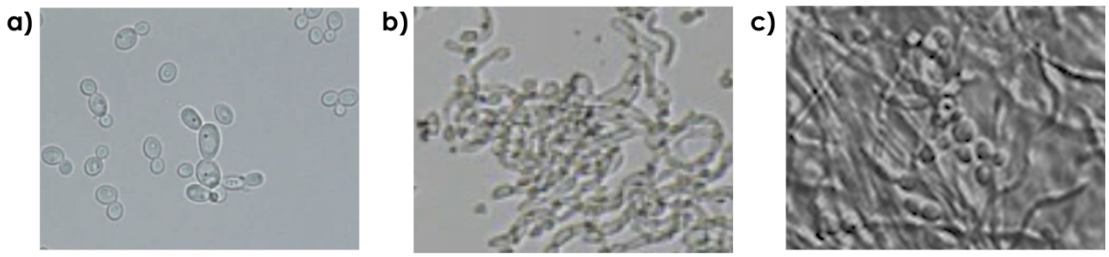

Figure 1.1 Polymorphic forms of *C. albicans*

a) Yeast form, b) Pseudohyphae form, c) both yeast and hyphae

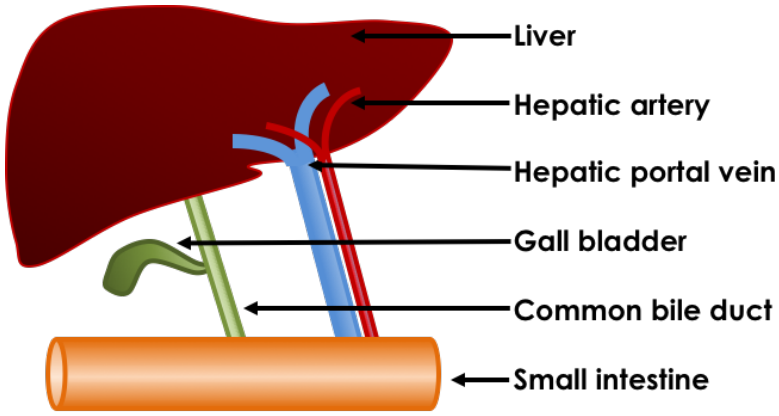

Figure 1.2 Liver and hepatic portal vein

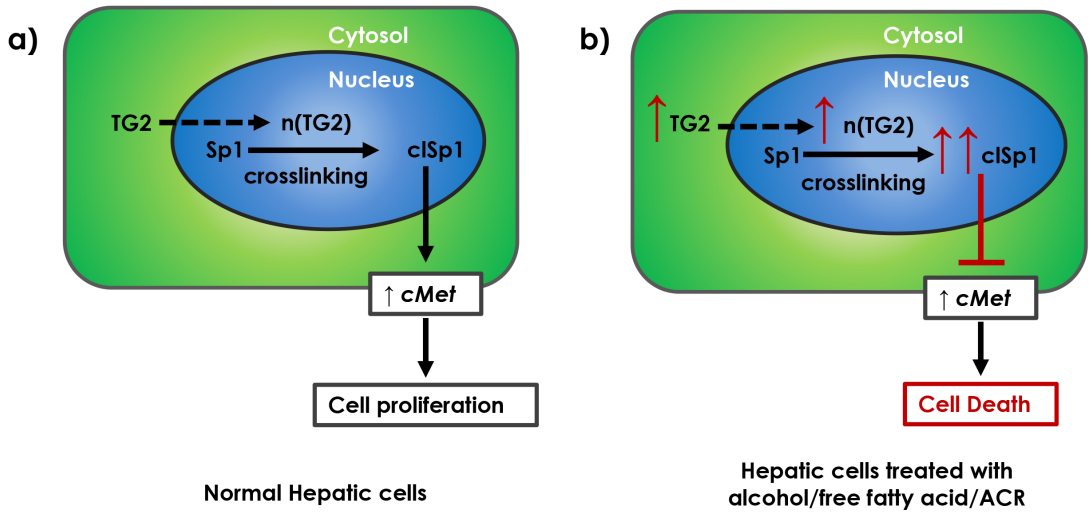

Figure 1.3 Role of TG2 in cell growth and death of hepatic cells

a) TG2 mediated cell growth in normal hepatic cell. **b)** TG2 mediated cell death in alcohol, free fatty acid and ACR treated hepatic cells.

Chapter 2

2. Fungi-host interaction and TG activity in the host cells

2.1 Introduction

Human liver receives majority of blood supply from intestine through portal vein. With blood flow, it therefore gets exposed to variety of gut-related factors including microbes and their products commensal to gut. A part of the microbes are potential systemic pathogens e.g. *C. albicans* and *C. glabrata* that habitually live in a benign state [28]. In immunocompromised individuals, e.g. in haematological malignancies [30], overgrowth of these fungi with invasion of intestinal lining is observed and they access to liver through the hepatic portal vein. It's reported that these fungi play an important role in gut microbiota in the pathogenesis of ASH and NASH [32-35]. However, the detailed relationship between *Candida* infection and hepatic injury has not been addressed yet.

TG2 has been associated with liver diseases. In several experimental models, TG2 induction and activation has been shown to cause both caspase-dependent and caspase-independent apoptotic cell death [55]. Several studies showed that, in carbon

tetrachloride–induced liver injury in rats and in acute human liver, there is an increase in TG2 crosslinking activity [56]. Increase in TG2 activity was also reported in the alcohol and free fatty acid treated hepatic cells [51, 52]. The role of induced cellular TG activity in hepatic cell death during the pathogenesis of both ASH and NASH has been linked with excessive crosslinking of Sp1 and trans-inactivation of c-Met. As a result, this signalling leads to caspase-independent hepatic cell death [51, 52]. Cell death in ACR treated hepatic cellular carcinoma cells induced by increased nuclear TG2 was also reported [53, 54]. This shows the important role of TG2 activity in liver injury.

Hence, to explore the effect of pathogenic fungi in the regulation of liver cell death, several fungi species were co-incubated with human hepatic cells and the TG2 activity in the hepatic cell was investigated.

2.2 Materials and methods

2.2.1 Cell culture

Human hepatic cells, (HC) cells, (Cell Systems, Kirkland, WA, USA) were grown in CSC complete medium, prepared by mixing cell system medium 4Z0-500-R containing 10% serum with culture boost-R containing human recombinant growth factors (Cell Systems, Kirkland, WA, USA). Hepatitis B virus integrated human hepatocellular carcinoma cell line (FLC-7) [57] was kindly supplied by Dr. Matsuura (The Jikei University School of Medicine, Tokyo, Japan), and human embryonic kidney cell line (HEK 298T) were cultured in Gibco^{TM} Dulbecco's modified Eagle's medium containing low glucose, L-Glutamine, and phenol red (DMEM) and 10% fetus bovine serum (FBS, Mediatech, Herndon, VA, USA). at 37 °C in a humidified incubator with 5 % CO_2. For the experiments, cells were plated in 96-well plates (2×10^4 cells) or 6-well plates (2×10^5 cells) bearing 15 mm round coverslips and cultured overnight.

2.2.2 Fungal strains and culture conditions

All fungal strains given in **Table 2.1** were grown on yeast peptone dextrose (YPD, 1 % yeast extract, 2 % peptone, 2 % dextrose) with 2 % agar. For co-incubation with HC cells, HEK 293T, and FLC-7 cells these fungi were pre-cultured in liquid YPD

medium with shaking at 160 rpm for 8 to 16 hours at 30 °C. The pre-cultures were washed twice with phosphate-buffered saline (PBS) and adjusted to the desired cell density per plate by measuring the optical density at 600 nm (OD600) using an Ultrospec 2000 spectrophotometer (Pharmacia Biotech, Piscataway, NJ, USA).

2.2.3 Immunostaining and immunofluorescence study

After the required incubation period, the treated cells were fixed for 15 mins with 10 % formaldehyde solution. They were then washed twice with PBS solution containing 1% tween-20 (PBST). The cells were permeabilized for 15 mins with PBS containing 0.1% Triton-X and washed with PBST twice for blocking with 2.5% bovine serum albumin (BSA) for 30 mins. After washing twice with PBST, the cells were immune-stained for 60 mins with streptavidin-tetramethylrhodamine isothiocyanate (TRITC) (1:5000, Jackson ImmunoResearch Laboratories, West Grove, PA, USA) for detection of incorporated 5-BAPA as TG activity. In some cases, the cells were also treated with primary antibody against cleaved caspase-3 (Asp175) (1:400, Cell Signaling Technology, Danvers, MA, USA) for detection of cleaved caspase-3. In the cases of cells treated with a primary antibody against cleaved caspase-3, after washing twice with PBST the cells were allowed to stand for 30 mins with a secondary antibody

anti-rabbit Alexa 488 (1:200, Jackson ImmunoResearch Laboratories, Inc. West Grove, PA, USA). The cells were also treated for 15 mins with Hoechst 33258 (1:5000) (Dojindo, Japan) to stain DNA and hence, the nuclei. The samples were washed and stored with PBST when the cells were grown in 96 well plates or mounted into slide using Fluromount (Diagnostic Biosystems, Pleasanton, CA, USA) when the cells were grown in coverslips. TG activity, cleaved caspase-3, and nuclei were detected as a fluorescence signal from TRITC, Alexa 488 and H 33258 using LSM 700 laser scanning confocal microscope (Carl Zeiss, Inc., Germany). Fluorescence intensities from TRITC in both the cytoplasm and nucleus and Alexa 488 were quantitated using ZEN 2011 software.

2.2.4 Determination of *in vitro* TG activity

The overnight human cell cultures were incubated for 4 hours in DMEM supplemented with 0.2 % FBS for serum starvation and co-incubated directly or indirectly with fungi in the presence of 0.2 mM 5-(biotinamido) pentylamine (5-BAPA, Thermo Scientific, Rockford, IL, USA) and 0.1 mM aminoguanidine in serum-free DMEM–for 24 hours. For indirect co-incubation, a transwell with a 0.4 μm pore size membrane was used creating a barrier between the HC cells and the fungal cells. After

the required incubation period, the treated cells were fixed, permeabilized and blocked and immunostained against 5-BAPA and cellular activity of TG was measured based on the incorporation of 5-BAPA into the cells as described previously

2.2.5 Treatment with a TG inhibitor(s)

Some HC cell cultures co-incubated with fungal cells were treated for 24 hours with 100 μM cystamine, a broad TG inhibitor [58] or 100 μM R283, a site-directed specific TG inhibitor [37], or 50 μM ZDON (Zedira, Darmstadt, Germany), a synthetic specific inhibitor to TG2 [59] or 10 μM phenosafranin (Sigma-Aldrich Co., St. Louis, MO, USA), an inhibitor to block nuclear localization of TG2 [60].

2.2.6 Determination of TG2 mRNA level

The overnight HC cell cultures were incubated alone and co-incubated with 5×10^6 *C. albicans* cells in an insert cup with a 0.4-μm pore size. After 8 hours, total RNA was isolated from cell cultures using an RNeasy kit (Qiagen, Valencia, CA, USA). The purity of the isolated RNA was evaluated using a NanoDrop spectrophotometer (NanoDrop products, Wilmington, DE, USA). PrimeScript RT Master Mix Kit (TaKaRa Bio, Otsu, Japan) was used to synthesized cDNA, and qPCR reactions were

performed using a LightCycler® 96 (Roche Diagnostics) with SsoAdvancedTM SYBR® Green Supermix (Bio-Rad Laboratories, Hercules, CA, USA). The primers used for the qPCR reaction is given in Table 2.2. Relative amounts of TG2 mRNA were plotted after normalization against the *GAPDH* mRNA levels in the same sample.

2.2.7 Determination of cellular TG2 level

After incubation, treated HC cells were fixed, permeablized and blocked as described previously. After washed twice with PBST, the cells were immune-stained for 60 mins with mouse monoclonal antibody Transglutaminase II Ab-1 (Clone CUB 7402, 1:200) (Thermo Fisher Scientific, Fermont, CA, USA) for detection of TG2, after washing twice with PBST the cells were allowed to stand for 30 mins with a secondary antibody anti-mouse Alexa Fluor-488 (1:200, Jackson ImmunoResearch Laboratories, Inc. West Grove, PA, USA). The cells were also treated for 15 mins with H 33258 (1:5000) to stain DNA and hence, the nuclei. The samples were washed with PBST and mounted into slide using Fluromount. The fluorescence signal from Alexa 488 and H 33258 using LSM 700 laser scanning confocal microscope (Carl Zeiss, Inc., Germany). Fluorescence intensities from Alexa 488 were quantitated using ZEN 2011 software.

2.2.8 Nuclear translocation study of EGFP tagged TG2

Nuclear translocation study of EGFP tagged TG2 was performed as described previously [54]. Briefly, HC cells were seeded at 2×10^5 cells per well in a 6-well plate with 15 mm round coverslip and incubated overnight. The next day, the cells were incubated for 4 hours in phenol red free DMEM supplemented with 0.2 % FBS for serum starvation. The cells were transiently transfected with 0.8 μg of *pEGFP*-C1 or *TG2-pEGFP*-C1 [54]. Twenty-four hours after transfection, the cells were co-incubated with 5×10^6 *C. albicans* cells for 24 hours. The cells were then fixed, and nuclei were stained with H 33258 dye. The blue fluorescence from the H 33258 dye along with the green fluorescence of EGFP was monitored using LSM 700 laser scanning confocal microscope (Carl Zeiss, Inc., Germany). Numbers of the cells overexpressing EGFP or EGFP-TG2 in the nuclei of cells in a 320 μm^2 area were counted, and the percentage of cells overexpressing EGFP or EGFP-TG2 relative to the total number of cells was calculated.

2.2.9 Determination of cleaved caspase-3

The treated HC cells were incubated for a certain period and then fixed, permeablized and blocked as mentioned previously. After washing twice with PBST,

the cells were immune-stained for 60 mins with Asp175 (1:400) for detection of cleaved caspase-3. After washing twice with PBST the cells were allowed to stand for 30 mins with anti-rabbit Alexa 488 (1:200). The cells were also treated for 15 mins with H 33258 (1:5000) to stain DNA and hence, the nuclei. The samples were washed again with PBST and mounted into slide using Fluromount. The cleaved caspase-3, and nuclei were detected as a fluorescence signal from Alexa 488 and H 33258 using LSM 700 laser scanning confocal microscope. Fluorescence intensities from Alexa 488 were quantitated using ZEN 2011 software.

2.2.10 Statistical analysis

Quantitative data are shown as the mean ± SD (n = 3-6). Statistical analyses were performed using GraphPad Prism version 6.0 for Windows (GraphPad Software, San Diego, CA, USA). A *p-value <0.05 and a **p-value <0.01 were considered statistically significant.

2.3Results

2.3.1 *C. albicans* increased cellular TG activity of co-incubated HC cells

To study the relation between TG2-mediated hepatic cell injury and fungus-host interaction, at first, *C. albicans* and *S. cerevisiae* were co-incubated with HC cells and alterations in TG activities as the crosslinking function for incorporation of 5-BAPA (a TG substrate) in HC cells were evaluated. Incubation of HC cells with *C. albicans*, but not with *S. cerevisiae*, enhanced the cellular incorporation of 5-BAPA **(**Figure 2.1 **a and b**, compare rows or columns 1 with 2 and 3, respectively). Next, to study the dose- and time-dependency of the fungus-host interaction, 2 x 10^5 HC cells were treated with different dose (0.2 x 10^6 - 10 x 10^6) cells of *C. albicans* for 24 hours and 5 x 10^6 cells of *C. albicans* for 0 to 36 hours. Maximum 2.5- and 6- fold level in TG activity were observed in cytosolic and nuclear regions, respectively, in dose- and time-dependent manners, reaching a plateau after the co-incubating of 2 × 10^5 HC cells with 5 × 10^6 *C. albicans* cells for 24 hours **(Figure 2.2 a and b)**.

In order to analyze the specificity of host cells, *C. albicans* was co-incubated with other human cells, HEK 293T and FLC-7 cells. Enhanced cellular TG activity was also observed in HEK 293T and FLC-7 cells following co-incubation with *C. albicans* **(Figure 2.3 a and b)**. In addition, other three fungal species except *C. albicans*, and *S.*

cerevisiae, were used for co-incubation with HC cells. These results showed only *C. glabrata,* was able to induce cellular TG activity, especially in the nucleus **(Figure 2.4 a and b**, compare rows or columns 1 with 2, 3 and 4-respectively**)**.

2.3.2 *C. albicans* increased mRNA expression level of TG2 and accumulation of TG2 in nucleus of HC cells

To investigate the mechanism of increased cellular TG activity in two *Candida spp* co-cultured with HC cells, alteration in expression levels of TG2 mRNA and TG2 protein were examined. Co-incubation of *C. albicans* and HC cells for 8 hours induced 1.5- fold amount of TG2 mRNA in HC cells **(**Figure 2.5 compare bar 1 with 2**)**. But, there was no significant difference in level of TG2 protein at 24 hours incubation **(**Figure 2.6 **a, b and c).**

Also, HC cells were transfected with pEGFP-C1 or TG2-pEGFP-C1 to study the localization of TG2 protein in HC cells. Co-incubation of *C. albicans* and transfected HC cells for 24 hours showed 4.0- fold increase in the accumulation of the EGFP-tagged TG2 in the nucleus rather than cytoplasm **(Figure 2.7 a and b)**.

2.3.3 TG inhibitors inhibited *C. albicans* induced TG activity in HC cells

To assure that the incorporation of 5-BAPA in HC cells is due to the cellular TG activity, inhibitors of TG were used. For this, HC cells were incubated with *C. albicans* cells in presence of 100 μM cystamine (a broad TG inhibitor) [58] and 100 μM R283 (a site-directed specific TG inhibitor) [37]. Both inhibitors of TG significantly inhibited the cellular TG activity induced by *C. albicans* in HC cells **(**Figure 2.8 **a and b**, rows or columns 3 and 4, respectively**)**, suggesting that more than 60 % of incorporated 5-BAPA into the nucleus of HC cells, detected as TG activity, was induced by *C. albicans*.

2.3.4 *C. albicans* induced caspaspe-3 activation in co-incubated HC cells

To investigate whether the increased cellular TG activity can lead to the cell death in HC cells, the co-cultures were observed for cell-death-related morphological sign and activation of caspase-3. No significant decrease in the number of HC cells was observed after co-incubation for 24 hours, but the cells became smaller in size. However, further co-incubation to 48 hours resulted in caspase-3 activation and cell death **(Figure 2.9 a and b**, compare rows and columns 1 with 2 and 3**)**. Next, pharmacological approaches were employed to determine whether inhibition of TG2 activation might

affect fungus-induced HC cell death. The addition of an irreversible inhibitor ofTG2, ZDON [59], into co-incubation of HC cells and *C. albicans* significantly inhibited HC cell death as measured by caspase-3 activation in FLC-7 **(Figure 2.10 a and b)**. Moreover, a nuclear TG2 inhibitor, phenosafranin, which inhibits nuclear localization of TG2 without affecting the transaminase activity itself, [60] also significantly inhibited *C. albicans*-induced caspase-3 activation in FLC-7 cells **(Figure 2.10 a and b)**, suggesting that nuclear TG2 activity is involved in *C. albicans*-induced HC cell death.

2.4Discussion

Co-incubation of HC cells and opportunistic fungi, *C. albicans* and *C. glabrata*, causes enhancement of cellular TG activity especially at the nuclear region, which was not observed in the case of *S. cerevisiae*, *Schizosacchromyces. pombe* and other edible *Candida* species, *C. utilis*. These phenomena are assumed to be commonly shown by pathogenic *Candida spp*. Enhanced cellular TG activity was also observed in HEK 293T and FLC-7 cells following co-incubation with *C. albicans*, suggesting this TG2 induction is not specific to host-cell types. These results may go to prove with the previous finding that *C. albicans* and *C. glabrata* are the two most common fungal pathogens among fungal infection in solid organs [4, 7, 10, 11].

The cellular TG activity of HC cells (2×10^5) increased dependent of fungal cell number. The co-incubation time, then reached plateau after the co-incubating with 5×10^6 *C. albicans* cells for 24 hours. Both TG2 mRNA level in HC cells and nuclear accumulation of EGFP tagged TG2 following 8 hours incubation with *C. albicans* were also observed. These results suggested this phenomenon was induced by *C. albicans*.

In order to confirm whether 5-BAPA incorporation in HC cells is due to the TG activity, non-specific TG inhibitors, cystamine and site-directed specific TG inhibitor, R283 were used in the co-incubations. These inhibitors showed no-induction of cellular

TG activity both in cytosolic and nuclear region suggesting that more than 60 % of the incorporated 5-BAPA causes to TG activity induced by *C. albicans*. However, this result did not demonstrate involvement of TG2. Hence, to examine the role of TG2 in the fungus-host interaction, a specific inhibitor of TG2, ZDON and a nuclear TG2 inhibitor, phenosafranin, were used and level of activated caspase-3 was monitored. Increase in caspase activity in HC cells co-incubated with *C. albicans* for 48 hours was observed. In FLC-7 cells, ZDON significantly inhibited cell death following activation of caspase-3. In addition, phenosafranin also significantly inhibited *C. albicans*-induced caspase-3 activation in FLC-7 cells, suggesting that nuclear TG2 activity is involved in *C. albicans*-induced hepatic cell death. This study corroborated the reports about cell apoptosis in response to enhanced TG2 activity in neuroblastoma cell lines [61, 62] and hepatic cell lines [51, 52, 54]. It`s suppose that the fungi *C. albicans* and *C. glabrata* underwent some stresses in the closer proximity of co-incubated hepatic cells then they release of some factor(s). These cellular stresses to enhance cellular TG2 activity in HC cells were thought to lead to cell death via activation of caspase-3 pathway.

Table 2.1 List of fungi used for study of fungi-host interaction induced TG activity

Species	Strain	Genotype	References
Candida albicans	SC5314	wild type	[63]
Saccharomyces cerevisiae	IFO10150	MATa ste-VC9 ura3-52 trp1-289 his3-D1 leu2-3,112	[64]
Candida glabrata	CBS138	wild type	[65]
Candida utilis	IFO0988	wild type	[66]
Schizosacchromyces pombe	IAM04863	wild type	JCM†

† Japan Collection of Microorganisms

Table 2.2 Primers for qPCR mRNA study

Primer Name	Sequence (5'-3')
TG2 F	CCTTACGGAGTCCAACCTCA
TG2 R	CCGTCTTCTGCTCCTCAGTC
GAPDH F	GCAGGGGGGAGCCAAAAGGG
GAPDH R	TGCCAGCCCCAGCGTCAAAG

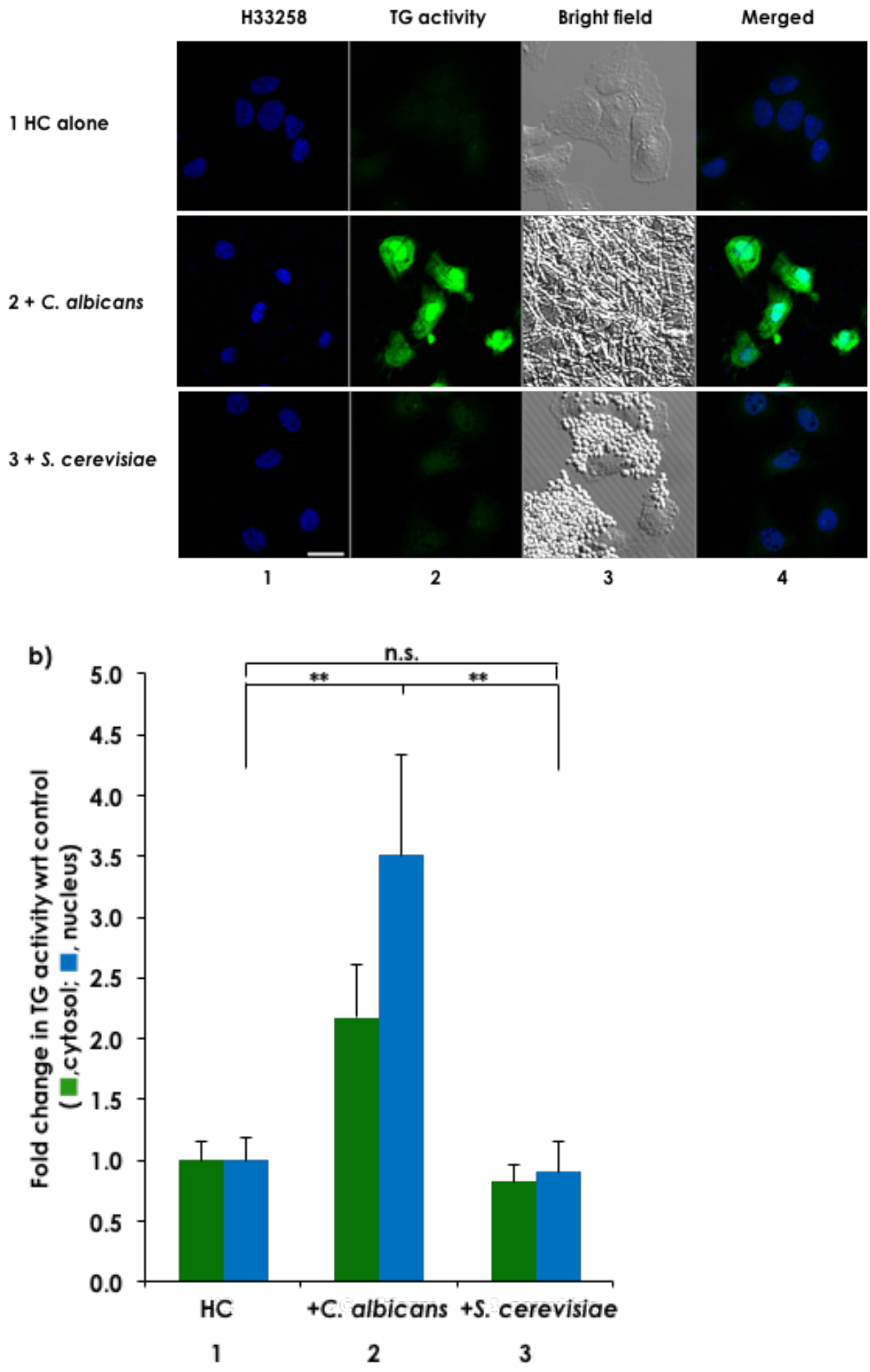

Figure 2.1 Cellular TG activity in HC cells co-cultured with *C. albicans*

HC cells were seeded at 2×10^5 cells per well in a 6-well plate and incubated overnight. After adding 5-BAPA, the cells were incubated **(a)** alone (row 1) or were co-incubated with 2.5×10^6 *C. albicans* cells (row 2) or *S. cerevisiae* cells (row 3) for 24 hours. Scale bars = 20 μm. Representative images from at least 3 fields from 3 independent experiments are shown. Fluorescence intensities from TRITC in both the cytoplasm and nucleus of panel **(b)** were quantitated using ZEN 2011 software, and relative TG activity levels in both locations are presented in bar graphs, with the levels from HC cells incubated (mean ± SD, n = 3). Asterisks represent statistical significance.

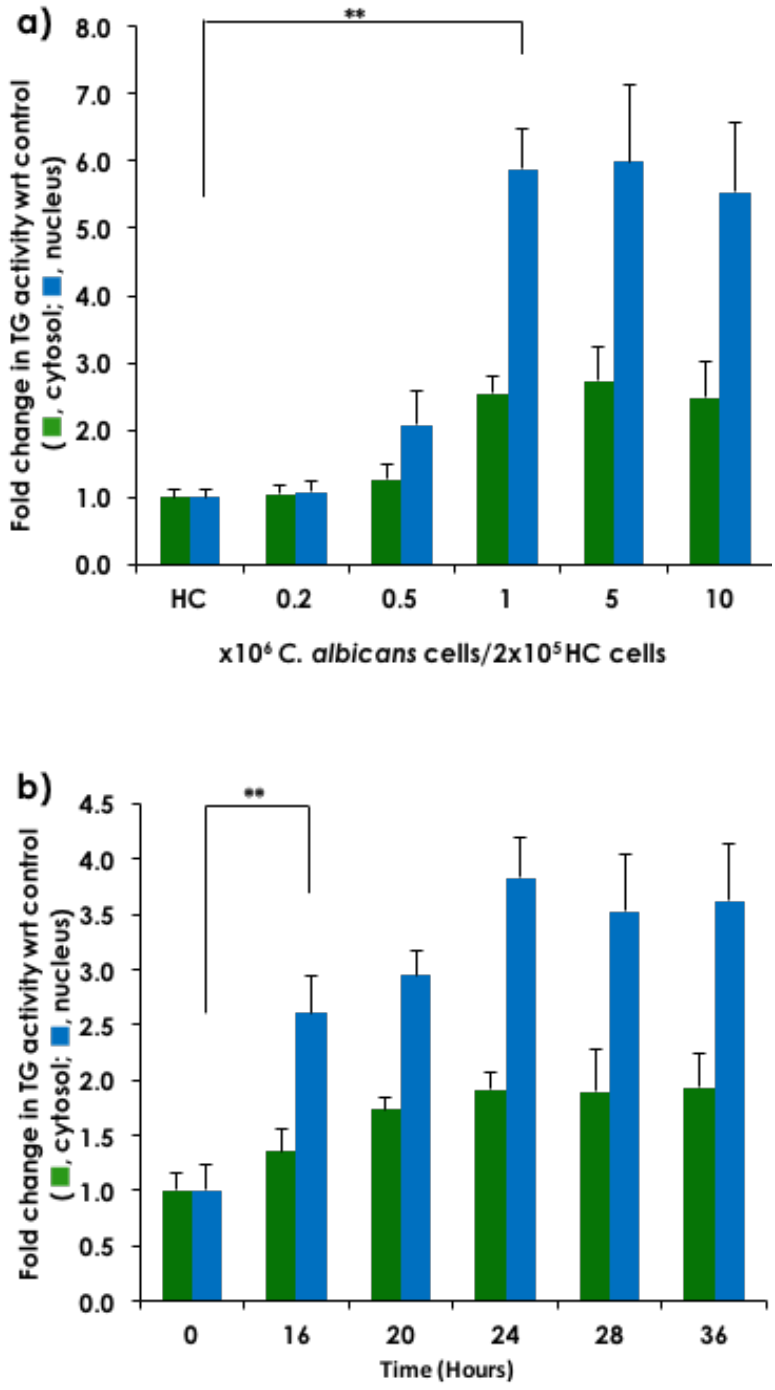

Figure 2.2 *C. albicans'* treatment- dose/time related cellular TG activity in HC cells

HC cells were seeded at 2×10^5 cells per well in a 6-well plate and incubated overnight. After adding 5-BAPA, the cells were incubated **(a)** with different doses of *C. albicans*

cells for 24 hours; **(b)** with 5 × 10^6 *C. albicans* cells for 0-36 hours. Fluorescence intensities from TRITC in both the cytoplasm and nucleus of panels **(a, b)** were quantitated using ZEN 2011 software, and relative TG activity levels in both locations are presented in bar graphs, with the levels from HC cells incubated alone **(**panels **a)** or at time 0 **(b)** used as the controls (mean ± SD, n = 3). Asterisks represent statistical significance.

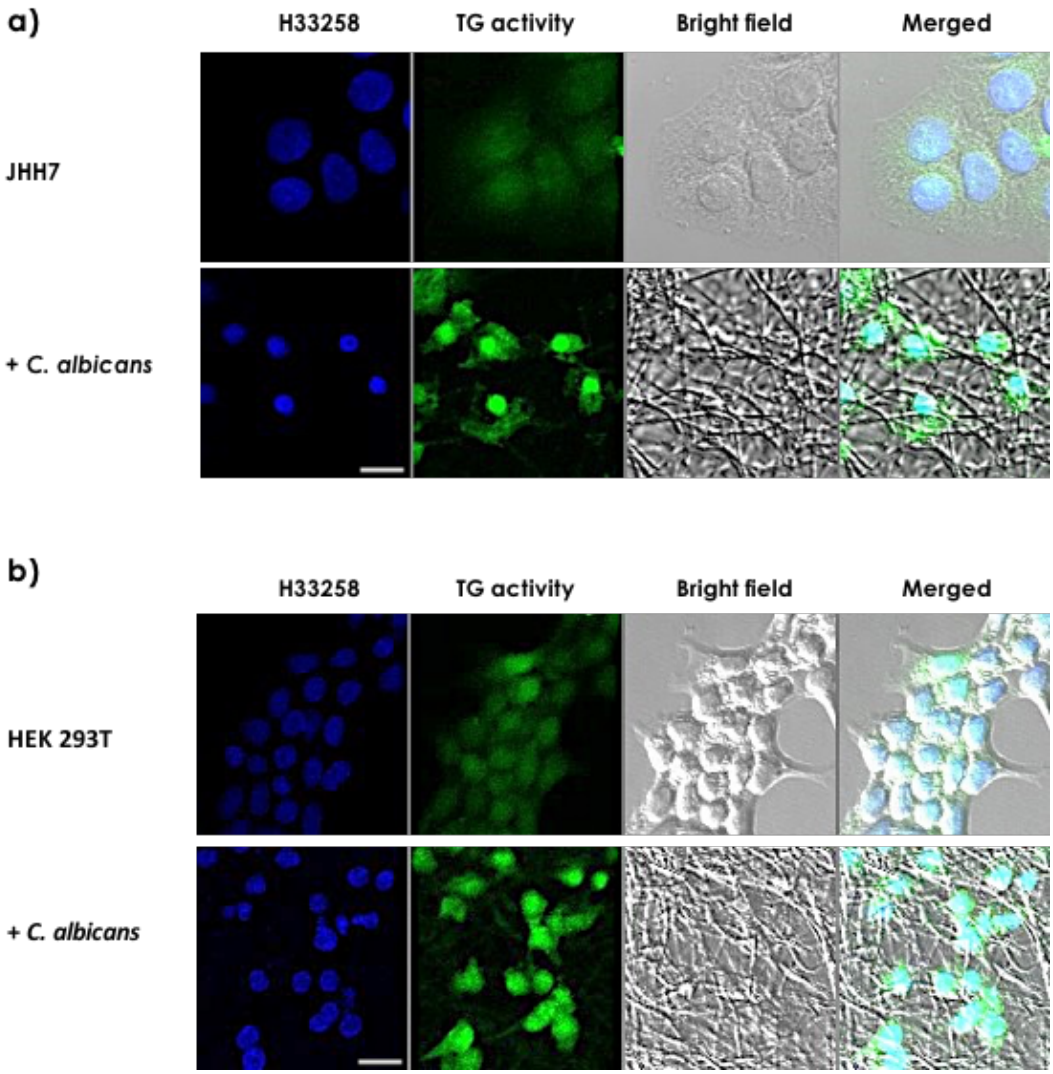

Figure 2.3 Cellular TG activity in *C. albicans* co-cultured FLC-7 and HEK 293T cells

a) FLC-7 cells and **b)** HEK 293T cells were seeded at 2×10^5 cells per well in a 6-well plate and incubated overnight. After adding 5-BAPA, the cells were incubated alone (row 1) or were co-incubated with 2.5×10^6 *C. albicans* cells (row 2) for next

twenty-four hours. Scale bars = 20 μm. Representative images from at least 3 fields from single experiments are shown.

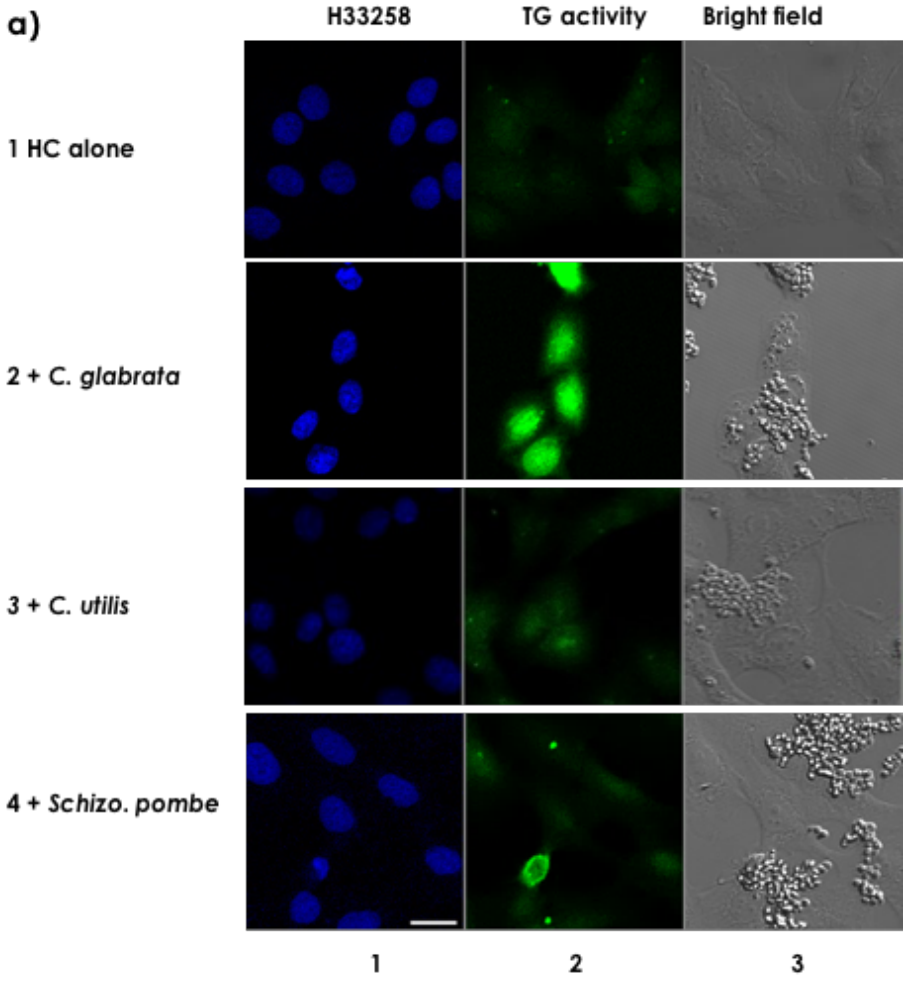
a)
H33258
TG activity
Bright field
1 HC alone
2 + C. glabrata
3 + C. utilis
4 + Schizo. pombe
1
2
3

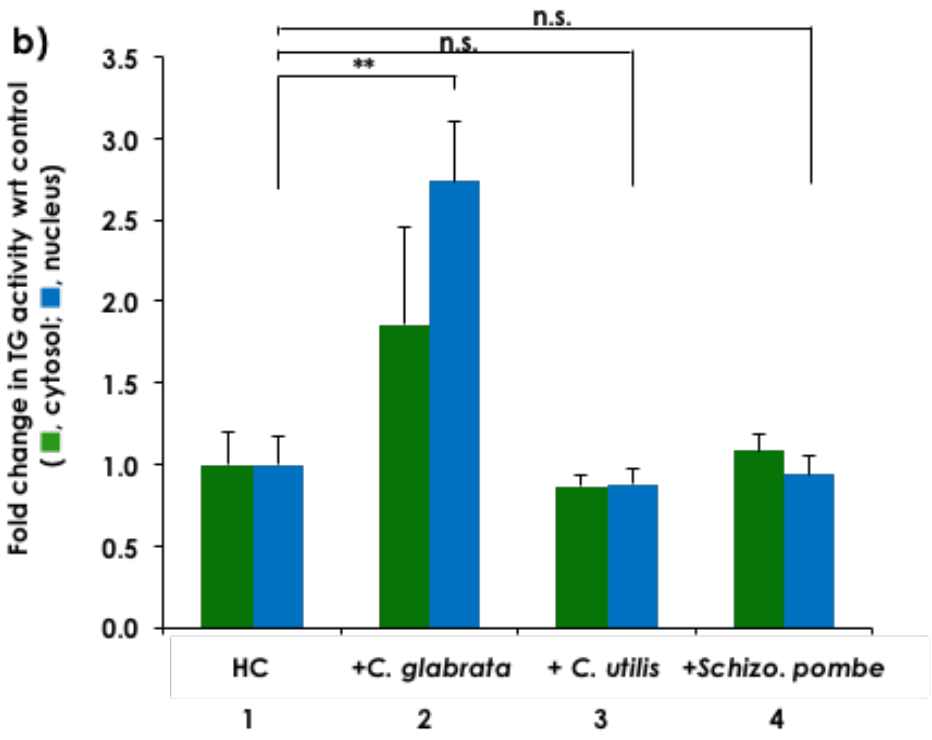

Figure 2.4 Cellular TG activity in non-pathogenic/ pathogenic fungi treated HC cells

HC cells were seeded at 2 × 10^5 cells per well in a 6-well plate and incubated overnight. The cells were incubated **(a)** alone (row 1) or were co-incubated with living 5 × 10^6 *C. glabrata* (row 2), *C. utilis* (row 3) and *Schizo. pombe* cells (row 4) for 24 hours. Scale bars = 20 µm. Representative images from at least 3 fields from 3 independent experiments are shown**. b)** Fluorescence intensities from TRITC in both the cytoplasm and nucleus of panels were quantitated using ZEN 2011 software, and relative TG activity levels in both locations are presented in bar graphs, with the levels from HC

cells incubated alone used as the controls (mean ± SD, n = 3). Asterisks represent statistical significance.

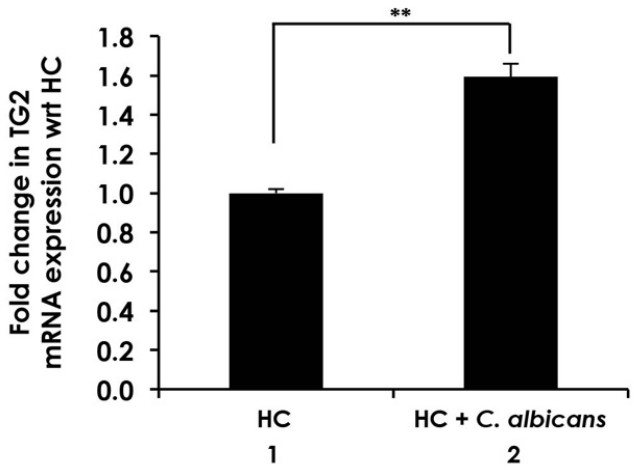

Figure 2.5 TG2 mRNA expression level in *C. albicans* co-cultured HC cells

HC cells were seeded at 2×10^5 cells per well in a 6-well plate and incubated overnight as previously described. Cells were incubated alone (sample 1) or co-incubated with 5×10^6 *C. albicans* cells in an insert cup with a 0.4-μm pore size (sample 2). After 8 hours, RNA was isolated from cell cultures. Relative amounts of TG2 mRNA were plotted after normalization against the GAPDH mRNA levels in the same sample.

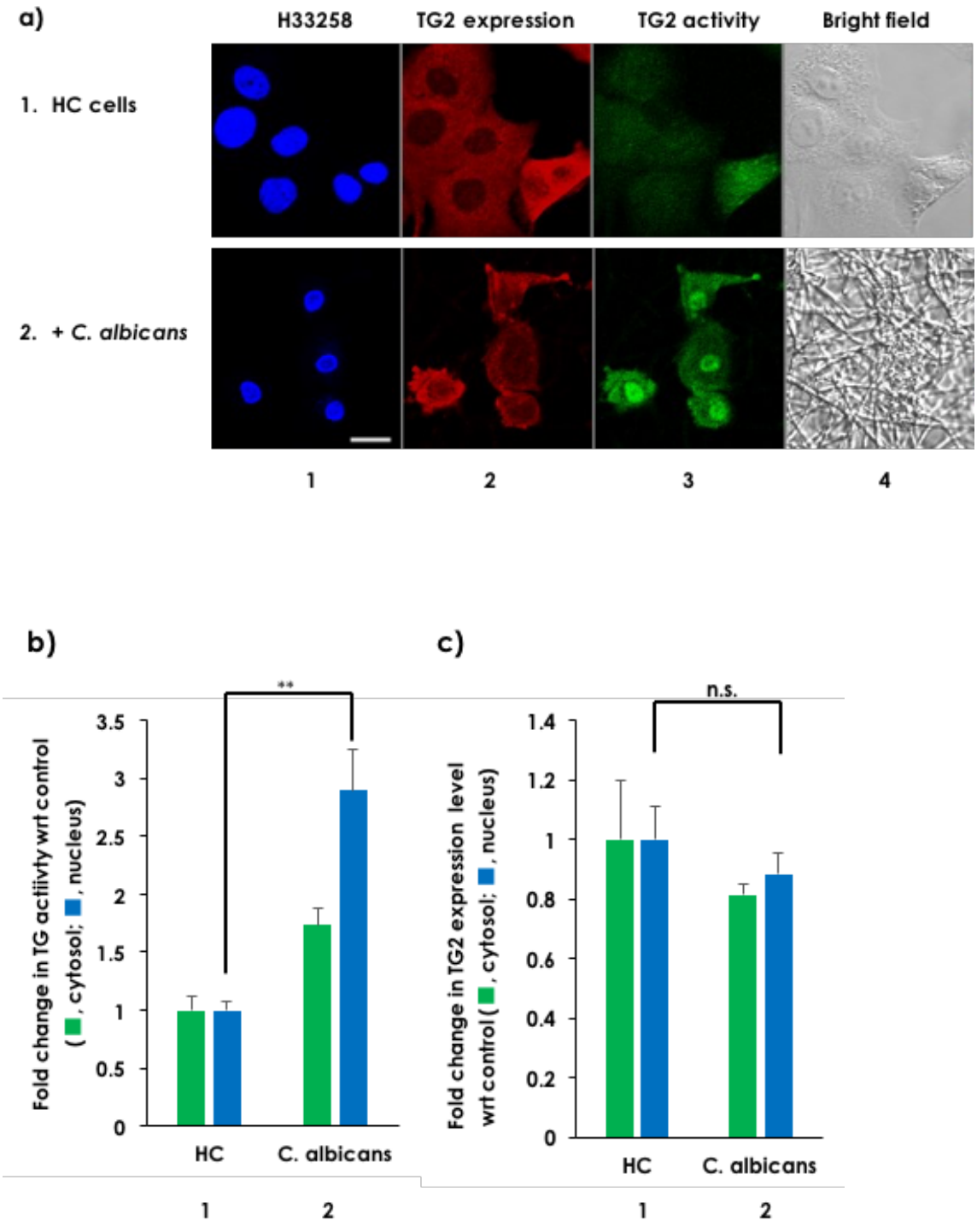

Figure 2.6 TG2 protein expression level in *C. albicans* co-cultured HC cells

HC cells were seeded at 2×10^5 cells per well in a 6-well plate and incubated overnight as previously described. **a)** HC cells were incubated (row 1) or co-incubated with 5×10^6 *C. albicans* (row 2). HC cells were stained with H 33258 (column 1), CUB7402 antibody against TG2 (column 2) and TRITC-conjugated Streptavidin (column 3). Bright field images of the cells (column 4). Scale bars = 20 μm. Fluorescence intensity from **b)** TRITC as TG activity and **c)** Alexa 488- CUB7402 as TG2 expression in cytosol and nucleus were quantitated using ZEN 2011 software and relative levels in both locations are presented in bar graphs with the levels from HC cells incubated alone used as the controls.

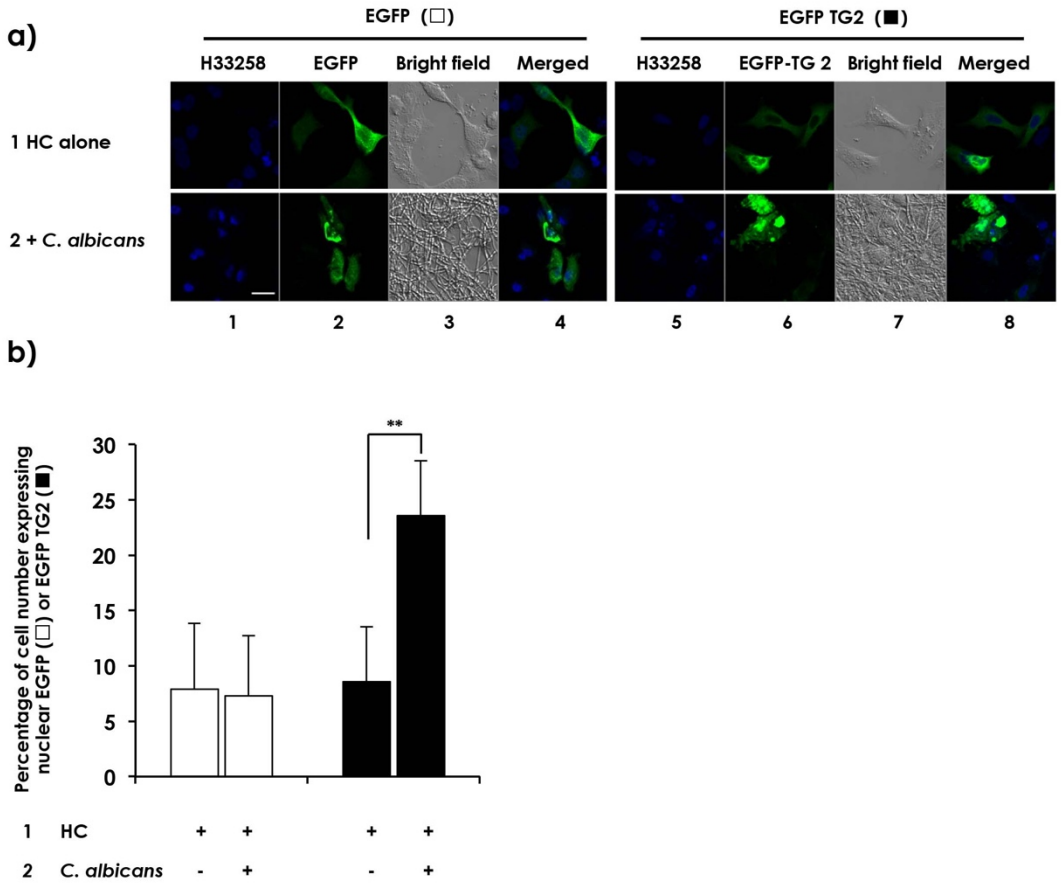

Figure 2.7 EGFP-TG2 accumulation in nucleus of *C. albicans* co-cultured HC cells

HC cells were seeded at 2×10^5 cells per well in a 6-well plate and incubated overnight as previously described. **(a)** Cells were transiently transfected with 0.8 µg of pEGFP-C1 or TG2-pEGFP-C1. Twenty-four hours after transfection, the cells were co-incubated with 5×10^6 *C. albicans* cells for another 24 hours. The cells were then fixed, stained with H 33258 dye and observed with a confocal microscope. The blue fluorescence from the H 33258 (columns 1 and 5) along with the green fluorescence of EGFP (columns 2 and 6) were monitored. Images taken under bright field (columns 3 and 7) and merged images are also shown (columns 4 and 8). Scale bars = 20 µm.

Representative images from at least 3 fields from a single experiment are presented. **(b)** Numbers of the cells overexpressing EGFP or EGFP-TG2 in the nuclei of cells in a 320 μm^2 area were counted, and the percentage of cells overexpressing EGFP or EGFP-TG2 relative to the total number of cells was calculated and plotted.

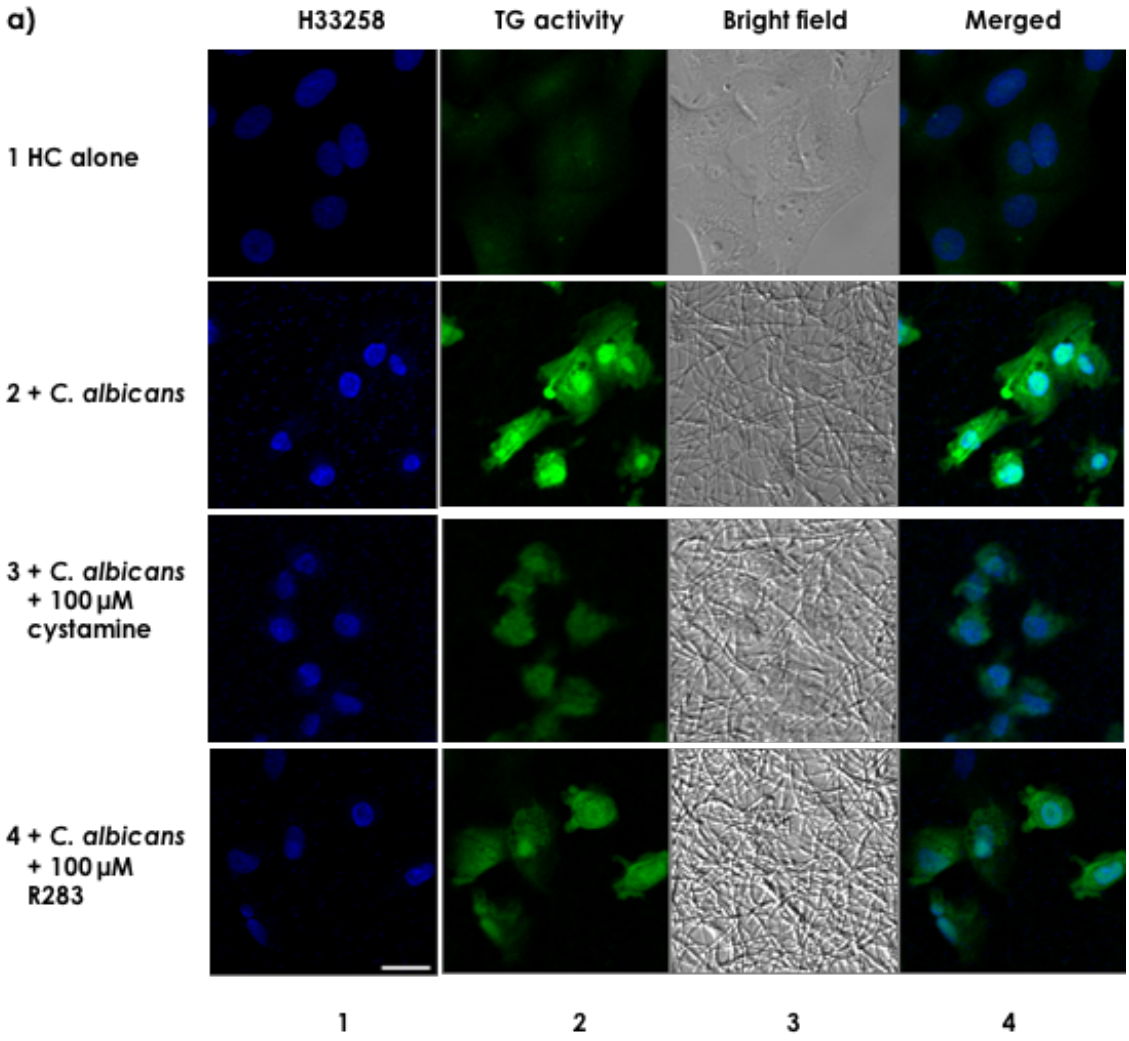
a)
H33258
TG activity
Bright field
Merged
1 HC alone
2 + C. albicans
3 + C. albicans + 100 µM cystamine
4 + C. albicans + 100 µM R283
1
2
3
4

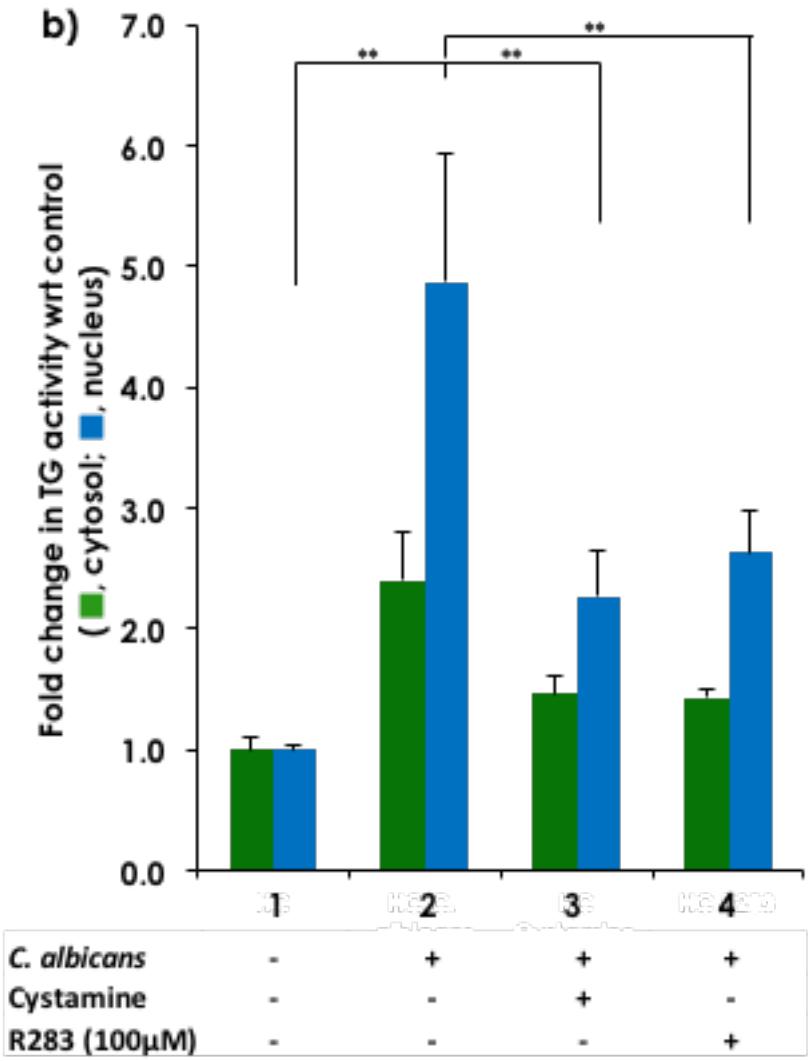

Figure 2.8 Cellular TG activity in *C. albicans* and TG inhibitors treated HC cells

HC cells were seeded at 2×10^5 cells per well in a 6-iwell plate and incubated overnight. After adding 5-BAPA, the cells were incubated **(a)** with 5×10^6 *C. albicans* cells in the absence (row 2) and presence of 100 µM of TG2 inhibitors, cystamine (row 3) or R283 (row 4) for 24 hours; Scale bars = 20 µm. Representative images from at least 3 fields from 3 independent experiments are shown for**.** Fluorescence intensities from TRITC in

both the cytoplasm and nucleus of panels **(b)** were quantitated using ZEN 2011 software, and relative TG activity levels in both locations are presented in bar graphs, with the levels from HC cells incubated alone used as the controls (mean ± SD, n = 3). Asterisks represent statistical significance.

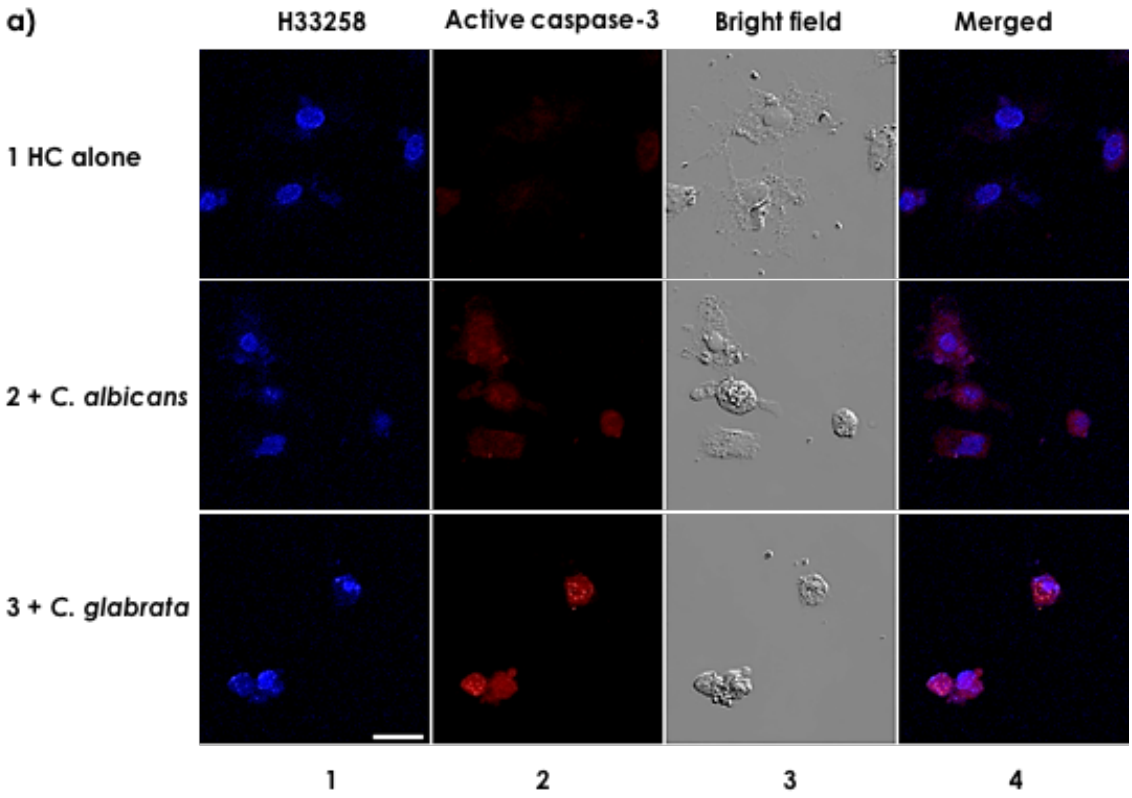
a)
H33258
Active caspase-3
Bright field
Merged
1 HC alone
2 + C. albicans
3 + C. glabrata
1
2
3
4

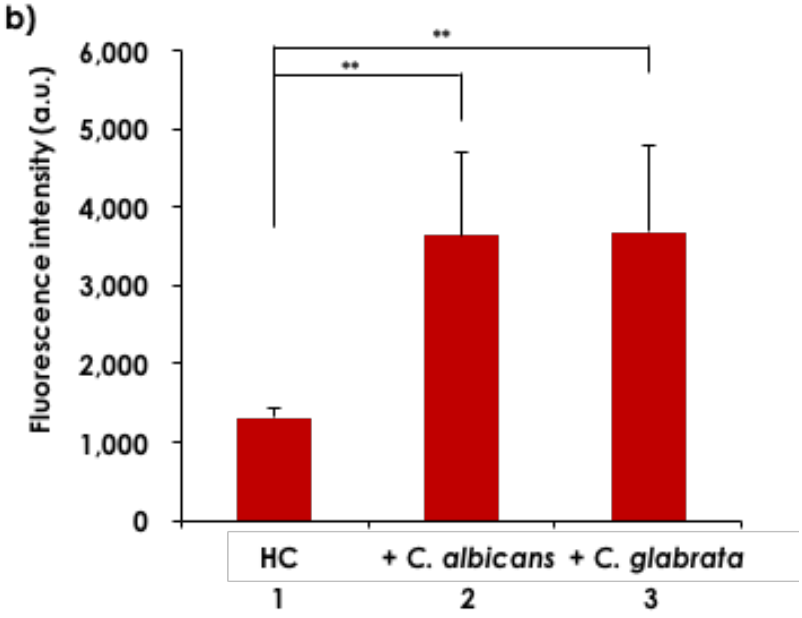
b)
Fluorescence intensity (a.u.)
6,000
5,000
4,000
3,000
2,000
1,000
0
**
**
HC
+ C. albicans
+ C. glabrata
1
2
3

Figure 2.9 Caspase-3 activity in pathogenic *Candida* species co-cultured HC cells.

HC cells were seeded at 2×10^5 cells per well in a 6-well plate and incubated overnight. The cells were incubated **(a)** alone (row 1) or were co-incubated with either 5×10^6 *C. albicans* cells (row 2) or the same number of *C. glabrata* cells (row 3) in an insert cup with a 0.4-μm pore size for 48 hours. Scale bars = 20 μm. Representative images from at least 3 fields from a single experiment are shown**.** Fluorescence intensities from Alexa 488 signal from panel **(b)** were quantitated using ZEN 2011 software, and caspase-3 activity are presented in bar graphs after subtraction of background intensities (mean ± SD, n = 3). Asterisks represent statistical significance.

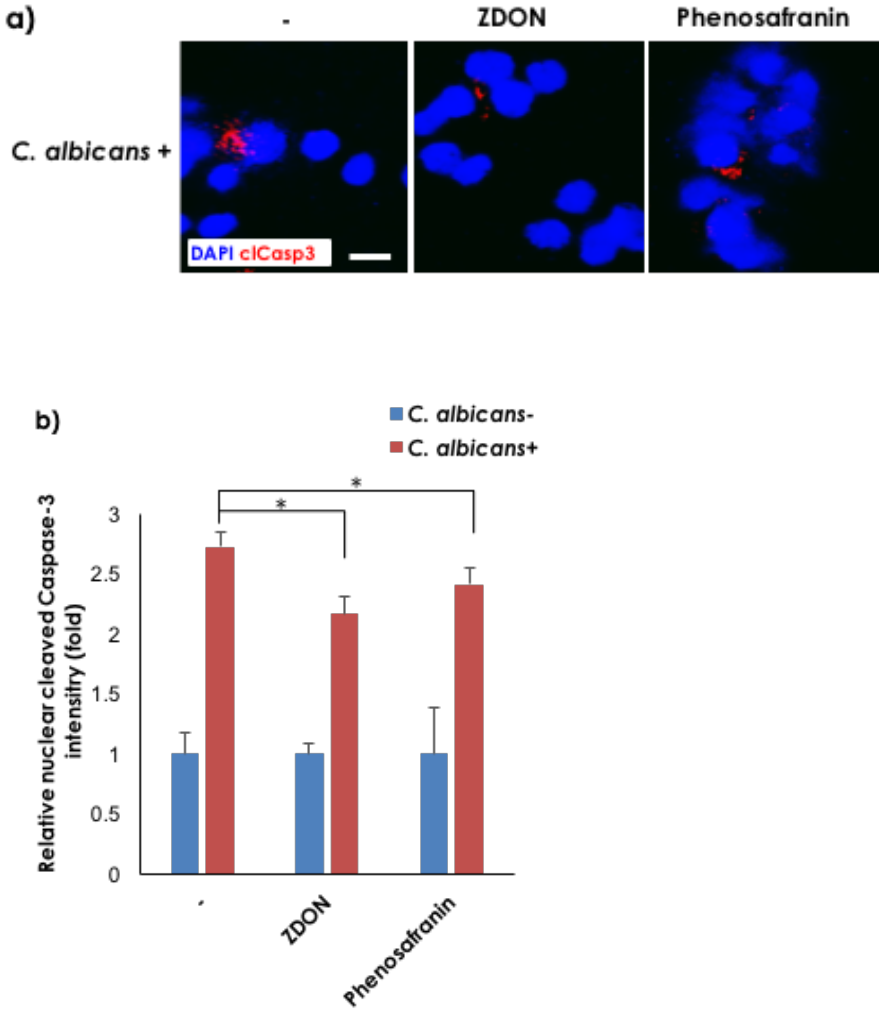

Figure 2.10 Cellular TG activity in *C. albicans* and TG2 inhibitors treated HC cells

FLC-7 cells were seeded at 1 × 10^4 cells per well in a 96-well plate and incubated overnight as previously described. Cells were incubated alone or co-incubated with 5 × 10^7 *C. albicans* cells in the absence and presence of 50 μM ZDON or 10 μM phenosafranin for 24 hours. Cell death was determined by fluorescence intensity with ImageXpress^{MICRO} High Content Screening System (Molecular Devices, Sunnyvale, CA, USA) and morphological analysis was performed using MetaXpress Image Analysis

software (Molecular Devices). **(a)** Representative fluorescence images from three biological samples of two independent experiments. Scale bar = 20 μm. DAPI: blue; cleaved caspase-3 (clCasp3): red. **(b)** The representative quantitative data of nuclear cleaved caspase-3 intensity were presented as mean ± SD from three biological samples of two independent experiments.

Chapter 3

3. Screening and identification of a fungal factor(s) responsible for the induction of TG activity of hepatic cells following co-incubation with fungus

3.1 Introduction

A large number of virulent factors have been identified and implicated in the pathogenesis of *C. albicans.* These factors depend on genetic, morphological and biochemical flexibilities of the strain of *C. albicans* and the host [14, 67]. Some major factors include morphological alteration, biofilm formation, adhesion, secreted hydrolytic enzymes, and reactive oxygen species (ROS). These properties as virulent factors are discussed in detail hereafter.

3.1.1 Polymorphism of *C. albicans*

C. albicans is a polymorphic fungus and the transition between yeast and hyphal forms is one of polymorphic phenomena of this fungus[68]. Both of cell forms and the ability to change between these forms have been considered important for pathogenicity. Several environmental factors such as pH, temperature, carbon dioxide levels, starvation,

and quorum-sensing molecules (farnesol, tyrosol, and dodecanol) induce change in morphology of the fungi into yeast, pseudohyphae, and hyphae [67, 68]. The yeast form is believed to be important in dissemination of *C. albicans* [69-71] and the hyphal form is believed to be more invasive and contributes to host tissue damage. However, the role of pseudohyphae is not well understood [70]. Hyphae formation is associated with the expression of subset of genes responsible for virulence of *C. albicans*. Such genes include hyphal wall protein Hwp1 [72], agglutinin-like sequence protein Als3 [73], secreted aspartic proteases Sap4, Sap5 and Sap6 [74] and the hypha associated proteins Ece1,Hyr1 and Hypha specific G1 cyclin-related protein Hgc1 [17, 75]. Mutants failing to form hyphae *in vitro* are shown to be associated with attenuation of virulence [17, 75].

Likewise, *GUP1* gene, identified in *S. cerevisiae* has been associated with glycerol uptake, and a series of complex and extensive cellular processes, such as cell wall maintenance, lipid composition, cytoskeleton orientation and secretory/endocytic pathway [76]. In *C. albicans*, Gup1 strongly interferes in hyphae formation along with other different virulent traits such as adhesion, invasion and biofilm formation. *Cagup1*Δ null mutant showed a weakened ability to form hyphae with decreased

adhesion, invasion and biofilm formation, which ultimately resulted in decreased virulence [77].

3.1.2 Adhesion, biofilm formation and invasion.

Biofilms are structured microbial communities attached to the surface of host cells. Capacity to form biofilm is thought to be another virulence trait of *C. albicans*. Biofilm formation is a sequential process which incorporates adherence of yeast cells to the substrate, proliferation of these yeast cells, formation of hypha cells in the upper part of the biofilm, accumulation of extracellular matrix materials and, finally, dispersion of yeast cells from the biofilm complex [73].

Adhesion is an essential step for colonization and establishment of *Candida* infections. The molecules responsible for adhesion are called adhesins, some of which include Als1-Als7 and Asl9. Of the eight Als proteins, the hypha-associated adhesin Als3 is important for adhesion [73]. Another important adhesin of *C. albicans* is Hwp1, a hypha-associated GPI-linked protein. Hwp1 serves as a substrate for mammalian TG and this reaction may covalently link *C. albicans* hyphae to host cells [72].

Likewise, *C. albicans* also has special sets of glycosylphosphatidylinositol (GPI)-linked cell surface glycoproteins (Eap1, Iff4 and Ecm33), non-covalent

wall-associated proteins (Mp65, a putative β-glucanase, and Phr1, a β-1,3 glucanosyl transferase), cell-surface associated proteases (Sap9 and Sap10) and the integrin-like surface protein Int1 also found to contribute to adhesion of this fungal cells [73]. Moreover, previous studies have shown that importance of cell wall protein such as a mannoprotein from the surface of *C. albicans* was identified as the β-1, 3-glucosyltransferase, Bgl2p in the delivery and accumulation of glucans for building of extracellular biofilm matrix and virulence [78]. Defects in biofilm formation were observed in bgl2Δ/Δ mutant making it less pathogenic [9].

3.1.3 Secretion of hydrolytic enzymes

The secreted hydrolytic enzymes expressed by *C. albicans* are classified into three different families; proteases, phospholipases and lipases. The family of secreted aspartic proteases (Saps) comprises ten members, Sap1-8 are secreted and released to the surrounding medium, whereas Sap9 and Sap10 remain bound to the cell surface [74]. The family of phospholipases consists of four different classes (A, B, C and D) [79]. Only the five members of class B (PLB1–5) are extracellular and may contribute to pathogenicity via disruption of host membranes [80, 81]. The third family, the lipases, consists of 10 members (LIP1–10) [82]. A lip8Δ/Δ mutant had reduced virulence in a

mouse model of systemic infection, supporting a role for these extracellular hydrolases in *C. albicans* pathogenicity [83].

It has been previously reported that *C. albicans* can secrete 70 kDa lipase extracellularly induced cytotoxicity and promoted the deposition of lipid droplets in the cytoplasm of macrophages and hepatocytes and induce injury and steatosis in immune and parenchymal cells [84]. The lipase-induced injury is protected by Ebelactone B, a serine esterase inhibitor known to inhibit fungal lipases [85].

3.1.4 Reactive oxygen species (ROS)

ROS is a collective term that describes the chemical species formed upon incomplete reduction of oxygen and includes the superoxide anion (O_2^-), H_2O_2 and the ·OH **(**Table 3.1**)**. ROS has long been known to free radicals of molecular oxygen. Recently, different roles of ROS in cell signaling including apoptosis and the signaling cascades has been demonstrated. The mitochondria in different morphological forms of *C. albicans* are capable of generating and extracellular releasing of ROS, which is the highest during formation of hyphae[86]. This indicates an important role of ROS in tissue invasion and infection, pathogenicity of *Candida* [86]. Subsequently, intracellular ROS have been reported to activate TG2 in different cell types of human [87-89].

In order to gain an insight for factors responsible for the enhancement of cellular TG activity, especially at the nuclear region of hepatic cells, different *C. albicans* mutants with defects in transition of yeast to hypha formation, adhesion on the host cells, biofilm formation and fungal lipase inhibitor are used. Similarly, segregation of HC cells to prevent contact with fungi cells directly was achieved by use of transwell system to verify the requirement of direct interaction. Additionally, another important fitness attribute of *C. albicans*, ability to secrete ROS was also studied.

3.2 Materials and methods

3.2.1 Cell culture

HC cells were maintained and prepared for experiments as described previously in Chapter 2.

3.2.2 Fungal strains and culture conditions

Fungal strains given in Table 3.2 were grown on YPD agar medium. For co-incubation with HC cells, these strains were pre-cultured in liquid YPD medium with shaking at 160 rpm for 8 to 16 hours at 30 °C. The pre-cultures were washed twice with PBS and adjusted to the desired cell density in plates by measuring the OD at 600 nm using an Ultrospec 2000 spectrophotometer.

3.2.3 Determination of *in vitro* TG activity

The cellular activity of TG2 was measured based on the incorporation of 0.2 mM 5-BAPA into the cells incubated in the presence of 0.1 mM aminoguanidine as described previously in Chapter 2.

3.2.4 Preparation of heat-killed *C. albicans* cells

C. albicans cells were routinely grown in YPD agar medium. These cells were pre-cultured in liquid YPD medium with shaking at 160 rpm for 8 to 16 hours at 30 °C. The pre-cultures were washed twice with PBS and adjusted to the cell density of 5 X 10^9 cells/mL by measuring the OD at 600 nm using an Ultrospec 2000 spectrophotometer. For heat killing, these cells were heated in DMEM at 70 °C for 20 minutes. The viability of heat-killed cells was confirmed after observing loss of the growth following incubation of the heated cells on YPD agar plates for 48 hours at 30 °C.

3.2.5 Preparation of hyphae form of *C. albicans.*

For the preparation of hyphae form of *C. albicans* cells, 5×10^6 cells of the overnight cultured cells were washed twice with PBS and grown in DMEM at 37 °C for 16 hours. The hyphae form of the *C. albicans* cells were confirmed after observing at 20X magnification under the light microscope.

3.2.6 Determination of inhibitory effect of Ebelactone B on cellular TG activity induced by *C. albicans*

Overnight culture of HC cells was plated and cultured in a 6-well plate bearing round coverslips at 37 °C in a humidified incubator with 5 % CO_2. The next day, these cells were incubated for 4 hours in DMEM supplemented with 0.2 % FBS for serum starvation. These HC cells were co-incubated with fungi in the presence and/or absence of 5 μM Ebelactone B. The cellular activity of TG2 was then measured based on the incorporation of 0.2 mM 5-BAPA into the cells as described previously.

3.2.7 Determination of inhibitory effect of Terbinafine on cellular TG activity induced by *C. albicans*

Overnight culture of HC cells was plated and cultured in a 6-well plate bearing round coverslips at 37 °C in a humidified incubator with 5 % CO_2. The next day, these cells were incubated for 4 hours in DMEM supplemented with 0.2 % FBS for serum starvation. These HC cells were co-incubated with fungi in the presence and/or absence of 1 μg/mL Terbinafine [90] found to be non-toxic to HC cells and *C. albicans*. The cellular activity of TG2 was then measured based on the incorporation of 0.2 mM 5-BAPA into the cells as described previously.

3.2.8 Determination of the effect of H_2O_2 on cellular TG activity of HC cells

HC cell line was cultured in CS-C complete medium at 37 °C in a humidified incubator with 5 % CO_2. For the experiments, $2x10^5$ cells was prepared and plated in 6-well plates bearing round coverslips. The next day, HC cells were incubated for 4 hours in DMEM supplemented with 0.2 % FBS for serum starvation. These cells were co-incubated with 100, 200, 500 and 1000 μM H_2O_2 in the presence of 5-BAPA in serum-free DMEM. The cellular activity of TG2 in HC cells was then measured based on the incorporation of 0.2 mM 5-BAPA as described previously.

3.2.9 Statistical analysis

Quantitative data are shown as the mean ± SD (n = 3-6). Statistical analyses were performed using GraphPad Prism version 6.0 for Windows (GraphPad Software, San Diego, CA, USA). A *p-value <0.05 and a **p-value <0.01 were considered statistically significant.

3.3 Results

3.3.1 Heat killed *C. albicans* lost the ability to increase TG activity in HC cells.

Heat-killed *C. albicans* were co-incubated with HC cells to see whether viable cells of *C. albicans* are necessary for the induction of TG activity in HC cells. Following co-incubation with heat-killed *C. albicans* cells, in contrast to living cells, the heat-killed *C. albicans* lost the capacity to increase TG activity in HC cells **(**Figure 3.1 **a and b**, compare rows or columns 1 with 3**)**. This indicated that living cells of *C. albicans* is required for the induction of increased TG activity of HC cells.

3.3.2 Both hyphae and yeast forms of *C. albicans* induced cellular TG2 activity.

Being a polymorphic fungus, *C. albicans* has the capacity to grow in a diversity of morphological forms, ranging from unicellular yeast form to pseudohyphae and later true hyphae. The effect of yeast and hyphae forms in the induction of TG activity of HC cells was studied. In this experiment, *Cagup1*, *C. albicans* mutant with delay in hyphae development [77] was used. HC cells co-incubated with the *Cagup1* cultured at 37 °C in DMEM medium enhanced cellular TG activity, especially at the nuclear region of HC cells was observed **(Figure 3.2 a and b**, compare row 1 with 2 and 3**)**. This result

suggested that the activation of TG in HC cells was independent of the morphological forms of *C. albicans*.

3.3.3 *C. albicans and C. glabrata* having defects in biofilm formation and adhesiveness induced cellular TG2 activity.

To understand the effect of another factors of *C. albicans,* morphology-dependent *Cabgl2* mutant [9], and *Caecm33* mutant defected in biofilm matrix formation and adhesive properties, and *C. glabrata* mutants *Cgbmt1* with altered cell wall structure were studied. Similarly, a mutant of *C. albicans*, *Cafad2* [91] defected in synthesis of linolenic acid previously shown to increase nuclear TG2 activity [51] was also studied. Following co-incubation of these mutants with HC cells, no attenuation in enhancement of cellular TG activity both at the cytosol and nuclear region was observed **(Figure 3.3)**., This suggested that these virulent traits of the pathogenic *Candida* species were not responsible for this phenomenon.

3.3.4 Ebelactone B did not decrease *C. albicans* induced cellular TG2 activity.

Considering lipase activity, a determinant factor in the pathogenicity of many bacteria and fungi, effect of Ebelactone B [84, 85, 92], a lipase inhibitor, was studied in

HC cells co-cultured with *C. albicans*. Inhibition effect of Ebelactone B in HC cells co-incubated with *C. albicans* showed no significant decrease in cellular TG activity (**Figure 3.4 a and b**), signifying that increase in TG activity was not related to the secreted virulent lipases.

3.3.5 A Small and unstable soluble factor(s) of fungus is required for induction of TG activity in HC cells.

After understanding the requirement of viable activity(s) of fungus, the requisite of direct contact of the body of fungal cell or nature of responsible mediator produced from fungi was investigated. For this HC cells were co-incubated with fungi plated in insert cup of pore size 0.4 μm creating a barrier between HC cells and *C. albicans*, and HC cells and *C. glabrata*. Enhanced nuclear TG2 activity was observed in the HC cells incubated with *C. albicans* **(**Figure 3.5 **a** and **b** compare rows or columns 1 with 2**)** as well as *C. glabrata* **(**Figure 3.5 **a** and **b** compare rows or columns 1 with 3**)** in insert cup. This suggests that direct contact between HC cells and fungus is not essential. I next, reduced the pore size of insert cup. HC cells were co-cultured with *C. albicans*, plated in a dialysis membrane (cutoff <10 kDa). Increased cellular TG activity was observed in HC cells treated with the fungus in transwell plates **(**Figure 3.5 **c and d**, compare rows

or columns 1 with 2**).** On the other hand, when I cultured HC cells with the *C. albicans*-cultured media, the increase in TG activity was not observed **(**Figure 3.5 **c and d**, compare rows or columns 1 with 3). This finding suggested that small molecule, which might be very unstable in nature, was secreted into the culture medium by *C. albicans* and caused increased cellular TG activity.

3.3.6 ROS might be small and unstable factor candidates.

To explore the factor(s) smaller in size and unstable, HC cells were co-incubated with *C. albicans* in the presence or absence of 1 μg/mL Terbinafine, an antifungal drug that inhibits ergosterol biosynthesis and acts as a free radical interceptor [90, 93]. At this concentration, terbinafine was non-toxic to both HC cells and *C. albicans*. Significant reduction in cellular TG activity in HC cells co-cultured with *C. albicans* in the presence of Terbinafine was observed after co-incubation for 24 hours **(Figure 3.6 a and b,** compare row or bar 2 with 3**)** and 36 hours **(Figure 3.6 c and d,** compare row or bar 2 with 3**)**.

Next, to screen whether the small, soluble and unstable factor(s) is ROS, HC cells were cultured with H_2O_2 (a kind of ROS) at different doses ranging from 100-1000 μM. Nearly, four-fold increase in nuclear TG activity was observed at dose at 1000 μM

of H_2O_2 **(**Figure 3.7 **a and b**, compare row or bar 1 with 6**)**. The result suggested that H_2O_2 and may be other ROS are responsible factors candidates for the enhancement of cellular TG activity in HC cells.

3.4 Discussion

The ability of *C. albicans* to infect a diverse host niche is supported by a variety of virulence factors. A number of attributes, such as morphological transition, adhesion, invasion and biofilm formation are considered to be virulent. For identification of the responsible factor(s) for induction of cellular TG activity, several virulence factors of *C. albicans* were evaluated. Lost in capacity to increase in cellular TG activity by heat-killed *C. albicans* signified the need of cell viability of these fungi for induction of TG activity in HC cells. On the other hand, HC cells co-cultured with hyphae form of *C. albicans* and yeast form of *C. albicans* (*Cagup1* mutant) showed enhancement of TG activity both in the cytosol and nuclear regions. These results suggested that the activation of cellular TG activity does not rely upon the morphological forms of *C. albicans*.

Mature biofilm formation of *C. albicans* cells on the biotic and abiotic surfaces involves a sequential process ranging from adhesion, aggregation , transition to hyphal form and secreting extra-matrix leads to the resistance to different antimicrobial agents and host immune system [94, 95]. Here, co-incubation of HC cells and *C. albicans* mutant, defect in adhesion and biofilm formation such *Caecm33* (extracellular matrix mutant having defect in biofilm formation), *Cabgl2* (1,3-beta-glucosyltransferase

mutants having defect in cell-wall and growth), *Cafad2* (fatty acid desaturase mutant having defect in production of poly-unsaturated fatty acid) did not show attenuation in fungus-induced enhancement of cellular TG activity. Furthermore, HC cells co-cultured with *C. albicans* cells in the presence of 5 μM Ebelactone B also could not show an inhibitory effect on cellular TG activity. Combining all the results, an increase in TG activity requires viable fungal cells and is not related to the virulence factors such as polymorphic change, biofilm formation, hyphae development, structural component of fungal cell wall and lipase, secreted by *C. albicans*.

After clarifying the requirement of viability of fungus, it was checked that whether direct contact of the fungi is necessary or not. Then HC cells were co-cultured with *C. albicans* plated in insert cup with pore size 0.4 μm, dialysis membrane (≤ 10kDa) and *C. albicans* cultured medium. Enhancement of TG activity in HC cells was observed even separated from *C. albicans* by using insert cup and dialysis membrane (≤ 10kDa). But the TG activity was not induced by addition of *C. albicans*-cultured medium. These results suggested that small molecule(s) which might be very unstable in nature, was secreted into the co-culture medium by *C. albicans* and caused increased cellular TG activity in HC cells.

Further to investigate whether the induction factor(s) is ROS or not, effect of Terbinafine was evaluated in fungus-HC co-culture. Terbinafine is an antifungal drug that inhibits biosynthesis of ergosterol of fungi and also a free radical interceptor [90, 93]. Even though no significant increase in TG activity was observed in HC cells co-incubated with *C. albicans* for 24 hours, a slight decrease in the growth of *C. albicans* was also observed, suggesting that inhibition of TG activity might be a consequence of decreased fungal cells. Hence, to overcome this condition, HC cells were incubated with *C. albicans* for 36 hours. The result showed no significant increase in cellular TG activity even in presence of sufficient number of *C. albicans* cells, suggesting that this no increase in TG activity is the resultant inhibitory action on ROS by Terbinafine [90]. Additionally, exogenously added H_2O_2 also showed significant enhancement of TG activity in HC cells. Combining the resultant effect of Terbinafine and H_2O_2, it could be speculated that ROS might be one of responsible factors for the enhancement of cellular TG activity in HC cells following co-incubation with *C. albicans*.

Table 3.1 Different ROS

Free radical	Representation
Superoxide	$O_2^{\cdot -}$
Hydroxyl radical	·OH
Hydrogen peroxide	H_2O_2
Peroxyl radical	RCOO·
Organic hydroperoxide	RCOOH
Singlet oxygen	$^1O_2$
Ozone	O_3

Table 3.2 List of fungi used for identification of TG activity inducing fungal factor(s)

Species	Strain	Genotype	References
C. albicans	SC5314	wild type	[63]
S. cerevisiae	IFO10150	MATa ste-VC9 ura3-52 trp1-289 his3-D1 leu2-3,112	[64]
C. glabrata	CBS138	wild type	[65]
Ca GUP1		*Cagup1*, a derivate of SC5315	[77]
Ca BGL2		*Cabgl2*, a derivate of SC5315	[9]
Ca ECM33		*Caecm33*, a derivate of SC5315	
Ca FAD2		*Cafad2*, a derivate of SC5315	[91]
Cg BMT1		*Cgbmt1*, a derivate of CBS138	From Professor. Chibana
Cg NOX1	CAGL0K05863g	*Cgnox1*, a derivate of CBS138	From Professor. Chibana

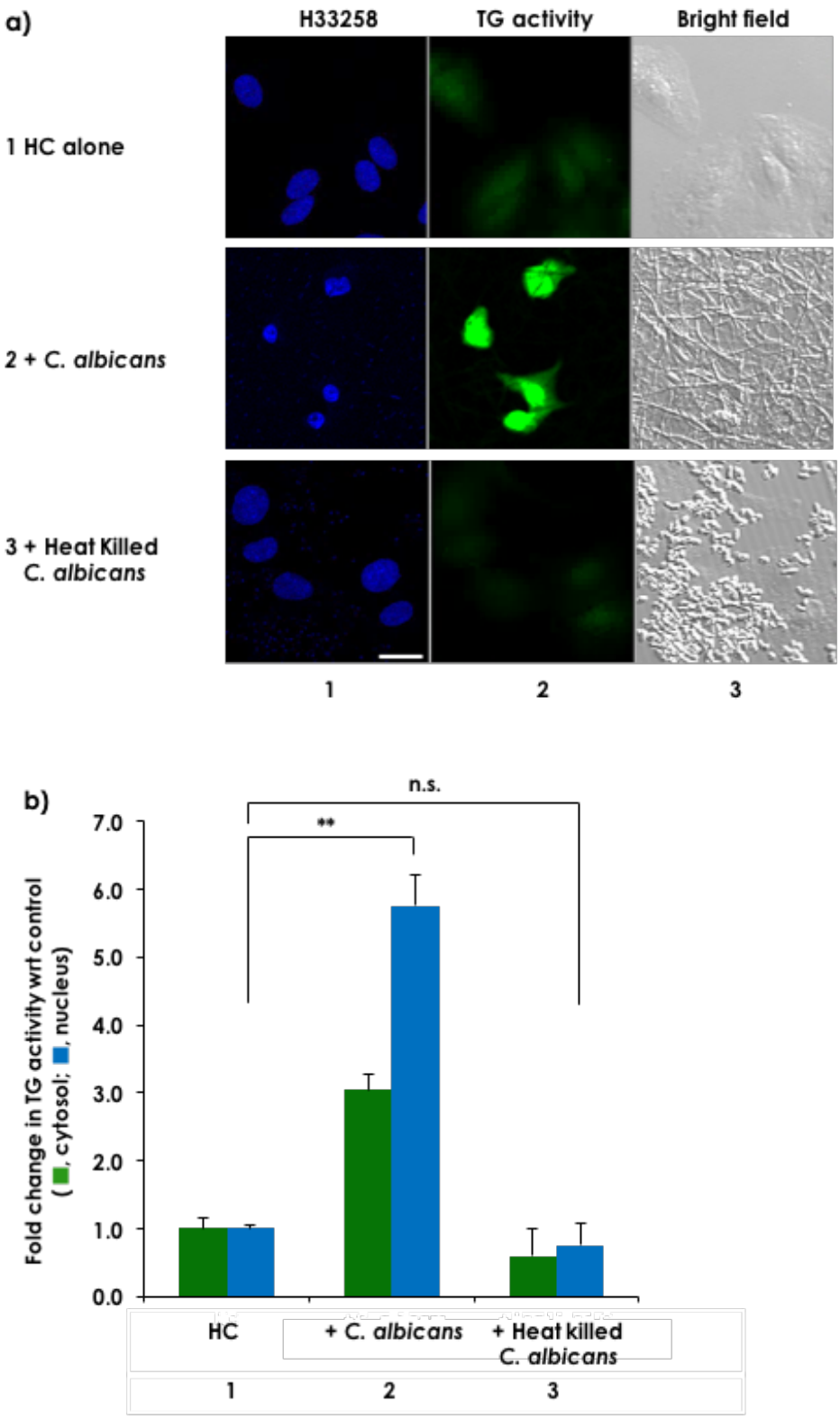

Figure 3.1 Cellular TG activity in HC cells treated with heat-killed *C. albicans*

HC cells were seeded at 2×10^5 cells per well in a 6-well plate and incubated overnight. After adding 5-BAPA, the cells were incubated **(a)** alone (row 1) or were co-incubated with living 5×10^6 (row 2) or heat-killed 5×10^9 (row 3) *C. albicans* cells for 24 hours; Scale bars = 20 μm. Representative images from at least 3 fields from 3 independent experiments are shown**.** Fluorescence intensities from TRITC in both the cytoplasm and nucleus of panels **(b)** were quantitated using ZEN 2011 software, and relative TG activity levels in both locations are presented in bar graphs, with the levels from HC cells incubated alone used as the controls (mean ± SD, n = 3). Asterisks represent statistical significance.

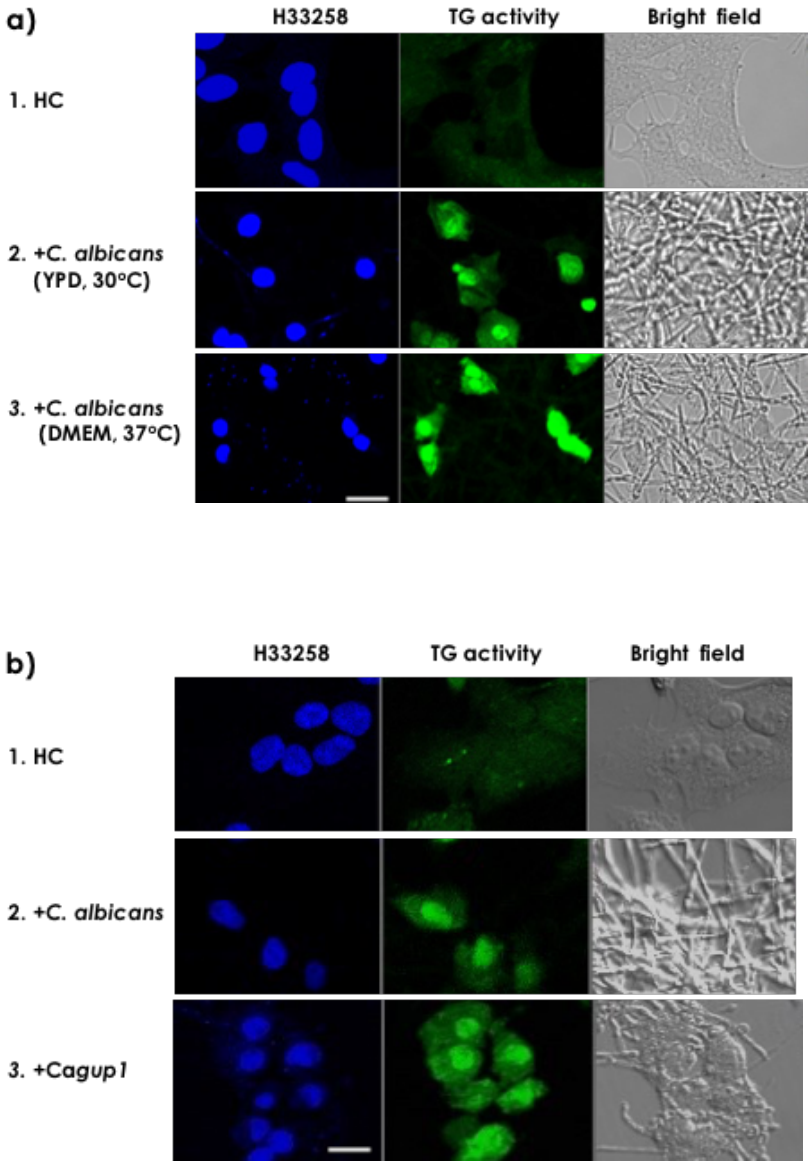

Figure 3.2 Cellular TG activity in yeast- and hyphae- *C. albicans* treated HC cells

HC cells were seeded at 2×10^5 cells per well in a 6-well plate and incubated overnight. After adding 5-BAPA, **(a)** the cells were incubated alone (row 1) or co-incubated with living 5×10^6 *C. albicans* cells grown in YPD media at 30°C (row 2) or 5×10^6 *C. albicans* cells grown in DMEM media at 37°C (row 2) for 24 hours. **b)** the cells were

incubated alone (row 1) or were co-incubated with living 5×10^6 *C. albicans* cells (row 2) or 5×10^6 *Cagup1* cells, a mutant of *C. albicans* (row 3) for 24 hours. Scale bars = 20 μm. Representative images from at least 3 fields from single experiments are shown.

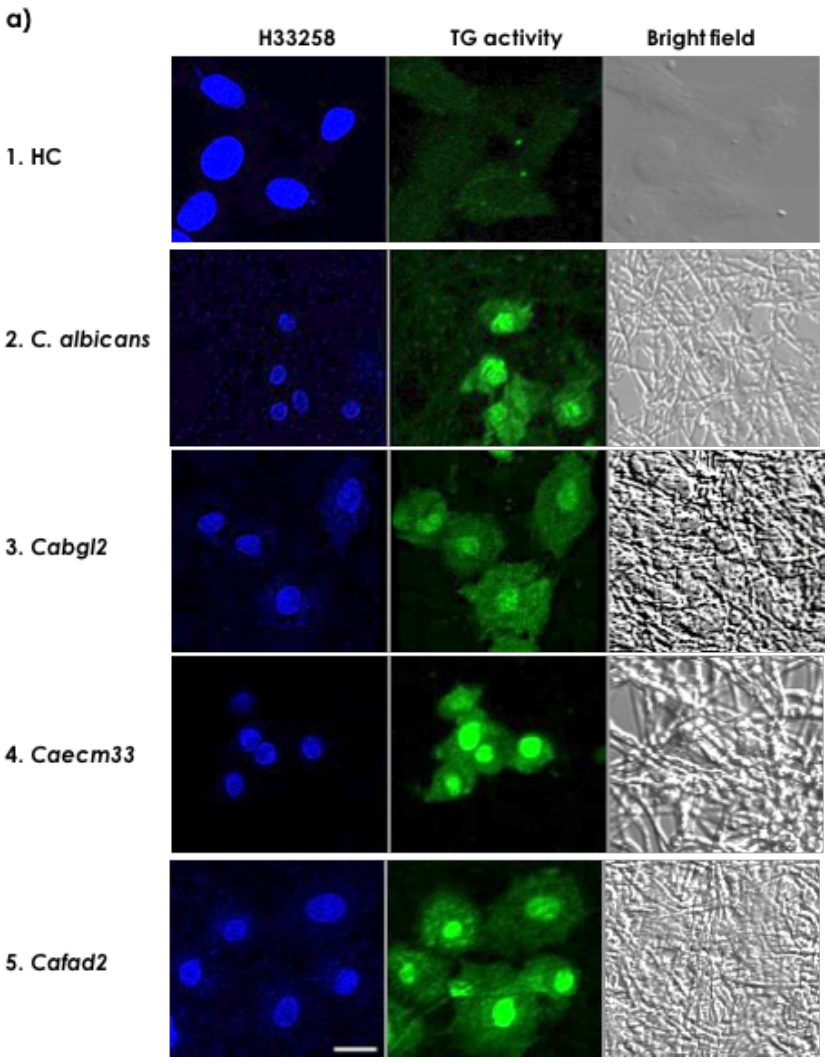
a)
H33258
TG activity
Bright field
1. HC
2. C. albicans
3. Cabgl2
4. Caecm33
5. Cafad2

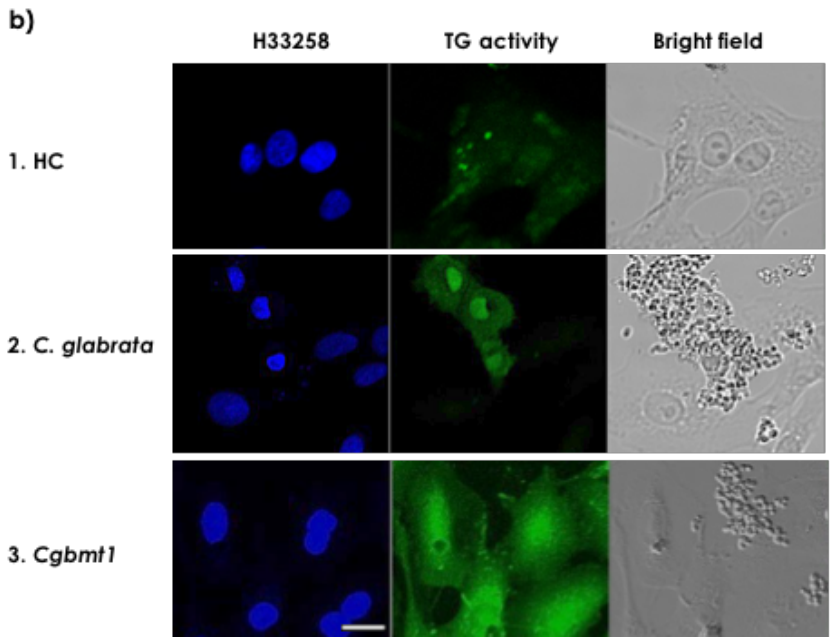

Figure 3.3 Cellular TG activity in *C. albicans*/ *C. glabrata* mutant treated HC cells

HC cells were seeded at 2 × 10^5 cells per well in a 6-well plate and incubated overnight. After adding 5-BAPA, **(a)** the cells were incubated alone (row 1) co-incubated with 5 × 10^6 cells of *C. albicans* (row 2), *Cabgl2* (row 3) *Caecm33* (row 4) and *Cafad2* (row 5) (**b)** the cells were incubated alone (row 1) or were co-incubated with 5 × 10^6 cells of *C. glabrata* (row 2) and *Cgbmt1* (row3) for 24 hours. Scale bars = 20 µm. Representative images from at least 3 fields from 2 experiments are shown**.**

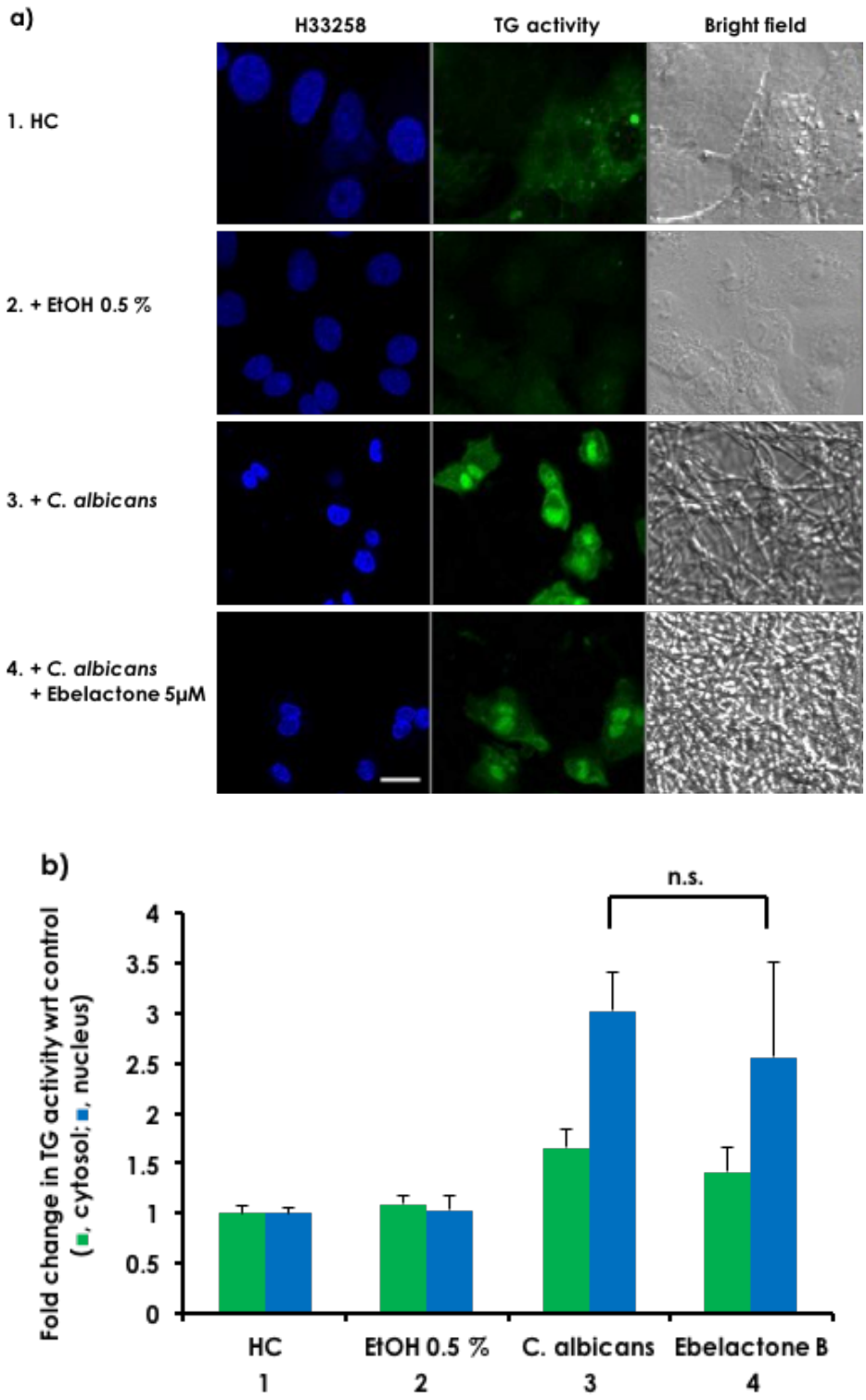

Figure 3.4 Cellular TG activity in *C. albicans* and a lipase inhibitor treated HC cells

HC cells were seeded at 2×10^5 cells per well in a 6-well plate and incubated overnight. After adding 5-BAPA, **(a)** the cells were incubated alone (row 1), or treated with 0.5% EtOH (row 2), or were co-incubated with living 5×10^6 *C. albicans* cells (row 3) or were co-incubated with living 5×10^6 *C. albicans* cells in presence 5μM Ebelactone (row 4) for 24 hours. Scale bars = 20 μm. Representative images from at least 3 fields from 2 independent experiments are shown**. (b)**Fluorescence intensities from TRITC in both the cytoplasm and nucleus of panels **(a)** were quantitated using ZEN 2011 software, and relative TG activity levels in both locations are presented in bar graphs, with the levels from HC cells incubated alone used as the controls (mean ± SD, n = 3). n.s. represent statistical non-significance.

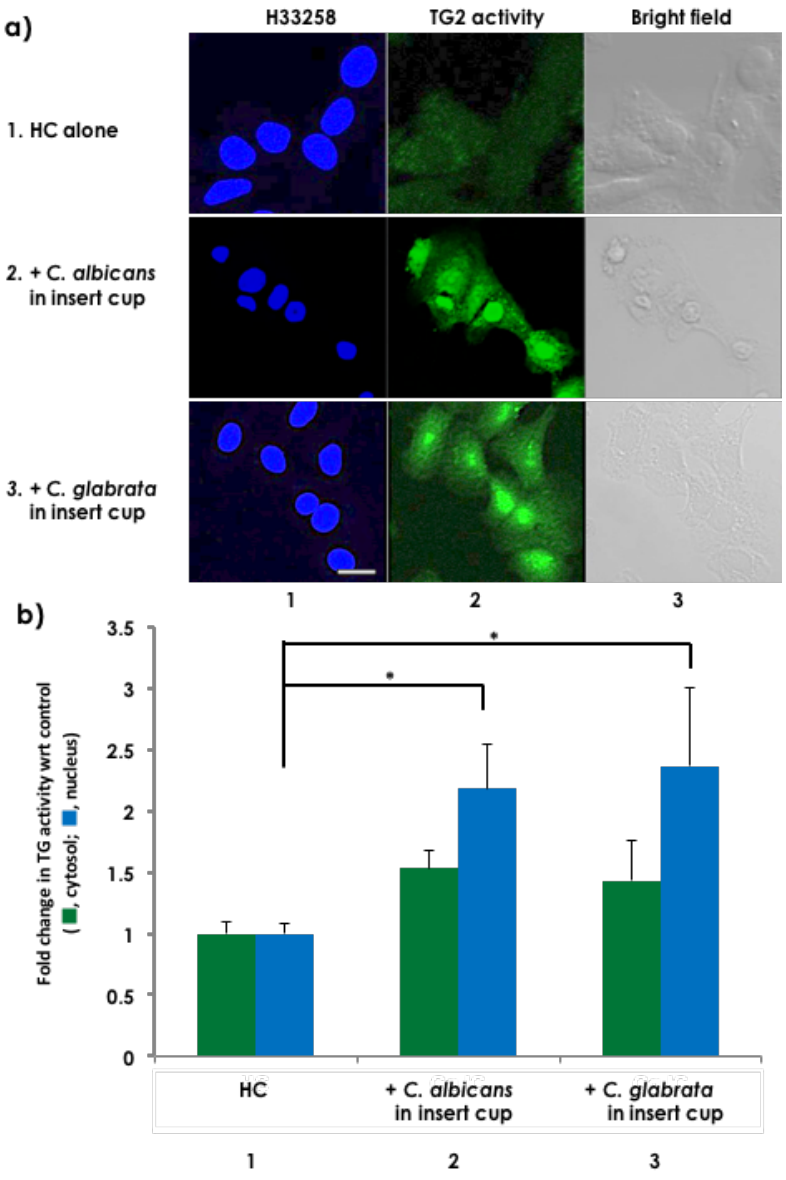
a)
H33258
TG2 activity
Bright field
1. HC alone
2. + C. albicans in insert cup
3. + C. glabrata in insert cup
1
2
3
b)
Fold change in TG activity wrt control (■, cytosol; ■, nucleus)
3.5
3
2.5
2
1.5
1
0.5
0
*
*
HC
+ C. albicans in insert cup
+ C. glabrata in insert cup
1
2
3

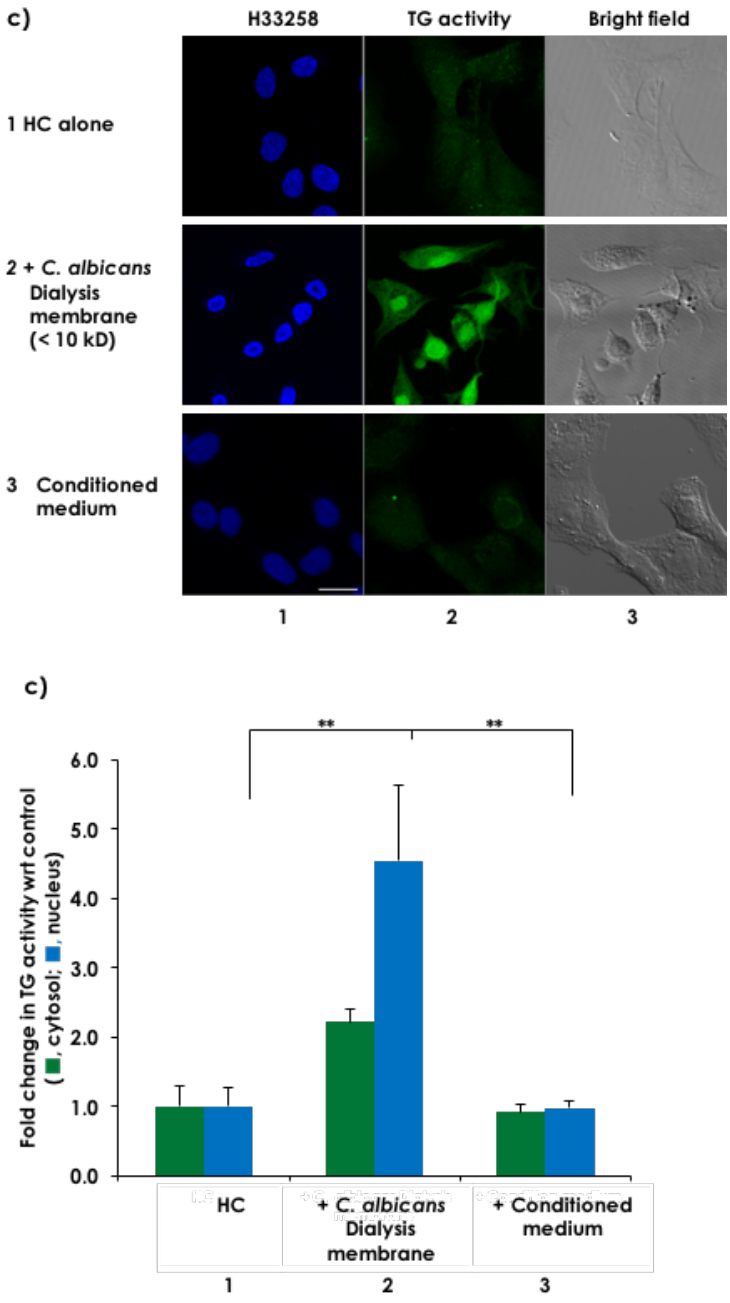

Figure 3.5 Nature of the factors (s) responsible for enhanced cellular TG activity in HC cells co-cultured with *C. albicans*

HC cells were seeded at 2 × 10^5 cells per well on a 35-mm glass-based dish or round cover slips plated in 6-well plates and were incubated overnight. **(a)** After adding

5-BAPA, the cells were incubated alone (row 1) or were co-incubated with 5×10^6 *C. albicans* cells grown insert cup (row 2) or were co-incubated with 5×10^6 *C. glabrata* cells grown insert cup (row 3). **(c)** After adding 5-BAPA, the cells were incubated alone (row 1) or were co-incubated with 5×10^6 *C. albicans* cells grown in a transwell separated by a dialysis membrane (row 2) and cultured with the conditioned medium prepared from *C. albicans* cultures following a 24-hour incubation (row 3). Scale bars = 20 μm. Representative images from at least 3 fields from 3 independent experiments are shown. Fluorescence intensities of TRITC in both the cytoplasm and nucleus were quantitated using ZEN 2011 software, and the relative TG activity levels in both locations of panels **(a)** are presented in bar graphs in **(b)** and of panel **(c)** in bar graphs in **(d)** with the levels from the HC cells incubated alone as the control (mean ± SD, n = 3). Asterisks represent statistical significance.

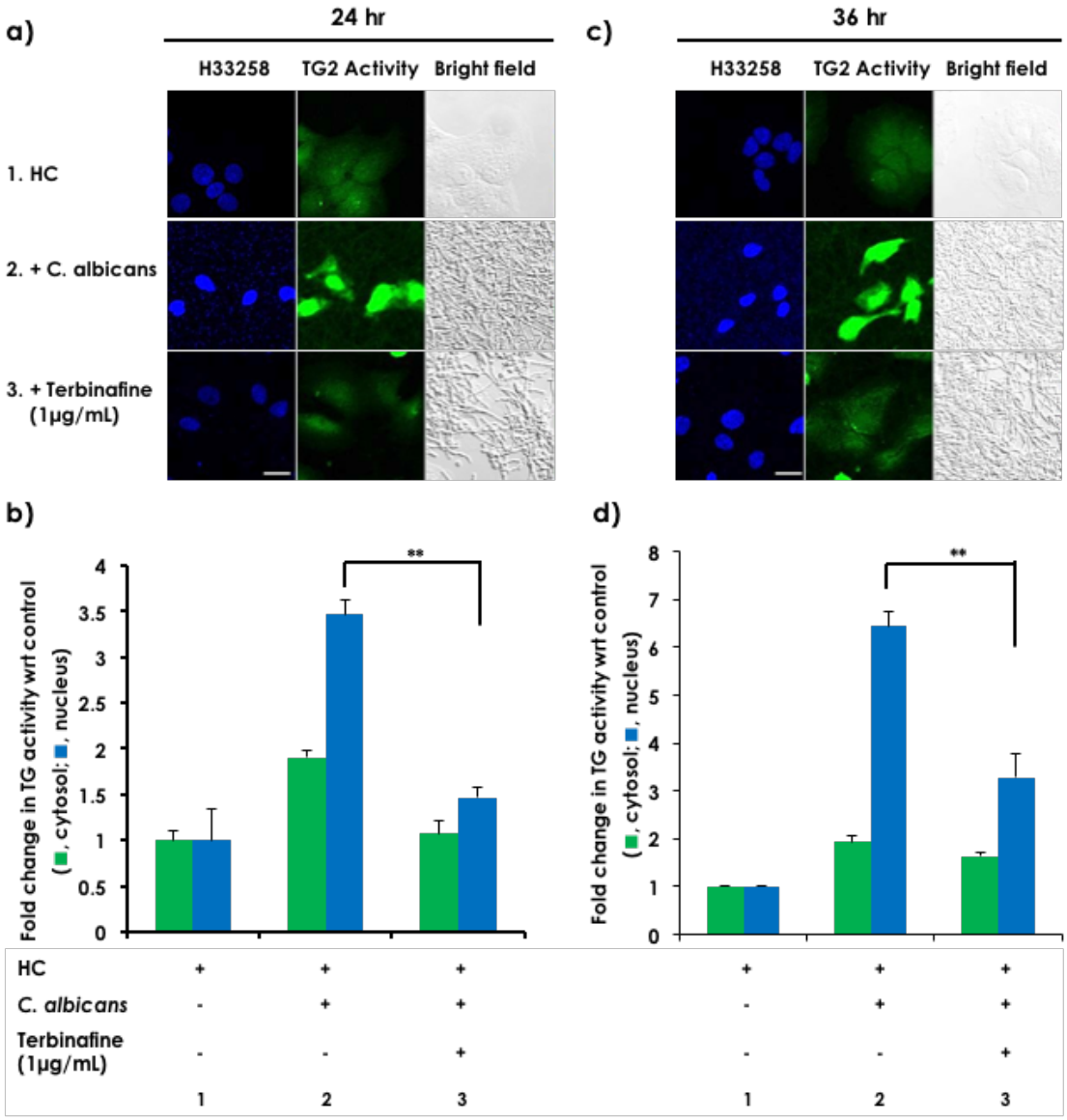

Figure 3.6 Cellular TG activity in Terbinafine and *C. albicans* treated HC cells

HC cells were seeded at 2 × 10^5 cells per well in a 6-well plate and incubated overnight. After adding 5-BAPA, the cells were incubated alone (row 1), or were co-incubated with living 5 × 10^6 *C. albicans* cells (row 2) or were co-incubated with living 5 × 10^6 *C. albicans* cells in presence of 1µg/mL Terbinafine (row 3) for **(a)** 24 hours or **(c)** 36 hours. Scale bars = 20 µm. Representative images from at least 3 fields from 2

independent experiments are shown**.** Fluorescence intensities from TRITC in both the cytoplasm and nucleus were quantitated using ZEN 2011 software, and relative TG activity levels in both locations of panels **(a)** are presented in bar graphs in **(b)** and of panel **(c)** in bar graphs in **(d)**, with the levels from HC cells incubated alone used as the controls (mean ± SD, n = 3). Asterisk represent statistical significance.

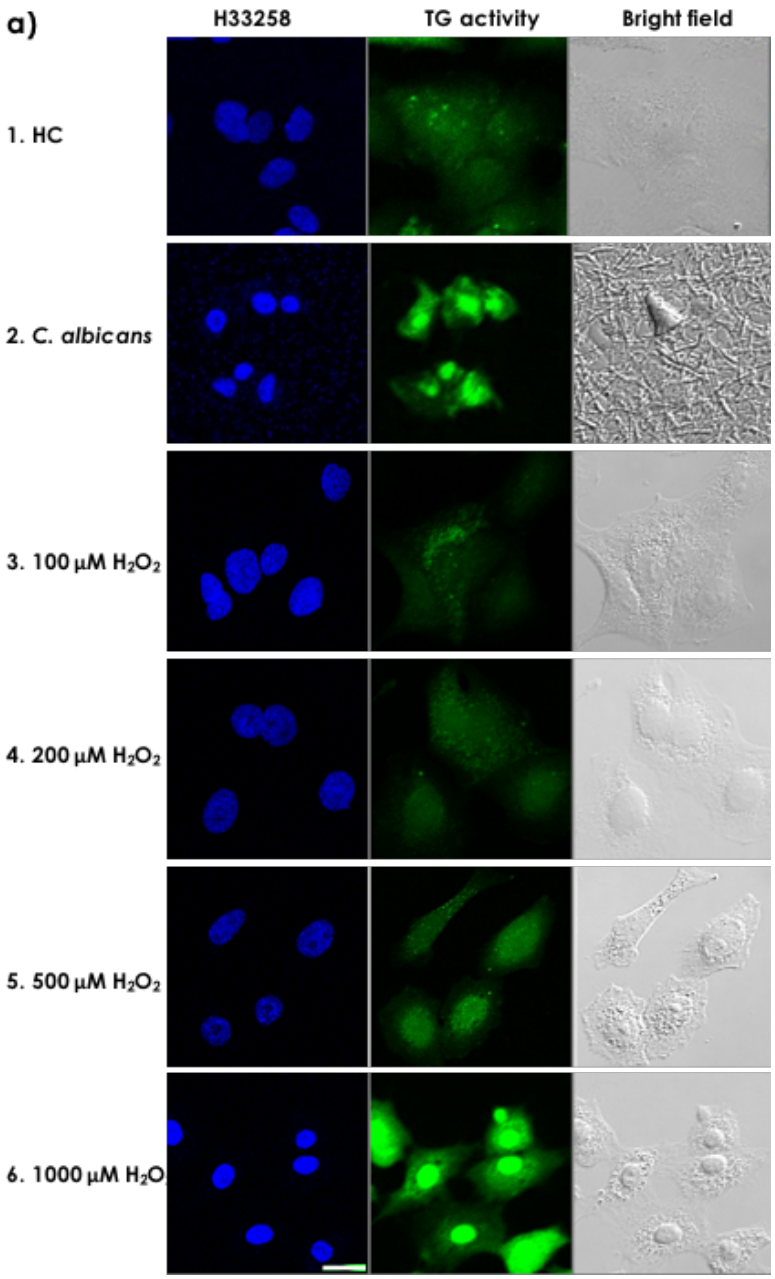
a)
H33258
TG activity
Bright field
1. HC
2. C. albicans
3. 100 µM H2O2
4. 200 µM H2O2
5. 500 µM H2O2
6. 1000 µM H2O

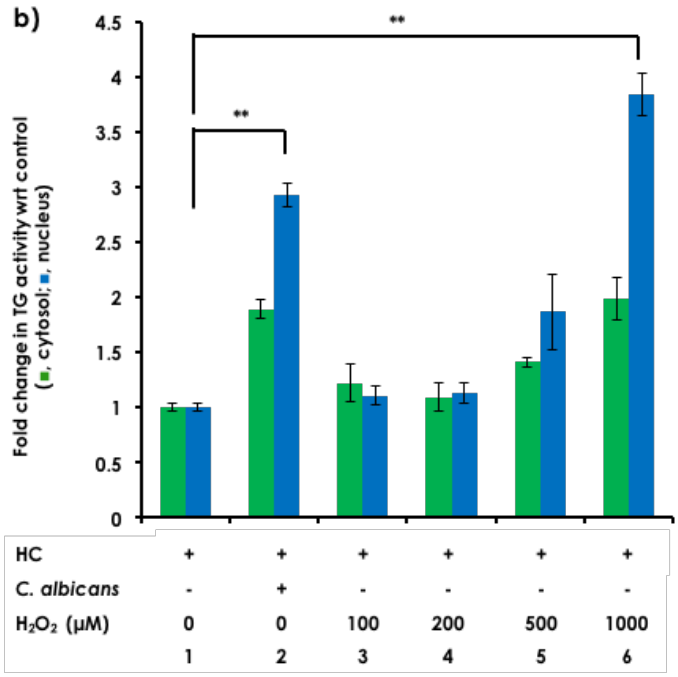

Figure 3.7 Cellular TG activity in H_2O_2 treated HC cells

HC cells were seeded at 2 × 10^5 cells per well in a 6-well plate and incubated overnight. After adding 5-BAPA, **(a)** the cells were incubated alone (row 1), or were co-incubated with living 5 × 10^6 *C. albicans* cells (row 2) and co-incubated with living 5 × 10^6 *C. albicans* cells in presence of 100 μm H_2O_2 (row 3), 200 μm H_2O_2 (row 4) 500 μm H_2O_2 (row 5) 1000 μm H_2O_2 (row 6) for 24 hours. Scale bars = 20 μm. Representative images from at least 3 fields from two independent experiments are shown**.** Fluorescence intensities from TRITC in both the cytoplasm and nucleus were quantitated using ZEN 2011 software, and relative TG activity levels in both locations of panels **(a)** are

presented in bar graphs in **(b)**. Levels from HC cells incubated alone is used as the controls (mean ± SD, n = 3). Asterisk represent statistical significance.

Chapter 4

4. Effect of Fungus-derived ROS to human hepatocytes and mouse primary hepatocytes.

4.1 Introduction

C. albicans is one of the most prominent etiological factors for causing opportunistic infection to human, which ranges from superficial infection to deep seated systemic infections. An interaction between virulence factors of *C. albicans* and immune environment of the host, determines well-being of human. In my research, it was suggested that one of the virulent attributes of *C. albicans* may be the ability of generating significant amounts of ROS.

In heterotrophic organisms, more than 90% of consumed oxygen under aerobic conditions is reduced directly to water via four-electron mechanisms by cytochrome oxidases coupled with oxidative phosphorylation to produce energy in ATP form. The system in eukaryotes is represented by electron transport chain (ETC) located in mitochondrial membrane. But, less than 10% of the consumed oxygen is reduced via alternative and successive one-electron pathway escaping from mitochondrial ETC mainly from coenzyme Q to form $O^{\cdot}_2$. This successive pathway of one-electron

reduction continues to reduce $O^{\cdot}_2$ to form H_2O_2 after parallel acceptance of two protons, and splits up H_2O_2 to ·OH and hydroxyl anion (OH^-) after accepting one more electron. Finally, OH^- interacts with one more electron and proton to form water. The formed $O^{\cdot}_2$, H_2O_2 and ·OH are collectively known as ROS **(**Table 3.1**)**. The term ROS also includes diverse peroxides like peroxides of lipid, proteins, and nucleic acids [96]. Over 90% of ROS are produced by electrons escaping ETC in mitochondria. In addition, small amount of ROS are also produced by ETC located in endoplasmic reticulum, plasmatic and nuclear membranes. Beside these, diverse oxidases are also producers of ROS. They oxidize carbohydrates, aldehydes, amino acids, heterocyclic compounds and other. Among them xanthine oxidases and NADPH oxidases are well studies ones. Xanthine oxidases are believed to be main ROS producers under hypoxic conditions and NADPH oxidases complex (Nox) are related to defense system for inactivation of bacteria by immune system cells.

In dying cells, intracellular ROS enhances TG2 activation, which facilitates Bax translocation to the mitochondria. Thus, the release of cytochrome *c* and apoptosis-inducing factors from the mitochondria can induce both caspase-dependent and caspase-independent apoptotic cell death, respectively [97].

In previous studies, increases in intracellular Ca^{2+} and endogenous ROS were reported with subsequent activation of TG2 and cell death of HUVEC cells treated with C-peptide, [89]. Similar apoptotic death was also reported in cancer cells following activation of TG2 due to increased ROS [98], in lysophosphatidic acid (LPA) and transforming growth factor-beta (TGF-β) treated Swiss 3T3 cell lines [87] and arachidonic acid treated NIH3T3 cell lines [88]. This study showed the ability to generate ROS on *Candida* species, which corroborates the finding of Sander CS. et. al., (2002) [90]. The exogenous ROS are highly toxic to the host cells and contributes the pathogenicity of *C. albicans* then leads to invasiveness and inflammatory responses of the host.

Hence, fungus-derived ROS mediating the activation of TG was evaluated about the association with hepatic cell death. For this, fluorescent probe CM-H2DCFDA and electron spin resonance (ESR) spectrometer were used for identification of ROS. HC cells were also co-incubated with *C. albicans* in the presence or absence of NAC, an inhibitor of ROS [99]. Further, *C. albicans*-derived ROS mediates induction of cellular TG activity, to a greater extent at the nuclear region, was verified by gain of- and loss of-function experiments in both human hepatic cell and mouse primary hepatocytes. Firstly, to examine the capacity of ROS to induce the TG activity, HC cells were treated

with H_2O_2 in the presence and absence of NAC. Secondly, HC cells co-incubated with *C. glabrata NOX1* mutant deficient in capacity to produce ROS. Finally, the activation of caspase 3 in human hepatic cells and mouse primary hepatocytes following to hepatic cell death was verified.

4.2 Materials and methods

4.2.1 Isolation of primary hepatocytes

Primary hepatocytes were isolated from the livers of male $TG2^{-/-}$ mice [100] and their $TG2^{+/+}$[101] littermates by collagenase digestion method as described previously [102].

4.2.2 Cell culture

Primary hepatocytes isolated form $TG2^{-/-}$ and $TG2^{+/+}$ were cultured in DMEM containing 10% FBS. HC cell line was grown in CSC complete medium. Both cell lines were incubated at 37 °C in a humidified incubator with 5 % CO_2. For the experiments, the cells were plated and cultured overnight in 96-well plates and 6-well plates bearing round coverslips. The next day, the cells were incubated for 4 hours in DMEM supplemented with 0.2 % FBS for serum starvation. These cells were co-incubated with fungi in the presence of 5-BAPA in serum-free DMEM.

4.2.3 Fungal strains and culture conditions

Fungal strains given in Table 4.2 were grown on YPD agar medium. For co-incubation with HC cells, the fungal cells were pre-cultured in liquid YPD medium

with shaking at 160 rpm for 8 to 16 hours at 30 °C. The pre-cultures were washed twice with PBS and adjusted to the desired cell density in plates by measuring the OD600 using an Ultrospec 2000 spectrophotometer.

4.2.4 Detection of *in vitro* ROS production by lucigenin

HC cells (4×10^3 cells in 200 μL of phenol red free DMEM) were seeded in each well of a 96-well plate and incubated at 37°C with 5 % CO_2 overnight as described previously. The next day, cells were co-incubated with 1×10^5 cells of different strains of fungi given in **Table 4.2** in phenol red free DMEM. Production of ROS in co-incubation culture was analyzed as based on the enhanced chemi-luminescence. Lucigenin was added (final concentration, 200 μM) (Sigma-Aldrich Co.) to the culture and incubated for 10 minutes at 37 °C. The chemi-luminescence was immediately measured using a microplate reader (Ensight, Perkin Elmer, USA).

4.2.5 Detection of *in vitro* ROS production by CM-H2DCFDA

HC cells (2×10^5 cells in the 2 mL of phenol red free DMEM medium) were seeded onto a 35-mm glass-based dish and incubated at 37 °C with 5 % CO_2 overnight as described previously. The next day, cells were co-incubated with *C. albicans* (5×10^6

cells) for 8 hours. ROS production was analyzed as based on the reaction between CM-H2DCFDA and ROS by measuring fluorescence signal. The cells were treated with CM-H2DCFDA (final concentration, 5 μM) (Life Technologies, Eugene, OR, USA) for 15 minutes at 37 °C, and cells were immediately monitored for their fluorescein isothiocyanate (FITC) fluorescence signals using LSM 700 laser scanning confocal microscope (Carl Zeiss, Inc., Germany).

4.2.6 Identification of a ROS by ESR spectroscopy

Semi-quantitative measurements of ROS were performed using a conventional spin trapping technique with ESR spectroscopy. HC cells (2×10^5 cells in the 2 mL of phenol red free DMEM medium) were seeded onto each well of a 6-well plate and incubated at 37 °C with 5 % CO_2 overnight. Cells were co-incubated with fungi (5×10^6 cells) for 8 hours. Culture medium was diluted in 100 mM phosphate buffer (pH 7.4) containing 25 μM diethylenetriaminepentaacetic acid (DPTA, Sigma-Aldrich Co.) and 25 mM 5-tert-Butoxycarbonyl-5-methyl-1-pyrrolin-N-oxide (BMPO, Enzo Life Sciences, Farmingdale, NY, USA) [103]. The mixtures were then transferred to a quartz flat cell and set inside the cavity of the ESR spectrometer. Then, ESR measurement of the spin adducts was performed under the following conditions: magnetic field,

336.7±10 mT; microwave frequency, 9.424 GHz; microwave power, 10.0 mW; sweep time, 0.5 minutes; time constant, 0.03 sec; and modulation field 1.0 × 0.1 mT (100 kHz). All ESR spectra were taken with 10 accumulation times. The generated ROS were evaluated using the data analyzer connected to the ESR spectrometer. Representative images obtained from a single experiment are shown.

4.2.7 Determination of *in vitro* TG activity and cleaved caspase-3

HC cells were seeded on round coverslips plated in a 6-well plate (2×10^5 cells) and incubated overnight at 37 °C with 5 % CO_2. The next day, the cells were directly co-incubated for 24 hours with fungi. The cellular activity of TG2 was measured based on the incorporation of 0.2 mM 5-BAPA into the cells incubated in the presence of 0.1 mM aminoguanidine. Some samples were also incubated with 10 mM NAC (Sigma-Aldrich Co.), as an ROS inhibitor [87], or 1 mM H_2O_2 as a positive control for producing ROS. Cells were then fixed with a 10 % formaldehyde solution, permeabilized, blocked and immunostained with streptavidin- TRITC (1:500) and cleaved caspase-3 (1:400). The TG activity was then detected as a fluorescence signal from TRITC and analyzed with an LSM 700 laser scanning confocal microscope (Carl Zeiss, Inc., Germany) and using ImageXpress^{MICRO} High Content Screening System

(Molecular Devices, Sunnyvale, CA, USA). Anti-rabbit Alexa 488 (1:200) was used to detect cleaved caspase-3 along with H 33258 (1:5000)

4.2.8 Use of a ROS inhibitor NAC

HC cells were cultured as described previously. Briefly, in 6-well plates bearing round coverslips $2x10^5$ HC cells was plated and incubated at 37 °C in a humidified incubator with 5 % CO_2 in presence and absence of fungus. The next day, the cells were incubated for 4 hours in DMEM supplemented with 0.2 % FBS for serum starvation (Mediatech, Herndon, VA, USA). These cells were treated with 10 mM of NAC prepared in DMEM. In some cases, 5-BAPA was also added to determine TG activity. The amount of NAC used was evaluated non-cytotoxic as determined by Cell counting kit-8 (CCK-8, Sigma-Aldrich) method and effective to inhibit ROS.

4.3Results

4.3.1 *C. albicans* and *C. glabrata* increased ROS in co-culture with HC cells

Suspecting that the unstable substances might be ROS from fungi for inducing TG activity in HC cells, time course for the production of ROS by fungus co-cultured with HC cells was measured using chemiluminescent probe lucigenin [86]. Co-incubation of HC cells and *C. albicans* led to produce higher amount of ROS in comparison to *C. glabrata* and *S. cerevisiae*, and the production was the highest amount at 8 hours after co-incubation **(**

Figure 4.1**)**. Next for further confirmation of ROS generation of fungus, fluorescent probe CM-H2DCFDA [104] was used **(**

Figure 4.2**)**. Significantly higher levels of ROS were produced by both *C. albicans* cultured with HC cells (row and column 2) and *C. glabrata* cultured with HC cells (row and column 3) than by HC cells alone (row and column 1) and by *S. cerevisiae* cultured with HC cells (row and column 4). In *C. glabrata*, only a gene (CAGL0K05863g) homologous to the genuine NADPH oxidase Yno1p/Aim14p of *S. cerevisiae* [105] was identified and named *CgNOX1*. *S. cerevisiae* Aim14p was already determined to be responsible for the generation of superoxide from oxygen [105].

Hence, *Cgnox1*-disruption mutant was co-incubated with HC cells and decrease in ROS generation (row and column 5) was confirmed.

4.3.2 *C. albicans* and *C. glabrata* increased ·OH in co-cultured HC cells

To determine the ROS species, ESR analyses of culture media were performed. Four split ESR line spectra of·OH with an intensity ratio of 1:2:2:1 were observed in the conditioned medium of HC cells with *C. albicans* **(**

Figure 4.3 **a)** and *C. glabrata* **(**

Figure 4.3 **b)** but not in that from HC alone **(**

Figure 4.3 **a)** with hyperfine parameters of (A_N = 1.4 mT, A_H = 1.3 mT). The intensities of the ·OH spectra were quite different for the different species of fungi. *C. albicans* showed the highest intensity. *C. glabrata* showed a spectrum for ·OH at a 2.5-fold higher sensitivity setting suggesting the amount of ·OH released by *C. glabrata* is relatively lower than that released by *C. albicans.* The order of the ·OH spectrum intensities was *C. albicans* > *C. glabrata* > *S. cerevisiae,* with an approximate ratio of 10:3:1, respectively **(**

Figure 4.3 **a and b).** The ·OH spectrum intensity of *Cgnox1* mutant was also quite small (almost the same as that of *S. cerevisiae*). Treatment of HC cells and *C.*

albicans / *C. glabrata* co-cultures with NAC also showed spectra similar to that of ·OH but with different hyperfine parameters (A_N=1.4 mT, A_H=1.5 mT). These results indicate that high amount of fungi derived ·OH is released as an exogenous ROS in adjacent hepatic cells.

4.3.3 *Candida* species-derived ROS induced higher cellular TG activity in HC cells

To explore whether fungus-derived ROS might mediate induction of cellular TG activity in HC cells, HC cells were co-incubated with *C. albicans* in the presence and absence of NAC [87]. Treatment of the co-cultures of *C. albicans* and HC cells with NAC completely blocked the enhanced cytosolic and nuclear TG activities in HC cells **(Figure 4.4 a and b**, compare rows or columns 2 with 3**)**. This result suggested that fungus-derived ROS might mediate the enhancement of cellular and, to a greater extent nuclear, TG activity in HC cells.

The hypothesis that *C. albicans*-derived ROS might mediate induction of cellular TG activity was further verified, by both gain- and loss-of-function experiments. First, to examine the capacity of ROS to induce TG activity, HC cells were treated with

H_2O_2 in the presence or absence of NAC. Similar to HC cells co-incubated with *C. albicans*, externally added H_2O_2 mimicked an increase in cellular TG activity in HC cells, which was blocked by NAC **(Figure 4.4 a and b**, compare rows or columns 4 with 5). However, HC cells co-incubated with the *Cgnox1* mutant failed to increase TG activity **(Figure 4.4 a and b**, compare row or column 6 with 7). These results suggested that fungus-derived ROS produced in the proximity of HC cells worked as a mediator(s) to increase cellular TG activity in HC cells.

4.3.4 *Candida* species-derived ROS induced TG2-mediated hepatic cell death

To explore the role of fungus-derived ROS to hepatic cell death, HC cells were incubated with pathogenic fungi and the caspase-3 activation in HC cells was analyzed. Enhanced cellular TG activity and caspase-3 activation were observed in this co-incubation and were attenuated by NAC **(Figure 4.5 a and b**, compare row or column 2 with 3).

Next to investigate the role of TG2 in fungus-derived ROS in hepatic cell death, primary hepatocytes from $TG2^{+/+}$ and $TG^{-/-}$ mice were treated with different strains of fungi **(Figure 4.5 a and b)**. Increased cellular TG and caspase-3 activities were observed following co-culturing *C. albicans* and *C. glabrata* with $TG2^{+/+}$ hepatocytes

(compare rows 1 with 3 and 5, respectively) but not with $TG2^{-/-}$ hepatocytes (compare rows 2 with 4 and 6, respectively) and $TG2^{+/+}$ hepatocytes treated with *Cgnox1*(row 9), *C. utilis* (row 10) or *S. cerevisiae* (row 11). The increased TG and caspase-3 activities were attenuated by NAC (compare rows 3 with 7 and 5 with 8), indicating that fungi-derived ROS was able to increase cellular TG activity, especially TG2, and increases caspase-3 activation, leading to cell apoptosis.

4.4 Discussions

In relation to unstable nature of factor(s) inducing TG2 activity in HC cells, ROS as a promising factor was monitored using the chemiluminescent probe lucigenin and fluorescent probe CM-H2DCFDA [104]. When co-cultured with HC cells, significantly higher yields of ROS were produced by both *C. albicans* and *C. glabrata* than by other fungi such as *S. cerevisiae*. The capacities of production of high yields of ROS in *C. albicans* and *C. glabrata* may characterize these fungi as pathogen. Schroter C. *et. al*. showed that *C. albicans* can produce significant yield of ROS in response to the morphological state and the virulence factor for invasive behavior [86]. Further, Sander CS. *et. al*., propounded the ability to generate remarkable yield of ROS, which are highly toxic to the cells and contributes for the pathogenicity of *C. albicans* in human host. Then, this phenomenon leads to invasiveness and inflammatory responses of the host [90].

Furthermore, ESR analysis was performed to identify ROS species. Four split ESR line spectra with an intensity ratio of 1:2:2:1 were observed in the conditioned medium of HC cells with *C. albicans* /*C. glabrata*. The origin of the split ESR lines comes from the hyperfine interactions of the nuclear spins and depends on the number of nuclear spins in the nitrone spin trap BMPO and the trapped ROS. If

·OH is trapped in BMPO, the total number of nuclear spins are I=3/2, and this splits the single ESR line into 2I+1 = 4 lines. The number of the splitting lines and the intensity ratio and the hyperfine parameters (A_N = 1.4 mT, A_H = 1.3 mT) suggested that the origin of the ESR was coming from the spin adducts BMPO/·OH. Therefore, the ROS was identified as ·OH.

High yield of ·OH in the conditioned medium co-incubated with HC cells and *C. albicans* /*C. glabrata* was observed. However, no similar spectrum was observed in conditioned medium co-incubated with HC cells and *S. cerevisiae* and in the medium in which only HC cells were cultured. The order of the ·OH spectrum intensities was *C. albicans* > *C. glabrata* > *S. cerevisiae*, with the approximate ratio of 10:3:1, respectively. Likewise, *NOX1* gene in *C. glabrata*, which eliminated the capacity to produce ROS, showed similar spectrum as that of *S. cerevisiae*. Treatment of HC cells and *C. albicans* / *C. glabrata* co-cultures by NAC also showed spectra similar to that of ·OH but with different hyperfine parameters (A_N=1.4 mT, A_H=1.5 mT). It was speculated that this might be an extrinsic effect due to the interactions of NAC, ·OH and BMPO. These results indicated that high yield of exogenous ROS triggers the induction of nuclear TG in adjacent hepatic cells.

ROS has been identified as the principal factor for activation of cellular TG activity in human hepatic cells following co-culture with leading opportunistic fungal pathogens *C. albicans* and *C. glabrata*. Next, the role of fungus derived ROS identified as ·OH was clarified by both gain of- and loss of-function. Here, HC cells were exogenously treated with H_2O_2 in the presence of NAC. and then TG activity in HC cells were monitored. Like as fungus-derived ROS, addition of H_2O_2 led to reproducible enhancement of cellular TG activity in HC cells, while NAC blocked these effects. Furthermore, co-incubation of HC cells and Cgnox1 mutant of *C. glabrata* abrogated the capacity to enhance cellular TG activity in HC cells. These results suggested that the ·OH produced by *C. albicans* /*C. glabrata* in close proximity to HC cells acted as a principal mediator to increase in the cellular, especially nuclear, TG activity in the HC cells and mouse primary hepatocytes, eventually, induced cell death **(Figure 4.5 and Figure 4.6)**. Intracellular ROS has been reported to be a principal mediator for TG2 activation in HUVEC lines treated with C-peptide [89], in Swiss 3T3 cell lines treated with lysophosphatidic acid (LPA) and transforming growth factor beta (TGF-β), [87] and in NIH3T3 cell lines treated with arachidonic acid [88]. In these studies, endogenous ROS enhanced cellular TG activity in HC cells, although the biological relevance of this enhancement was not addressed. Similarly, H_2O_2 has been revealed as

a principal contributor of cartilage degradation through chrondrocyte apoptosis via caspase 1 and 3 activation and increased TG2 activation and expression. However, the possibility that *C. albicans* and *C. glabrata* might also stimulate endogenous ROS production in HC cells cannot be ruled out. Thus far, this study showed that ROS enhances both the gene expression and nuclear localization of TG2 in HC cells. In addition, it has been reported that *C. albicans* produces ROS under certain conditions [86]. The roles of the gut microbiota and bacteria-liver interactions are fairly well understood in the context of ASH and NASH [32-35], Recently Yang et al. reported the contribution of *C. albicans* in development of ASH disease [36]. Here, in this study, for the first time, an association of ROS-high producing fungi, such as *C. albicans* and *C. glabrata* with enhanced nuclear TG2 activity in hepatic cells leading to apoptosis is demonstrated. Combining these previous findings and the results of my study suggested that host cell (tissue) injury by two *Candida* species via the ROS-mediated induction of nuclear TG2 might be a general phenomenon in human body. Indeed, a similar induction of nuclear TG2 was observed in HEK 293T and FLC-7 cells upon co-incubation with *C. albicans*.

Table 4.1 Steps involved in *in vivo* formation of ROS

Reaction	ROS
$O_2 + e^- \rightarrow {}^{\cdot}O_2^-$	Superoxide
$2H^+ + {}^{\cdot}O_2^- + {}^{\cdot}O_2^- \rightarrow H_2O_2 + O_2$	Hydrogen peroxide
$H_2O_2 + e^- \rightarrow HO^- + {}^{\cdot}OH$	Hydroxyl radical
$2H_2O_2 \rightarrow 2H_2O + O_2$	

Table 4.2 List of fungi used in study of fungal-derived ROS in human hepatocytes

Species	Strain	Genotype	References
C. albicans	SC5314	wild type	[63]
S. cerevisiae	IFO10150	MATa ste-VC9 ura3-52 trp1-289 his3-D1 leu2-3,112	[64]
C. glabrata	CBS138	wild type	[65]
CgNOX1	CAGL0K05863g	*Cgnox1*, a derivate of CBS138	From Professor Chibana

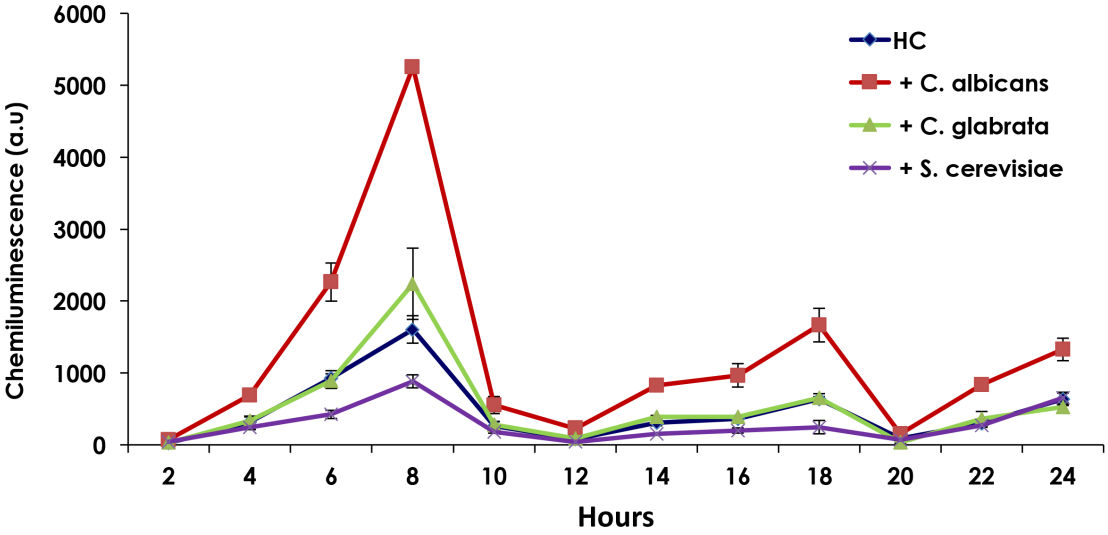

Figure 4.1 Time dependent ROS level in fungus-HC co-culture

HC cells were seeded onto a 96-well plate (4×10^3 cells per 200µL) in phenol red free DMEM and incubated at 37 °C with 5 % CO_2 overnight. The next day, cells were co-incubated with different strains of fungi (1×10^5 cells) in phenol red free DMEM. After inoculation of the fungi the plate was incubated at 37 °C with 5 % CO_2 and in 2 hours interval, ROS production was measured immediately after addition of lucigenin in final concentration of 200 µM for 10 minutes. The chemi-luminescence was immediately measured using a microplate reader.

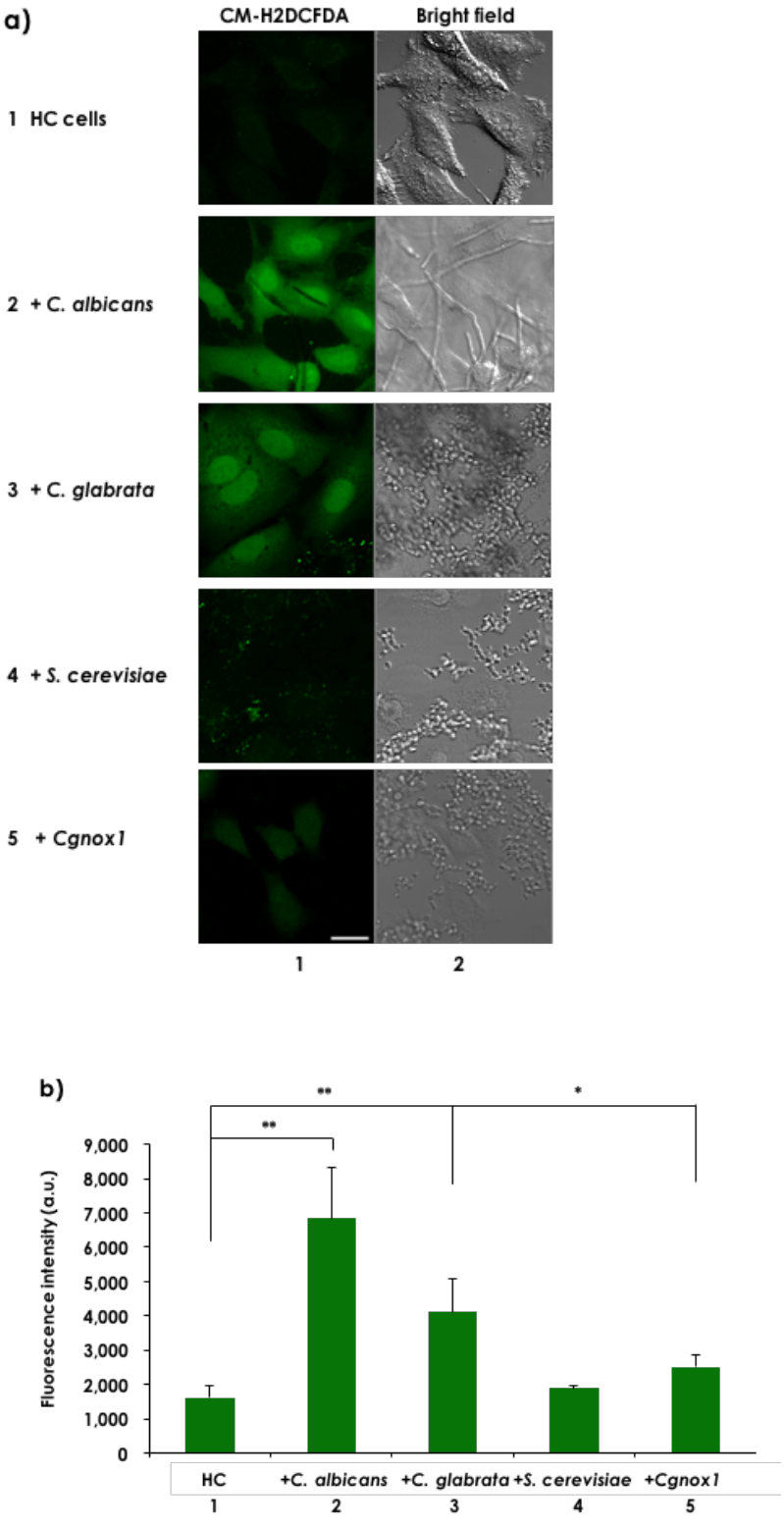

Figure 4.2 Level of ROS in HC cells co-incubated with fungus

HC cells were seeded at 2×10^5 cells per well on a 35-mm glass-based dish or round cover slips plated in 6-well plates and were incubated overnight. **(a)** Cells were incubated alone (row 1) or were co-incubated for 8 hours with the different fungal strains, including *C. albicans* (row 2), *C. glabrata* (row 3), *S. cerevisiae* (row 4), and a *CgNOX1* gene mutant of *C. glabrata* (row 5), with 5 μM CM-H2DCFDA. Scale bars = 20 μm. **(b)** Fluorescence intensities from reacted CM-H2DCFDA were quantitated using ZEN 2011 software and are represented in bar graphs (mean ± SD, n = 3). A 100-μL test mixture was prepared containing 40 μL DPTA, 10 μL BMPO. Asterisks represent statistical significance.

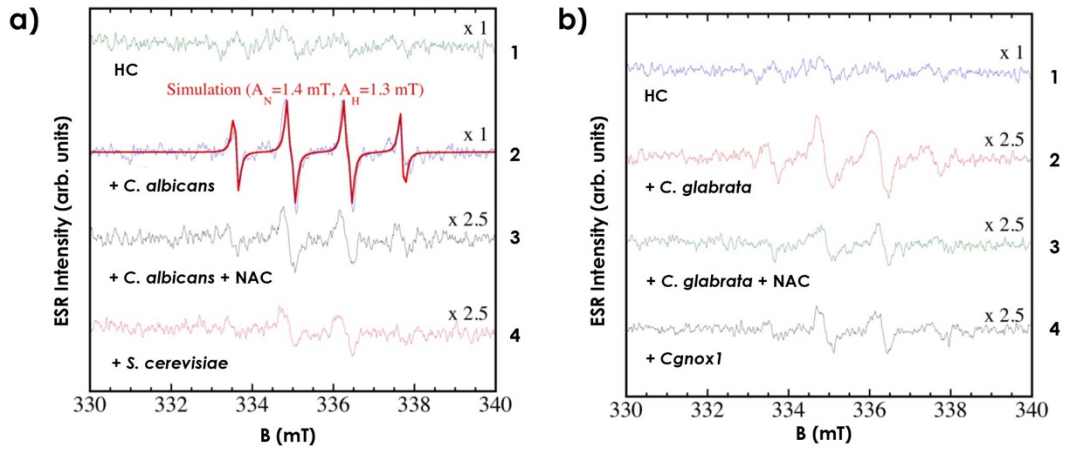

Figure 4.3 Level and species of ROS in fungus-HC cells cultured medium

HC cells were seeded at 2 × 10^5 cells per well on a 35-mm glass-based dish or round cover slips plated in 6-well plates and were incubated overnight. **(a)** 50 µL of culture medium from the HC cells (spectrum 1) or HC cells co-incubated with *C. albicans* in the absence (spectrum 2) or presence (spectrum 3) of NAC or *S. cerevisiae* (spectrum 4) cultivated for 8 hours or with **(b)** 50 µL of culture medium from HC cells (spectrum 1), or HC cells were co-incubated with *C. glabrata* in the absence (spectrum 2) or presence (spectrum 3) of NAC or *Cgnox1* (spectrum 4) for 8 hours. The mixture was transferred to a quartz flat cell and set inside the cavity of the ESR spectrometer and analyzed using the data analyzer connected to the ESR spectrometer.

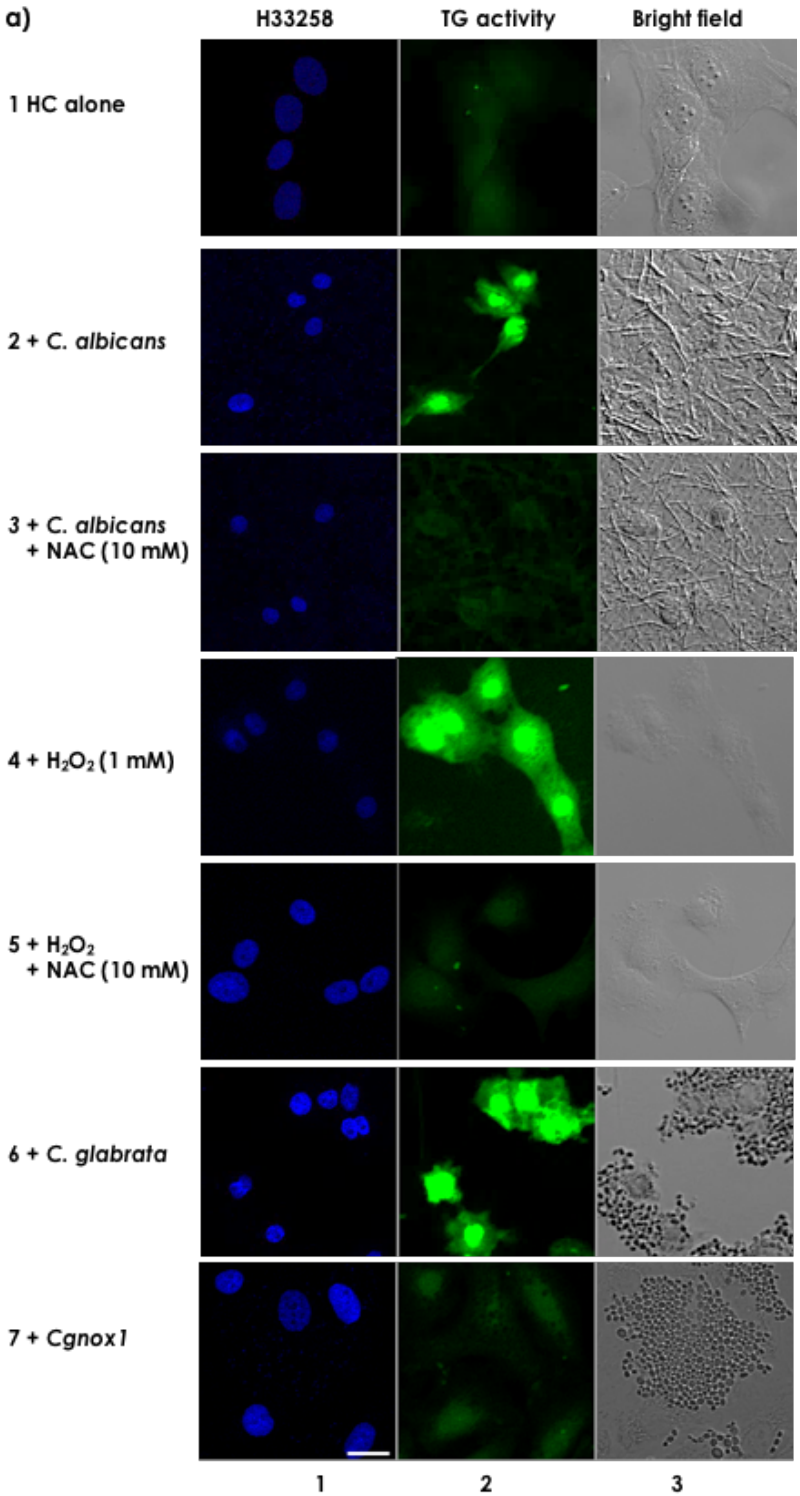
a)
H33258
TG activity
Bright field
1 HC alone
2 + C. albicans
3 + C. albicans
+ NAC (10 mM)
4 + H2O2 (1 mM)
5 + H2O2
+ NAC (10 mM)
6 + C. glabrata
7 + Cgnox1
1
2
3

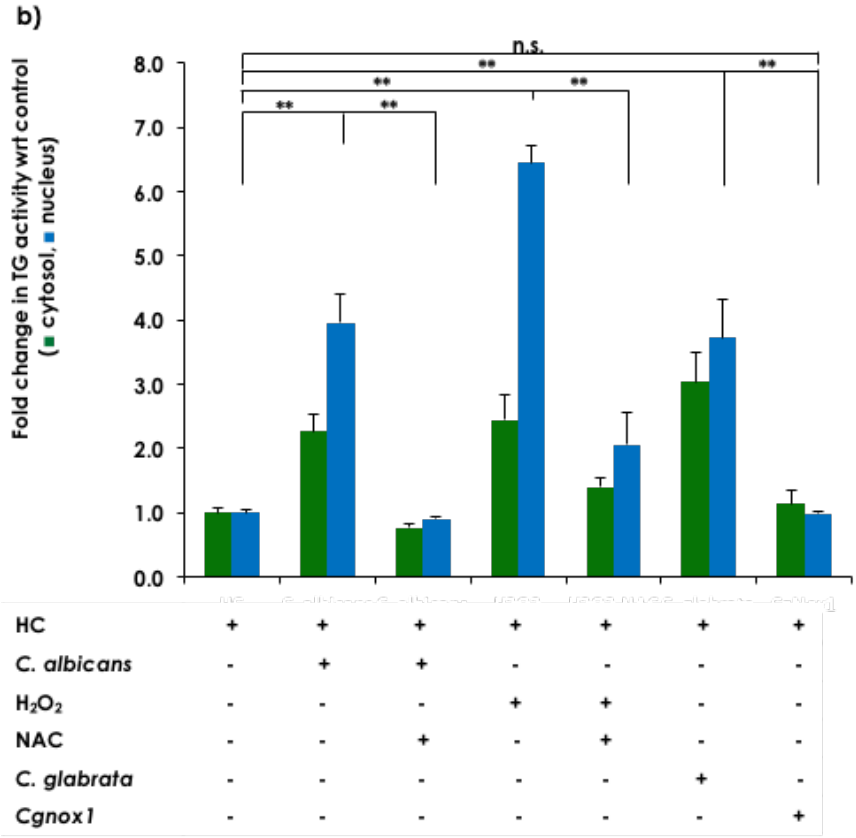

Figure 4.4 Cellular TG activity in HC cells induced by ROS

HC cells were seeded at 2 × 10^5 cells per well in a 35-mm glass-based dish or on round cover slips plated in 6-well plates and incubated overnight as previously described. **(a)** After adding 5-BAPA, the HC cells were incubated alone (row 1) or were co-incubated for 24 hours with 5 × 10^6 *C. albicans* cells in the absence (row 2) or presence (row 3) of 10 mM NAC, with 1 mM H_2O_2 in the absence (row 4) or presence (row 5) of 10 mM NAC, or with 5 × 10^6 *C. glabrata* cells (row 6) or *Cgnox1*-mutant cells (row 7). The cells were fixed and stained with streptavidin-TRITC and H 33258 dye. Both the blue fluorescence signals from H 33258-stained nuclei (column 1) and the green

fluorescence signals representing TG activity (column 2) were detected using a confocal microscope. Images taken under the bright field (column 3) are also shown. Scale bars = 20 μm. Representative images from at least 3 fields from 3 independent experiments are shown. **(b)** Fluorescence intensities from TRITC in both the cytoplasm and nucleus were quantitated using ZEN 2011 software, and the relative TG activity levels in both locations are represented in bar graphs, with the level from HC cells incubated alone used as the control (mean ± SD, n = 3). Asterisks represent statistical significance.

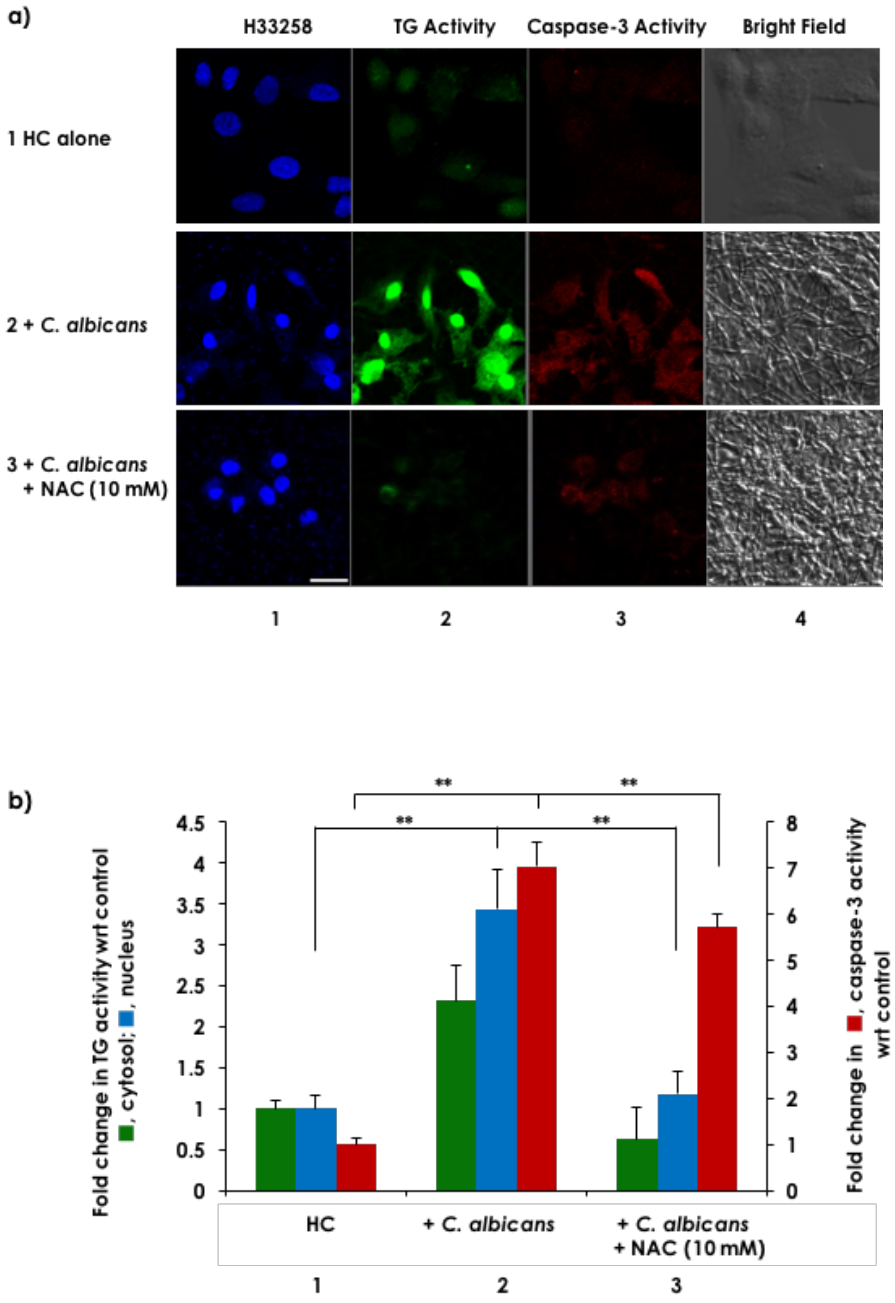

Figure 4.5 TG mediated cell death of HC cells induced by fungus derived ROS

(a) HC cells were seeded at 2 × 10^5 cells per well in a 6-well plate and were incubated overnight and then treated with 5-BAPA and were incubated alone (row 1) or were

co-incubated with 5×10^6 *C. albicans* cells (row 2) in the presence of 10 mM NAC (row 3). The blue fluorescence from H 33258 dye (column 1) was observed along with the green fluorescence signals from TRITC staining 5-BAPA representing TG activity (column 2) and red fluorescence from Alexa 488 representing caspase-3 activity (column 3) using a confocal microscope. An image taken under bright field (column 4) is also shown. Scale bar = 20 μm. Representative images from at least 3 fields from a single experiment are shown. (b). Fluorescence intensities from TRITC in both the cytoplasm and nucleus along with fluorescence intensities from Alexa 488 were quantitated using ZEN 2011 software, and after subtraction of background intensities, the relative TG and caspase-3 activity levels are represented in bar graphs, with the levels from HC cells incubated alone as the control (mean ± SD, n = 3). Asterisks represent statistical significance.

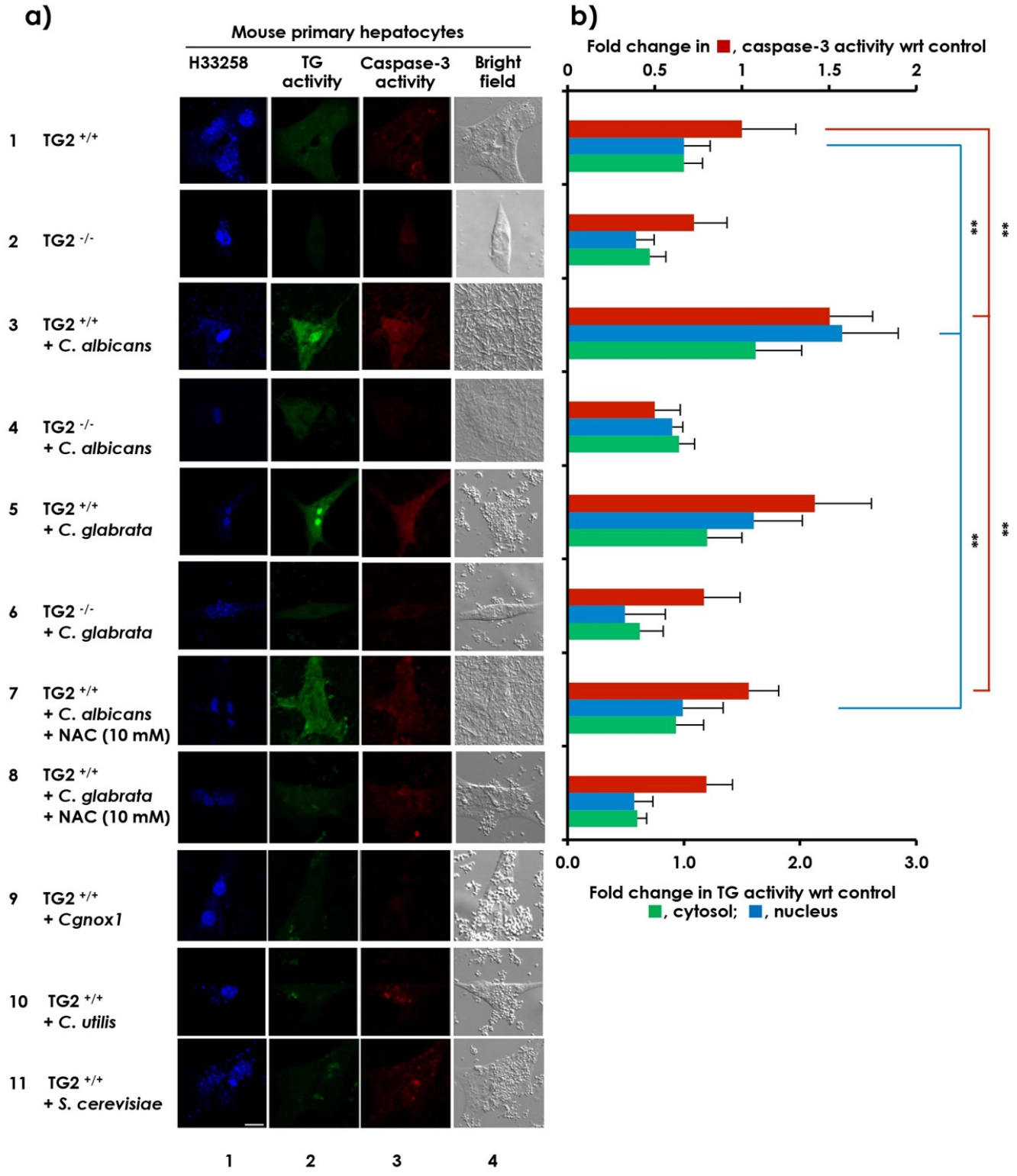

Figure 4.6 TG2 mediated hepatic cell death induced by fungus derived ROS

(a) Primary hepatocytes isolated from livers of $TG^{-/-}$ mice and their $TG^{+/+}$ littermates were seeded at 5×10^5 cells per well in a 6-well plate and incubated overnight. The next day, the cells were treated with 5-BAPA and incubated alone (rows 1 and 2) or were co-incubated with 5×10^6 *C. albicans* cells (rows 3 and 4) in the presence of 10 mM NAC (row 7) or with the same number of *C. glabrata* cells (rows 5 and 6) in the presence of 10 mM NAC (row 8), *Cgnox1* (row 9), *C. utilis* (row 10), and *S. cerevisiae* (row 11). The blue fluorescence from H 33258 dye (column 1) was observed along with the green fluorescence signals from TRITC staining 5-BAPA representing TG activity (column 2) and red fluorescence from Alexa 488 representing caspase-3 activity (column 3) using a confocal microscope. An image taken under bright field (column 4) is also shown. Scale bar = 20 μm. Representative images from at least 3 fields from a single experiment are shown. **(b)**. Fluorescence intensities from TRITC in both the cytoplasm and nucleus along with fluorescence intensities from Alexa 488 were quantitated using ZEN 2011 software, and after subtraction of background intensities, the relative TG and caspase-3 activity levels are represented in bar graphs, with the levels from $TG2^{+/+}$ primary hepatocytes incubated alone as the control (mean ± SD, n = 3). Asterisks represent statistical significance.

Chapter 5

5. Conclusion

Role of TG2 and existence of pathogenic fungus like *C. albicans* and *C. glabrata* in human liver damage were previously reported. But, role of these fungi in hepatic injury was still not clear. Hence, in this study investigation in the direction of involvement of TG2 and in the regulation of liver cell death after infection with *C. albicans* and *C. glabrata* was conducted.

Increased cellular TG activity, increased TG2 mRNA level and nuclear accumulation of EGFP tagged TG2 were observed following incubation of human liver cell with these pathogenic fungi. TG inhibitors cystamine and R283, inhibited the increased cellular TG activity, suggesting that observed TG activity in HC cells was induced by these *Candida*. Furthermore, ZDON and phenosafranin significantly inhibited cell death following activation of caspase-3 in FLC-7 cells, suggesting that nuclear TG2 activity is involved in *C. albicans*-induced hepatic cell death. This study suggested that fungi *C. albicans* and *C. glabrata* release some factor/s, causing cellular stress and enhancing cellular TG2 activity in host cells and then lead to cell death via activation of caspase-3 pathway.

For screening and identification of the responsible factor(s) for induction of cellular TG activity, several virulence factors of *C. albicans* were evaluated. HC cells co-cultured with heat-inactivated *C. albicans,* hyphae form of *C. albicans, C. albicans* with delayed hyphae development and *C. albicans* mutant cells with defect in adhesion and biofilm formation such *Caecm33*, *Cabgl2*, *Cafad2*. In addition, HC cells were incubated with *C. albicans* in the presence of 5 μM Ebelactone B, a lipase inhibitor. The results showed that an increase in TG activity in HC cells requires viable fungus cells and is not related to the polymorphic form of *C. albicans*, the ability to form biofilm, hyphae development, structural component of fungal cell wall and lipase secreted by *C. albicans*. Further, to evaluate the necessity of the direct contact of these fungi and the stability of some factor(s) of these fungi, HC cells were co-cultured with living fungus plated in dialysis membrane (≤ 10kDa) and cultured with fungus-cultivated media. Enhancement of TG activity in HC cells in living fungus plated in dialysis membrane was observed but not with the fungus-cultivated media, suggesting that a certain soluble factor(s), which might be very unstable in nature, was secreted into the culture medium by *C. albicans* and increased cellular TG activity.

Further to verify whether the responsible factor is ROS or not, effect of Terbinafine (a free radical interceptor) in fungus-HC co-culture and exogenously added

H_2O_2 in HC cells were evaluated. These results suggested that ROS might be the responsible factor further verified by using fluorescent probe of ROS CM-H2DCFDA. Furthermore, ESR analyses were performed. The result showed higher levels of •OH in the conditioned medium co-incubated with HC cells and *C. albicans* /*C. glabrata*. Next, the role of fungus derived ROS (identified as •OH) was clarified by both gain of-and loss of-function. HC cells were exogenously treated with H_2O_2 in the presence of NAC, then the TG activity was checked. And also, HC cells were co-incubated with a *NOX1*-deleted mutant in *C. glabrata* and the TG activity was monitored. Reproducible enhancement of cellular TG activity by exogenously added H_2O_2 were observed, while the ROS scavenger NAC blocked these effects. Furthermore, a mutation in NOX1 in *C. glabrata* abrogated the capacity to enhance cellular TG activity in *C. glabrata*. These results suggested that the ROS produced by *C. albicans* and *C. glabrata* in close proximity to HC cells acted as a principal mediator for increase in cellular, especially nuclear TG activity in the host cells, and eventually induced cell death.

This study demonstrated that pathogenic fungi *C. albicans* and *C. glabrata* increase cellular TG activity levels in hepatic cells. This increase eventually leads to cell death due to the release of ROS, which acts as a principal mediator (**Fig. 5.1**). This observation suggested that production of high levels of ROS and ROS-mediated

induction of nuclear TG2 might be a basic feature of pathogenic fungi. ROS plays a vital role in host defense and has been involved in various pathological conditions, including cardiovascular disease, [106] neurodegenerative diseases such as Alzheimer's disease [107] and Parkinson's disease [15], diabetes [89] and renal cell carcinoma [108]. TG2 has also been associated with these diseases. [109-113] In such situations, suitable inhibitors of exogenous ROS may serve as promising therapies for liver injury in hepatitis patients by inhibiting the enhancement of cellular TG activity.

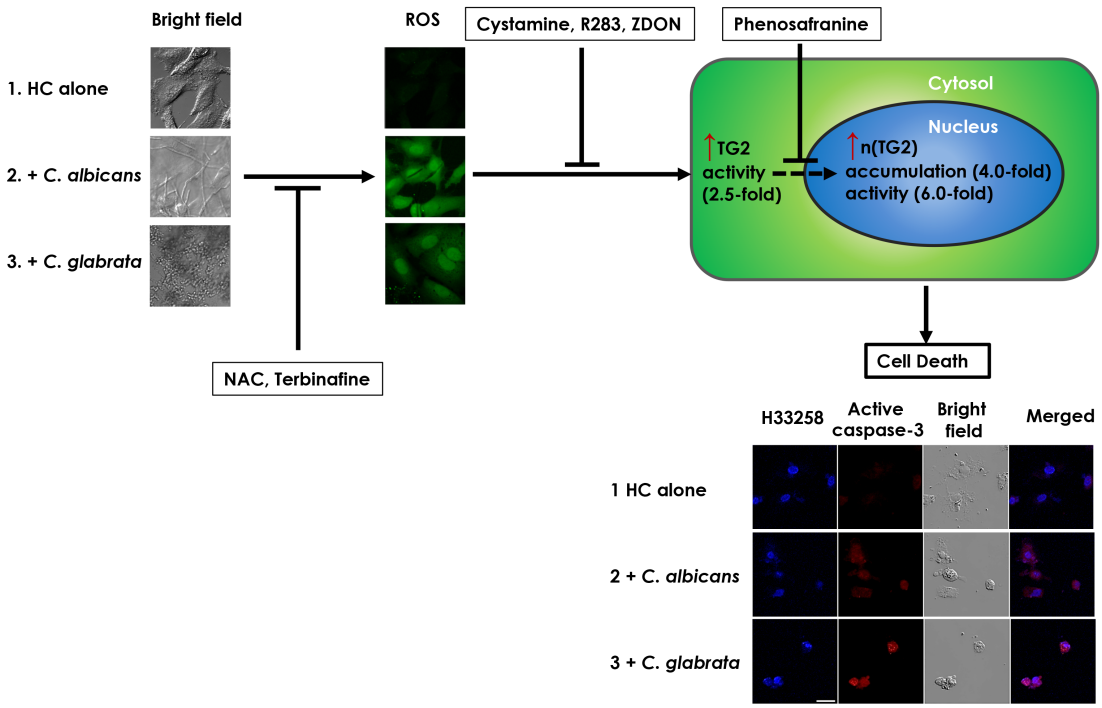

Figure 5.1 Mechanism of *C. albicans* & *C. glabrata*-induced cell death in HC cells

Both *C. albicans* and *C. glabrata* produce high amount of ROS that induces cellular TG activity leading to HC cell death. NAC and natural antioxidant are effective in preventing this cell death by blocking the action of ROS.

Acknowledgements

I am highly obliged to my professors, Prof. Susumu Kajiwara and Prof. Soichi Kojima for believing me and kindly giving the opportunity and environment to foster the doctoral research under their supervision. The valuable skills that I have gained under their supervisions are my precious assets. I am very confident that the skills will certainly help me to excel further in my career.

I cannot thank enough to all contributors who helped me publish my paper and prepare this thesis work, including Dr. Xian-Yang Qin, Dr. Yugo Oshima, Dr. Shun Iwatani, Prof. Reizo Kato, Prof. Hiroji Chibana, Dr. Mitsuko Hara, Dr. Ryu Teraoka, Fujii-san, Li-san, and to my all my lab colleagues from RIKEN and Tokyo tech; Dr. Yutaka Furutani, Mariko Toguchi-san, Ikuyo Inoue-san, Yumi Sato-san, Chen-san, Tee-san, Siribun-san, Den-san, Mori-san, Tejima-san and Simamura-san for helping me performing my experiments, providing needful materials, analyzing the results and suggesting for my experiments. Without their support, I could not have completed my thesis work. I am also indebted to Kimie Tajima-san, Yasuyo Takayama-san and Reina Kojima-san for their unconditional support and making my stay at lab and Japan comfortable.,

I would like to express my sincere gratitude to International Program Associate (IPA) program from the RIKEN and Tokyo Institute of Technology for awarding me PhD fellowship.

I am very grateful to my beloved husband Dr. Rajan Shrestha, Love from my heart-core to my sweet daughter Anvesha Shrestha (Anvi) and my dear mother for continuously encouraging me and being by my side whenever in needs. Special thanks also go to all other family members and friends for their indispensable encouragement.

Bibliography

1. Ruggiero, M.A., et al., *A Higher Level Classification of All Living Organisms.* PLoS One, 2015. **10**(4): p. e0119248.
2. Mahanty, T., et al., *Biofertilizers: a potential approach for sustainable agriculture development.* Environ Sci Pollut Res Int, 2017. **24**(4): p. 3315-3335.
3. Adrio, J.L. and A.L. Demain, *Fungal biotechnology.* Int Microbiol, 2003. **6**(3): p. 191-9.
4. Schmiedel, Y. and S. Zimmerli, *Common invasive fungal diseases: an overview of invasive candidiasis, aspergillosis, cryptococcosis, and Pneumocystis pneumonia.* Swiss Med Wkly, 2016. **146**: p. w14281.
5. Das, R.R., R., *An Overview of Changing Trends in Systemic Fungal Infections.* WebmedCentral MICROBIOLOGY, 2012. **3**(5): p. WMC003386.
6. Perlroth, J., B. Choi, and B. Spellberg, *Nosocomial fungal infections: epidemiology, diagnosis, and treatment.* Med Mycol, 2007. **45**(4): p. 321-46.
7. Lockhart, S.R., et al., *Comparison of in vitro susceptibility characteristics of Candida species from cases of invasive candidiasis in solid organ and stem cell transplant recipients: Transplant-Associated Infections Surveillance Network (TRANSNET), 2001 to 2006.* J Clin Microbiol, 2011. **49**(7): p. 2404-10.
8. Dujon, B., et al., *Genome evolution in yeasts.* Nature, 2004. **430**(6995): p. 35-44.
9. Chen, X., et al., *The role of Bgl2p in the transition to filamentous cells during biofilm formation by Candida albicans.* Mycoses, 2017. **60**(2): p. 96-103.
10. Brieland, J., et al., *Comparison of pathogenesis and host immune responses to Candida glabrata and Candida albicans in systemically infected immunocompetent mice.* Infect Immun, 2001. **69**(8): p. 5046-55.
11. Neofytos, D., et al., *Epidemiology and outcome of invasive fungal infections in solid organ transplant recipients.* Transpl Infect Dis, 2010. **12**(3): p. 220-9.
12. Odds, F.C., *Candida infections: an overview.* Crit Rev Microbiol, 1987. **15**(1): p. 1-5.
13. Chai, L.Y., et al., *Fungal strategies for overcoming host innate immune response.* Med Mycol, 2009. **47**(3): p. 227-36.
14. Polke, M., B. Hube, and I.D. Jacobsen, *Candida survival strategies.* Adv Appl Microbiol, 2015. **91**: p. 139-235.
15. Zhang, Y., V.L. Dawson, and T.M. Dawson, *Oxidative stress and genetics in the pathogenesis of Parkinson's disease.* Neurobiol Dis, 2000. **7**(4): p. 240-50.

16. Murad, A.M., et al., *NRG1 represses yeast-hypha morphogenesis and hypha-specific gene expression in Candida albicans.* EMBO J, 2001. **20**(17): p. 4742-52.
17. Lo, H.J., et al., *Nonfilamentous C. albicans mutants are avirulent.* Cell, 1997. **90**(5): p. 939-49.
18. Eckert, R.L., et al., *Transglutaminase regulation of cell function.* Physiol Rev, 2014. **94**(2): p. 383-417.
19. Nakagawa, Y., T. Kanbe, and I. Mizuguchi, *Disruption of the human pathogenic yeast Candida albicans catalase gene decreases survival in mouse-model infection and elevates susceptibility to higher temperature and to detergents.* Microbiol Immunol, 2003. **47**(6): p. 395-403.
20. Frohner, I.E., et al., *Candida albicans cell surface superoxide dismutases degrade host-derived reactive oxygen species to escape innate immune surveillance.* Mol Microbiol, 2009. **71**(1): p. 240-52.
21. Wellington, M., K. Dolan, and D.J. Krysan, *Live Candida albicans suppresses production of reactive oxygen species in phagocytes.* Infect Immun, 2009. **77**(1): p. 405-13.
22. Jenne, C.N. and P. Kubes, *Immune surveillance by the liver.* Nat Immunol, 2013. **14**(10): p. 996-1006.
23. Berg, R.D., *Bacterial translocation from the gastrointestinal tract.* Trends Microbiol. , 1995. **3**(4): p. 149-54.
24. Son, G., M. Kremer, and I.N. Hines, *Contribution of gut bacteria to liver pathobiology.* Gastroenterol Res Pract, 2010.
25. Balmer, M.L., et al., *The liver may act as a firewall mediating mutualism between the host and its gut commensal microbiota.* Sci Transl Med, 2014. **6**(237): p. 237ra66.
26. Adams, L.A., P. Angulo, and K.D. Lindor, *Nonalcoholic fatty liver disease.* CMAJ, 2005. **172**(7): p. 899-905.
27. Ma, C., Q. Zhang, and T.F. Greten, *Non-alcoholic fatty liver disease promotes hepatocellular carcinoma through direct and indirect effects on hepatocytes.* FEBS J, 2017.
28. Brunke, S. and B. Hube, *Two unlike cousins: Candida albicans and C. glabrata infection strategies.* Cell Microbiol, 2013. **15**(5): p. 701-8.
29. Renna, M.S., et al., *Hepatocellular apoptosis during Candida albicans colonization: involvement of TNF-alpha and infiltrating Fas-L positive lymphocytes.* Int Immunol, 2006. **18**(12): p. 1719-28.

30. Fleischhacker, M., et al., *Diagnosis of chronic disseminated candidosis from liver biopsies by a novel PCR in patients with haematological malignancies.* Clin Microbiol Infect, 2012. **18**(10): p. 1010-6.
31. Rolando, N., et al., *Fungal infection: a common, unrecognised complication of acute liver failure.* J Hepatol, 1991. **12**(1): p. 1-9.
32. Kirpich, I.A., et al., *Probiotics restore bowel flora and improve liver enzymes in human alcohol-induced liver injury: a pilot study.* Alcohol, 2008. **42**(8): p. 675-82.
33. Zhu, L., et al., *Characterization of gut microbiomes in nonalcoholic steatohepatitis (NASH) patients: a connection between endogenous alcohol and NASH.* Hepatology, 2013. **57**(2): p. 601-9.
34. Llorente, C. and B. Schnabl, *The gut microbiota and liver disease.* Cell Mol Gastroenterol Hepatol, 2015. **1**(3): p. 275-284.
35. Mutlu, E.A., et al., *Colonic microbiome is altered in alcoholism.* Am J Physiol Gastrointest Liver Physiol, 2012. **302**(9): p. G966-78.
36. Yang, A.M., et al., *Intestinal fungi contribute to development of alcoholic liver disease.* J Clin Invest, 2017. **63**.
37. Griffin, M., R. Casadio, and C.M. Bergamini, *Transglutaminases: nature's biological glues.* Biochem J, 2002. **368**(Pt 2): p. 377-96.
38. Kuo, T.F., H. Tatsukawa, and S. Kojima, *New insights into the functions and localization of nuclear transglutaminase 2.* FEBS J, 2011. **278**: p. 4756-4767.
39. Furutani, Y. and S. Kojima, *Control of TG Functions Depending on Their Localization.* 2015: p. 43-62.
40. Fesus, L. and Z. Szondy, *Transglutaminase 2 in the balance of cell death and survival.* FEBS Lett, 2005. **579**(15): p. 3297-3302.
41. Liu, S., R.A. Cerione, and J. Clardy, *Structural basis for the guanine nucleotide-binding activity of tissue transglutaminase and its regulation of transamidation activity.* Proc Natl Acad Sci USA, 2002. **99**(5): p. 2743-2747.
42. Han, B.-G., et al., *Crystal structure of human transglutaminase 2 in complex with adenosine triphosphate.* Int J Biol Macromol, 2010. **47**(2): p. 190-195.
43. Nakaoka, H., et al., *Gh: a GTP-binding protein with transglutaminase activity and receptor signaling function.* Science, 1994. **264**(5165): p. 1593-1596.
44. Lorand, L. and R.M. Graham, *Transglutaminases: crosslinking enzymes with pleiotropic functions.* Nat Rev Mol Cell Biol, 2003. **4**: p. 140-156

45. Wu, J., et al., *Roles of tissue transglutaminase in ethanol-induced inhibition of hepatocyte proliferation and alpha 1-adrenergic signal transduction.* J Biol Chem, 2000. **275**(29): p. 22213-22219.
46. Pinkas, D.M., et al., *Transglutaminase 2 undergoes a large conformational change upon activation.* Plos Biol, 2007. **5**(12): p. 2788-2796.
47. Casadio, R., et al., *The structural basis for the regulation of tissue transglutaminase by calcium ions.* Eur J Biochem, 1999. **262**: p. 672-679.
48. Venere, A.D., et al., *Opposite effects of Ca(2+) and GTP binding on tissue transglutaminase tertiary structure.* J Biol Chem, 2000. **275**(6): p. 3915-3921.
49. Begg, G.E., et al., *Mechanism of allosteric regulation of transglutaminase 2 by GTP.* Pro Natl Acad Sci U S A, 2006. **103**(52): p. 19683-19688.
50. Fesus, L. and M. Piacentini, *Transglutaminase 2: an enigmatic enzyme with diverse functions.* Trends Biochem Sci, 2002. **27**(10): p. 534-9.
51. Kuo, T.F., et al., *Free fatty acids induce transglutaminase 2-dependent apoptosis in hepatocytes via ER stress-stimulated PERK pathways.* J Cell Physiol, 2012. **227**(3): p. 1130-7.
52. Tatsukawa, H., et al., *Role of transglutaminase 2 in liver injury via cross-linking and silencing of transcription factor Sp1.* Gastroenterology, 2009. **136**(5): p. 1783-95 e10.
53. Tatsukawa, H., et al., *Dual induction of caspase 3- and transglutaminase-dependent apoptosis by acyclic retinoid in hepatocellular carcinoma cells.* Mol Cancer, 2011. **10**: p. 4.
54. Shrestha, R., et al., *Molecular mechanism by which acyclic retinoid induces nuclear localization of transglutaminase 2 in human hepatocellular carcinoma cells.* Cell Death Dis, 2015. **6**: p. e2002.
55. Volokhina, E.B., et al., *Tissue transglutaminase mRNA expression in apoptotic cell death.* Apoptosis, 2003. **8**(6): p. 673-9.
56. Chen, C.S., et al., *NF-kappaB-activated tissue transglutaminase is involved in ethanol-induced hepatic injury and the possible role of propolis in preventing fibrogenesis.* Toxicology, 2008. **246**(2-3): p. 148-57.
57. Fujise K, N.S., Hasumura S, Homma S, Sujino H, Matsuura T, Shimizu K, Niiya M, Kameda H, Fujita K,, *Integration of hepatitis B virus DNA into cells of six established human hepatocellular carcinoma cell lines.* Hepatogastroenterology 1990. **37**(5): p. 457-460.
58. Jeitner, T.M., et al., *Mechanism for the inhibition of transglutaminase 2 by cystamine.* Biochem Pharmacol, 2005. **69**(6): p. 961-70.

59. McConoughey, S.J., et al., *Inhibition of transglutaminase 2 mitigates transcriptional dysregulation in models of Huntington disease.* EMBO Mol Med, 2010. **2**(9): p. 349-70.
60. Furutani, Y., et al., *Phenosafranin inhibits nuclear localization of transglutaminase 2 without affecting its transamidase activity.* Amino Acids, 2017. **49**(3): p. 483-488.
61. Melino, G., et al., *Tissue transglutaminase and apoptosis: sense and antisense transfection studies with human neuroblastoma cells.* Mol Cell Biol, 1994. **14**(10): p. 6584-96.
62. Tucholski J, J.G., *Tissue transglutaminase differentially modulates apoptosis in a stimuli-dependent manner.* J Neurochem, 2002. **81**: p. 780–791.
63. Fonzi, W.A. and M.Y. Irwin, *Isogenic strain construction and gene mapping in Candida albicans.* Genetics, 1993. **134**(3): p. 717-28.
64. Kajiwara, S., et al., *Polyunsaturated fatty acid biosynthesis in Saccharomyces cerevisiae: expression of ethanol tolerance and the FAD2 gene from Arabidopsis thaliana.* Appl Environ Microbiol, 1996. **62**(12): p. 4309-13.
65. Ueno, K., et al., *Intestinal resident yeast Candida glabrata requires Cyb2p-mediated lactate assimilation to adapt in mouse intestine.* PLoS One, 2011. **6**(9): p. e24759.
66. Tomita, Y., et al., *Genome and transcriptome analysis of the food-yeast Candida utilis.* PLoS One, 2012. **7**(5): p. e37226.
67. Mayer, F.L., D. Wilson, and B. Hube, *Candida albicans pathogenicity mechanisms.* Virulence, 2013. **4**(2): p. 119-28.
68. Sudbery, P., N. Gow, and J. Berman, *The distinct morphogenic states of Candida albicans.* Trends Microbiol, 2004. **12**(7): p. 317-24.
69. Berman, J. and P.E. Sudbery, *Candida Albicans: a molecular revolution built on lessons from budding yeast.* Nat Rev Genet, 2002. **3**(12): p. 918-30.
70. Saville, S.P., et al., *Engineered control of cell morphology in vivo reveals distinct roles for yeast and filamentous forms of Candida albicans during infection.* Eukaryot Cell, 2003. **2**(5): p. 1053-60.
71. Jacobsen, I.D., et al., *Candida albicans dimorphism as a therapeutic target.* Expert Rev Anti Infect Ther, 2012. **10**(1): p. 85-93.
72. Sundstrom, P., E. Balish, and C.M. Allen, *Essential role of the Candida albicans transglutaminase substrate, hyphal wall protein 1, in lethal oroesophageal candidiasis in immunodeficient mice.* J Infect Dis, 2002. **185**(4): p. 521-30.

73. Murciano, C., et al., *Evaluation of the role of Candida albicans agglutinin-like sequence (Als) proteins in human oral epithelial cell interactions.* PLoS One, 2012. **7**(3): p. e33362.
74. Naglik, J.R., S.J. Challacombe, and B. Hube, *Candida albicans secreted aspartyl proteinases in virulence and pathogenesis.* Microbiol Mol Biol Rev, 2003. **67**(3): p. 400-28.
75. Zheng, X., Y. Wang, and Y. Wang, *Hgc1, a novel hypha-specific G1 cyclin-related protein regulates Candida albicans hyphal morphogenesis.* EMBO J, 2004. **23**(8): p. 1845-56.
76. Ferreira, C. and C. Lucas, *The yeast O-acyltransferase Gup1p interferes in lipid metabolism with direct consequences on the sphingolipid-sterol-ordered domains integrity/assembly.* Biochim Biophys Acta, 2008. **1778**(11): p. 2648-53.
77. Ferreira, C., et al., *Candida albicans virulence and drug-resistance requires the O-acyltransferase Gup1p.* BMC Microbiol, 2010. **10**: p. 238.
78. Jeng H.W., H.A.R., Cannon R.D., *Characterization of two Candida albicans surface mannoprotein adhesins that bind immobilized saliva components.* Med Mycol., 2005. **43**(3): p. 209-17.
79. Niewerth, M. and H.C. Korting, *Phospholipases of Candida albicans.* Mycoses, 2001. **44**(9-10): p. 361-7.
80. Leidich, S.D., et al., *Cloning and disruption of caPLB1, a phospholipase B gene involved in the pathogenicity of Candida albicans.* J Biol Chem, 1998. **273**(40): p. 26078-86.
81. Theiss, S., et al., *Inactivation of the phospholipase B gene PLB5 in wild-type Candida albicans reduces cell-associated phospholipase A2 activity and attenuates virulence.* Int J Med Microbiol, 2006. **296**(6): p. 405-20.
82. Hube, B., et al., *Secreted lipases of Candida albicans : cloning, characterisation and expression analysis of a new gene family with at least ten members.* Archives of Microbiology, 2000. **174**(5): p. 362-374.
83. Gacser, A., et al., *Lipase 8 affects the pathogenesis of Candida albicans.* Infect Immun, 2007. **75**(10): p. 4710-8.
84. Paraje, M.G., et al., *Candida albicans-secreted lipase induces injury and steatosis in immune and parenchymal cells.* Can J Microbiol, 2008. **54**(8): p. 647-59.
85. Trofa, D., et al., *Acetylsalicylic acid (aspirin) reduces damage to reconstituted human tissues infected with Candida species by inhibiting extracellular fungal lipases.* Microbes Infect, 2009. **11**(14-15): p. 1131-9.

86. Schroter, C., et al., *Generation of reactive oxygen species by Candida albicans in relation to morphogenesis.* Arch Dermatol Res, 2000. **292**(5): p. 260-4.
87. Lee, Z.W., et al., *Activation of in situ tissue transglutaminase by intracellular reactive oxygen species.* Biochem Biophys Res Commun, 2003. **305**(3): p. 633-40.
88. Yi, S.J., et al., *Arachidonic acid activates tissue transglutaminase and stress fiber formation via intracellular reactive oxygen species.* Biochem Biophys Res Commun, 2004. **325**(3): p. 819-26.
89. Bhatt, M.P., et al., *C-peptide prevents hyperglycemia-induced endothelial apoptosis through inhibition of reactive oxygen species-mediated transglutaminase 2 activation.* Diabetes, 2013. **62**(1): p. 243-53.
90. Sander, C.S., et al., *Inhibitory effect of terbinafine on reactive oxygen species (ROS) generation by Candida albicans.* Mycoses, 2002. **45**(5-6): p. 152-5.
91. Murayama, S.Y., et al., *Construction and functional analysis of fatty acid desaturase gene disruptants in Candida albicans.* Microbiology, 2006. **152**(Pt 5): p. 1551-8.
92. Juntachai, W., et al., *The lipolytic enzymes activities of Malassezia species.* Med Mycol, 2009. **47**(5): p. 477-84.
93. Camera, E., et al., *Scavenging effects of terbinafine on free radicals in vitro.* Br J Dermatol, 1999. **140**(4): p. 640-4.
94. Fanning, S. and A.P. Mitchell, *Fungal biofilms.* PLoS Pathog, 2012. **8**(4): p. e1002585.
95. Finkel, J.S. and A.P. Mitchell, *Genetic control of Candida albicans biofilm development.* Nat Rev Microbiol, 2011. **9**(2): p. 109-18.
96. Semchyshyn, H.M. and L.M. Lozinska, *Fructose protects baker's yeast against peroxide stress: potential role of catalase and superoxide dismutase.* FEMS Yeast Res, 2012. **12**(7): p. 761-73.
97. Yoo, J.O., et al., *Transglutaminase 2 promotes both caspase-dependent and caspase-independent apoptotic cell death via the calpain/Bax protein signaling pathway.* J Biol Chem, 2012. **287**(18): p. 14377-88.
98. Yoo, J.O., et al., *Differential cytotoxic responses to low- and high-dose photodynamic therapy in human gastric and bladder cancer cells.* J Cell Biochem, 2011. **112**(10): p. 3061-71.
99. Zafarullah, M., et al., *Molecular mechanisms of N-acetylcysteine actions.* Cell Mol Life Sci, 2003. **60**(1): p. 6-20.

100. Iismaa, S.E., et al., *Transglutaminases and disease: lessons from genetically engineered mouse models and inherited disorders.* Physiol Rev, 2009. **89**(3): p. 991-1023.
101. Nanda, N., et al., *Targeted inactivation of Gh/tissue transglutaminase II.* J Biol Chem, 2001. **276**(23): p. 20673-8.
102. Akita, K., et al., *Impaired liver regeneration in mice by lipopolysaccharide via TNF-α/kallikrein–mediated activation of latent TGF-β.* Gastroenterology, 2002. **123**(1): p. 352-364.
103. Zhao, H., et al., *Synthesis and biochemical applications of a solid cyclic nitrone spin trap: a relatively superior trap for detecting superoxide anions and glutathiyl radicals.* Free Radic Biol Med, 2001. **31**(5): p. 599-606.
104. Koopman, W.J., et al., *Simultaneous quantification of oxidative stress and cell spreading using 5-(and-6)-chloromethyl-2',7'-dichlorofluorescein.* Cytometry A, 2006. **69**(12): p. 1184-92.
105. Rinnerthaler, M., et al., *Yno1p/Aim14p, a NADPH-oxidase ortholog, controls extramitochondrial reactive oxygen species generation, apoptosis, and actin cable formation in yeast.* Proc Natl Acad Sci U S A, 2012. **109**(22): p. 8658-63.
106. Dhalla, N.S., R.M. Temsah, and T. Netticadan, *Role of oxidative stress in cardiovascular diseases.* J Hypertens, 2000. **18**(6): p. 655-73.
107. Qin, B., et al., *A key role for the microglial NADPH oxidase in APP-dependent killing of neurons.* Neurobiol Aging, 2006. **27**(11): p. 1577-87.
108. Liao, D., et al., *Hypoxia-inducible factor-1alpha is a key regulator of metastasis in a transgenic model of cancer initiation and progression.* Cancer Res, 2007. **67**(2): p. 563-72.
109. Sane, D.C., J.L. Kontos, and C.S. Greenberg, *Roles of transglutaminases in cardiac and vascular diseases.* Front Biosci, 2007. **12**(1): p. 2530-45.
110. Hartley, D.M., et al., *Transglutaminase induces protofibril-like amyloid beta-protein assemblies that are protease-resistant and inhibit long-term potentiation.* J Biol Chem, 2008. **283**(24): p. 16790-800.
111. Citron, B.A., et al., *Protein crosslinking, tissue transglutaminase, alternative splicing and neurodegeneration.* Neurochem Int, 2002. **40**(1): p. 69-78.
112. Bernassola, F., et al., *Role of transglutaminase 2 in glucose tolerance: knockout mice studies and a putative mutation in a MODY patient.* FASEB J, 2002. **16**(11): p. 1371-8.

113. Erdem, M., et al., *Up-regulation of TGM2 with ITGB1 and SDC4 is important in the development and metastasis of renal cell carcinoma.* Urol Oncol, 2014. **32**(1): p. 25 e13-20.